Mendelova univerzita v Brně

Lesnická a dřevařská fakulta

Ústav hospodářské úpravy lesů a aplikované geoinformatiky

The use and processing of TLS data for purposes of forestry and forest ecology

Disertační práce

2016/2017

Ing. Jan Trochta

Prohlašuji, že jsem práci: The use and processing of TLS data for purposes of forestry and forest ecology *zpracoval samostatně a veškeré použité prameny a informace uvádím v seznamu použité literatury. Souhlasím, aby moje práce byla zveřejněna v souladu s § 47b Zákona č. 111/1998 Sb., o vysokých školách ve znění pozdějších předpisů a v souladu s platnou Směrnicí o zveřejňování vysokoškolských závěrečných prací.*

Jsem si vědom, že se na moji práci vztahuje zákon č. 121/2000 Sb., autorský zákon, a že Mendelova univerzita v Brně má právo na uzavření licenční smlouvy a užití této práce jako školního díla podle §60 odst. 1 autorského zákona.

Dále se zavazuji, že před sepsáním licenční smlouvy o využití díla jinou osobou (subjektem) si vyžádám písemné stanovisko univerzity, že předmětná licenční smlouva není v rozporu s oprávněnými zájmy univerzity a zavazuji se uhradit případný příspěvek na úhradu nákladů spojených se vznikem díla, a to až do jejich skutečné výše.

V Brně, dne 29. Září 2016

Poděkování:

Rád bych na tomto místě poděkoval všem mým blízkým za trpělivost, cenné rady, důvěru, podporu a radost, které mě posunovali a pořád posunují kupředu.

Jan Trochta: The use and processing of TLS data for purposes of forestry and forest ecology

ABSTRACT:

The use of terrestrial laser scanner in forestry seems to be promising technology for new findings about forest ecosystem together with precise information for forest managers and planners. With new technology comes also new methodology of data acquisition, data processing and presentation of results. In this thesis are proposed methodological aspects of scanning setup if forest with analysis of two main obstacles - terrain and tree stems together with estimation of synergic effect of additional scan and optimal distance of such scan. In the following section software for processing of TLS data from forest environment - 3D Forest - is introduced and briefly described. In the last part original and early attempt of the below ground tree biomass reconstruction and volume estimation using TLS data is presented as a part of coppice forest study.

KEY WORDS: Terrestrial laser scanning; 3D Forest; scanning setup; LiDAR;

Jan Trochta: Využití a zpracování dat z TLS pro účely lesnictví a ekologie lesa.

ABSTRAKT:

Využití pozemního laserového skenování v lesnictví se zdá být velmi slibnou technologií přinášející nové poznatky o lesním ekosystému stejně jako přesné informace pro vlastníky a správce lesa. S novou technologií přichází také nové způsoby sběru dat, jejich zpracování a prezentace výsledků. Tato disertační práce přibližuje možné metodologické postupy, které lze uplatnit pro lepší sběr dat v lesním prostředí s minimalizací ztrát způsobených překážkami (terén, kmeny stromů) a zároveň určit velikost synergického efektu, který přináší další sken z určité vzdálenosti. Následující sekce se zaobírá samotným zpracováním dat v nově vytvořené softwarové aplikaci 3D Forest a srovnáním základních stromový parametrů s běžnými metodami. Poslední část je věnována jednomu z prvních pokusů odhalit množství biomasy skrývající se pod zemí pomocí pozemního skenování.

KLÍČOVÁ SLOVA: Pozemní laserové skenování; 3D Forest; LiDAR; pozice skenování;

The use and processing of TLS data for purposes of forestry and forest ecology

1. INTRODUCTION

Forests cover about one third (about 3 999 000 000 ha) of earth surface (Keenan *et al.*, 2015) and thus play an important role in human society as a source of timber, fuel or paper products. In addition, forests depends on and also contribute to many complex processes that have great impact on all components of ecosystem: production of clear water, soil protection, stabilizing air temperature and humidity, mitigation of CO_2 emissions, ensure shelter for wildlife plants and animals and many more (Duffy, 2009; Hector and Bagchi, 2007; Naeem *et al.*, 2009). To keep all possible functions present in our forests we need to understand their spontaneous anatomy, physiology and dynamics on forests unchanged by direct human impact.

Such forests are widely named as primary forest or old-growth forests. Based on FAO assessment (Keenan *et al.*, 2015) primary forests cover about 33% of total forest area, but more than half of the area is based only in three states: Russian Federation, Canada and Brazil. The two biomes mostly found there – tropical and boreal forests - cover more than 88% of all primary forest on earth. Primary forests in temperate forest biom are rare since this biom is historically affected by rise of human civilization. In Europe primary forests cover less than 3 % of forested area (Forests of Europe, 2011) with hotspots in Scandinavia and south-east part of Europe. Primary forests in Czech Republic (Ministerstvo Zemědělství, 2015) cover about 1.1% of forested area. Such places needs to be protected from human impact but still studied by forest researchers in order to uncover numerous processes and relationships that create the forest ecosystem so unique.

Forest system can be studied by appropriate methods at many scales – from micro-organisms (López-Mondéjar *et al.*, 2015) to global scale (Crowther *et al.*, 2015). However, up-scaling or down-scaling of various investigations at different scales is not straightforward and sometimes very difficult. Spatially-explicit methods with high accuracy, precision, great detail and broad reach are needed (not only) to overcome these scaling issues and bring new insight into forest ecosystem.

Recently the methods based on LiDAR technology came in sight of researchers as fast, precise and detailed acquisition method of spatially oriented data. Laser combined with fast recording device, precise mechanics and time measurement build together a laser scanner. The scanner

emits laser beams into surrounding space, some of the beams are backscattered from surrounding objects/surfaces back into the scanner and the scanner records precise distance of the reflecting points from scanner (Fig. 1). Depending on mounting type laser scanning can be distinguished into: Airborne Laser Scanning (ALS), Terrestrial Laser Scanning (TLS) and Mobile Laser Scanning (MLS). Each method has similar output - point cloud, but with different perspective, point density and methods of further processing. TLS can be used for the most detailed studies on branch and leaf scale (Côté *et al.*, 2009) to plot scale, ALS is better suited from tree to regional scale studies (Naesset, 1997) and MLS in places where it´s possible to use vehicle – streets, parks or plantations (Rutzinger *et al.*, 2010).

This work further focuses on the TLS technology only (sometimes also called ground-based laser scanning). Speed of terrestrial scanners in present time reach 1 000 000 points per second with horizontal 360° and vertical 290° field of view with resolution 0.009° cover greatly surrounding of the scanner.

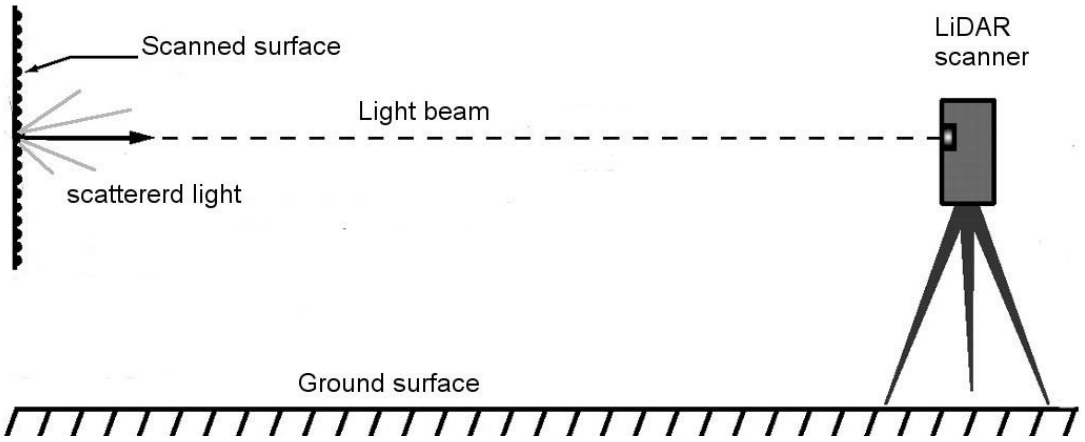

Fig. 1: Illustrative figure of terrestrial laser scanner technology used on tripod.

Expected results of laser scanning are georeferenced point clouds of target objects, detailed models with parameters of scanned objects or other spatial information that can be extracted. The advantage of laser scanning is that the real 3D shapes of target objects are recorded with only little simplification of reality compared to other recent non-destructive filed methods. The TLS field measurements are also fast and easy to repeat with respect to the level of detail recorded.

Despite indisputable advantages of the TLS mentioned above, there are also many obstacles that are recently a subject of intensive research. Some of the current issues of TLS have been addressed in these Ph.D. Thesis in a form of three Papers and/or manuscripts in different stage of publication process attached at the end of this work (further referred to as Papers I to III). The first question arise immediately with design of data collection since the complex forest environment constitutes so many obstacles (like stems, branches, terrain, etc.) for effective TLS. The Paper I thus address the question how to setup the scanner positions for area-wide stem mapping of natural forests. After data acquisition one needs to process the point clouds by specific algorithms designed to handle big data and produce outputs with good accuracy in reasonable time. Such algorithms are greatly appreciated by user community, no less than a stand-alone application that can provide the whole pipeline and make the data-processing a lot easier. These issues are addressed in the Paper II, where the powerful algorithms built-in new stand-alone software application - 3D Forest - are described and tested. The TLS has been usually used for description and quantification of above-ground biomass (AGB) of forest stands. The AGB however constitutes only 80% of the total tree biomass (Barbaroux *et al.*, 2003). Paper III thus presents one of the pioneer attempts applying TLS technology for examination of belowground tree root structures. In following sections the three individual Papers are set in a specific context and introduced in more detail.

2. SCANNING SETUP

With TLS data collection Liang *et al.* (2016) define three main approaches – single scan, multiple single scans and multiple scans.

2.1. Single scan setup

Single scan setup is mainly used in forest inventories (Liang *et al.*, 2011), detailed gap analysis (Seidel *et al.*, 2015) or LAI estimation similar to hemispherical photos (Danson *et al.*, 2007). The main advantage of such setup is in short time data acquisition due to the simple setup – just put

scanner into the center of the plot, setup the scanner and start scanning. Straightforward concept of single scan setup can be applied in national forest inventories or other statistical inventories as presented in Liang *et al.* (2011). Disadvantage of such concept is in occlusion effect leading to missing trees or their parts in resulting point cloud and relatively small diameter of dense point cloud. This was acknowledged in multiple studies from various types of forest e.g. (Brolly and Kiraly, 2009; Liang and Hyyppä, 2013; Maas *et al.*, 2008; Olofsson *et al.*, 2014). An approach how to compensate the occlusions was introduced by Ducey and Astrup (2013) who try to statistically define the portion of occlusion and estimate probability of tree nondetection. This approach thus try to deal with the biggest disadvantages of the single scan setup and might significantly improve its use.

2.2. Multiple single scans setup

Multiple single scanning setup is used only rarely (e.g. (Liang and Hyyppä, 2013) in order to minimize disadvantages of multiple setup, i.e. the need of co-registration and alignment of the multiple scans. On the other hand, it loses the advantage of a "synergic effect" of multiple scans described in the Paper I (Trochta *et al.* 2013).

2.3. Multiple scans setup

Multiple scanning setup is used in the most studies for tree reconstruction or estimation of tree parameters e.g. (Hopkinson *et al.*, 2004; Maas *et al.*, 2008; Van der Zande *et al.*, 2011) since it provides point cloud with less occlusions and generally better coverage of trees, as they are scanned from different angles and sides. On the other hand, this setup needs more time for setup the scanner on more positions and setup control points that create correspondence between scans. The multiple scanning setup is particularly tricky in unfavorable wind and day time conditions, where tree tops and branches might be considerably shifted in individual scans. The distance among scanning position in many studies have been set only intuitively, usually in a range from 10 to 100 m and differed substantially among individual studies (Calders *et al.*, 2015; Puttonen *et*

al., 2013). The issue of effective arrangement of scanner positions in the multiple scanning setup was thoroughly studied in the Paper I.

The paper focused on the effect of occlusion, successful stem recognition rate of trees with DBH ≥10 cm and effect of forest stand conditions for multiple scanning setup in various primary forests. It demonstrated that with the single scan setup the stem recognition rate decrease almost linearly with the distance from scanner and reach about 80 % at distance of 15-20 m. However, with three additional scans the 80 % recognition rate can be still achieved at the 25-30 m distance. The multiple scans thus significantly reduce the sharp decline of the recognition rate at further distances from the scanner. For are-wide stem mapping of trees with DBH ≥10 cm the most effective distance among scanner positions (i.e. the one with the highest synergic effect) appeared to be about 40m. The effect of occlusion was tested separately for terrain and tree stems. The results suggest that total occlusion is usually formed the by combination of both factors rather than by one of the factors only. However, in sites with rough terrain, the relief configuration (especially deep depressions) has a more significant effect of occlusion than present tree stems. More detailed information can be found in the PAPER I of this thesis.

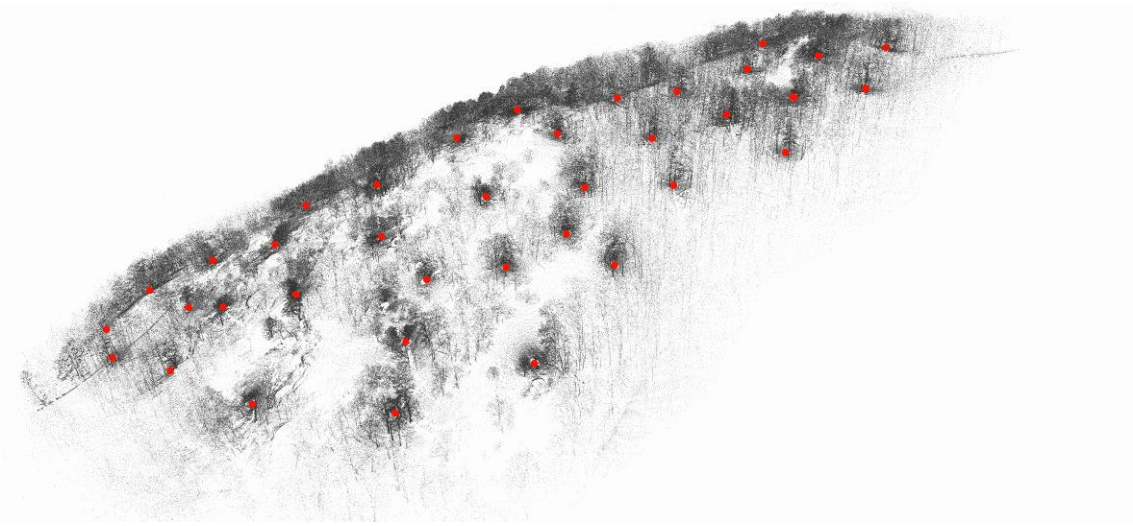

Fig. 2: Multiple scanning setup used on study site Velká Pleš (10 ha). Point cloud data were reduced to display only 1% of all points. Scanning positions are represent by red dots.

3. POINT CLOUD PROCESSING

After data acquisition user have to process scans – align scans and register them to coordinate system, select scanned area representing study plot and segment into target objects. Such process pipeline is almost universal for any scanning setup where object-oriented processing is followed.

The first steps – scan alignment, registration and area selection are often solved by scanner manufactures that provide special software suited for those tasks. Such software can read binary data from scanner, find targets identifying the control points in various scans, find the best match of scans and register them to selected coordinate system. After this all is done, a user can export point cloud into various formats for further use. This part of process line is quite straightforward and thanks to scanner manufactures partly automated using predefined scanning settings.

Further processing of the point cloud from forest environment is more complicated since the target objects (trees) are not parametric, each tree has its specific shape, trees are ingrown into other trees and trees and branches are frequently occluded.

3.1. Tree segmentation

Successful tree segmentation usually precede the tree reconstruction. Selection of all points representing given tree is the first really important task in the process line. In present time, tree segmentation is conducted either by manual or automated segmentation. Manual segmentation is quite simple but time consuming. On contrary, automatic way is very complex task composed of numerous interconnected algorithms. Up to present time, the automatic tree segmentation is a bottleneck of the process line and a development of highly reliable segmentation algorithm would undoubtedly contribute to wider applicability of TLS in forestry in general.

Alternative approaches can be employed, avoiding the step of tree segmentation itself and instead only try to estimate and export selected tree parameter like DBH or tree height e.g. (Bienert *et al.*, 2006; Brolly and Kiraly, 2009; Maas *et al.*, 2008) mainly using cylindrical fitting, or height difference between terrain and the topmost point in its neighborhood.. The first attempts of automated parameter segmentation were based on estimation of a circle or cylindrical form of

stem (Aschoff and Spiecker, 2004; Pfeifer *et al.*, 2004). Since tree structure is very complex, more sophisticated methods based on tree skeleton were developed later (Bremer *et al.*, 2013; Livny *et al.*, 2010). Those simplified approaches however can't fully exploit the potential of detailed and complex TLS data.

The real breakthrough was made by Raumonen *et al.* (2013), defining spatially exact small patches of point cloud and their merging based on its distance to neighboring patch and its shape. Similar approach but with not defined size of the patch was used also by Tao *et al.* (2015). This segmentation approach was independently adopted also in the Paper II (Trochta *et al.* (2016). It is based on point clusters that meets the user-given criteria of point density and minimal distance among points. Such clusters are then connected into 'tree clouds' based on rules of distance and angle among neighboring cluster centroids. In an oak forest with relatively sparse understory this procedure reached in average accuracy of 90% of correctly assigned points representing a particular tree. The omission and commission error rates were around 3 % for each (tested on 824 trees segmented both automatically and manually). The segmentation results are comparable to those attained by Raumonen *et al.* (2013) and Tao *et al.* (2015), there are still some lacks in problematic places such as crossing of branches of two trees, occlusions and mistaking of tree base with terrain points through all suggested methods. More testing is needed to prove the segmentation reliability also in other forest types and terrain conditions. Prior to individual trees the point cloud is also automatically segmented into terrain / vegetation. For details see the section Segmentation of trees (3.2) in the Paper II.

3.2. Tree reconstruction

Once the individual trees are segmented it´s possible to reconstruct each tree though its important parameters. The first tree parameters being extracted were tree position, DBH and tree height as usual in forest inventories (Hopkinson *et al.*, 2004; Maas *et al.*, 2008). More parameters can follow for tree crown (Bayer *et al.*, 2013; Fernández-Sarría *et al.*, 2013; Seidel *et al.*, 2011; Trochta *et al.*, 2016; Zheng and Moskal, 2012) describing its size, LAI, planar projection, estimation of crown volume and surface. The issue of tree parameters is also addresses in the PAPER II in the section Tree parameters (3.3). It introduces the algorithms employed for

extraction of individual tree parameters such as tree base position, DBH, tree height, stem curve, tree planar projection and a number of crown parameters. The PAPER II also presents a comparison of two principal tree parameters – DBH and tree height - derived from TLS with conventional field measurements (section 4.2). In addition, the detailed sensitivity analysis of DBH estimation is provided there (section 5).

3.3. Tree modeling

Tree reconstruction is not only a parametrization of tree, but also a creation of solid representation of the object that helps in characterization of tree physiology; inter tree interactions and understanding the role of each tree in plot. Detailed models as presented in (Côté *et al.*, 2011; Widlowski *et al.*, 2014) can help in estimation of architectural properties and topology of trees with high fidelity. Tree parameters can be created automatically based on Quantitative Surface Models (QSM) algorithm that can produce detailed tree representation build automatically (Calders *et al.*, 2015).

Most studies focus on the reconstruction and precise volume estimation of trunk, branches or the AGB of the whole tree (Calders *et al.*, 2015; Hackenberg *et al.*, 2014; Hauglin *et al.*, 2013; Hosoi *et al.*, 2013; Srinivasan *et al.*, 2014). On the contrary, PAPER III (Vrška *et al*., 2016) introduce an original and early attempt of the below ground tree biomass reconstruction and volume estimation. Tree roots system of one oak stool in ancient coppice forest of Lipina (Fig. 3) was excavated using hand tools, pneumatic drills and an air-spade supersonic nozzle. The soil was removed to the underlying bedrock at a maximum depth of 65 cm. Right after uncovering the roots the stool was scanned from multiple positions to record the state and architecture of the entire system with as much details as possible. Point clouds were aligned, merged and further processed in the Geomagic Studio software to create the 3D mesh model of the stool composed of seven stems and one snag interconnected by complex underground root-system. With the model it was then easy to estimate volume of above-ground and below-ground biomass. The mass of root-system was estimated to 1.02 m^3 of woody biomass lying below ground. On contrary the above-ground biomass was estimated to 2.13 m^3 in 7 stems and one snag.

Fig. 3 Exposed coppice stool root system (Lipina research plot). The current state was excavated and captured by a terrestrial laser scanner and saved as a mesh object for further analysis.

From known center of the root-system, average distance to the stems and an average annual radial increment we concluded that age of the whole system was about 825 years (SE ± 145 years). More details are provided in the PAPER III.

3.4. Forest TLS data processing software

Apart of individual algorithm using for special purpose, a common user appreciate a set of such algorithms built into ne stand-alone and application that can provide complete processing of the raw point cloud, compute and export tree parameters and visualize point clouds or model representations of the trees. In present time a potential user can choose from multiple applications that each has its focus on different part of point cloud processing or tree reconstruction.

One of specialized software is AutoStem (TreeMetrics, 2015), commercial software made for forestry purposes developed by TreeMetrics Company. Primary target of TreeMetrics based on their web site is to create new technology to preserve the environment and ensure sustainable use

of the natural resources. In present time AutoStem is provided only as a service and not as an application for own use.

Another commercial software on the market is LiForest (True Reality Geospatial Solutions, 2015). LiForest focuses its processing mainly into ALS data from forest environment, but in recent version introduced also the processing of TLS data and extraction of basic tree parameters like DBH, tree position and tree height.

Not only commercial software but also development of open source and free applications has great potential to take a leading role in TLS data processing. Almost all these applications are based on two platforms that handle cloud storage, accessing and various methods for filtering, segmenting, etc. – more general Point Cloud Library (Rusu and Cousins, 2011) and specialized CompuTree (Piboule *et al.*, 2015). CompuTree is also a standalone application with possible plugins that allow user to segment trees and compute their parameters (DBH, tree height, QSM) and their visualization. Various parameters and methods can be computed based on installed plugins.

Similar tree parameters can be estimated in SimpleTree (Hackenberg *et al.*, 2015). This application focused on detailed tree reconstruction is based on Point Cloud Library. Tree model is composed of detailed branch models with parameters like branch order, branch length, and crown volume

The last (but not least) application is thoroughly described in the PAPER II (Trochta *et al.*, 2016). The original 3D Forest application represents "created by foresters to foresters" style of application. This application is developed for three-dimensional studies of forest structure and dynamics. 3D Forest combines automated methods of terrain and tree segmentation with tree reconstruction of position, DBH, tree height, planar area or stem profile. The application can describe forest plot in detail of a single tree and its parts as well as interaction of the trees in canopy level. This is important as foresters and forest ecologists are actively using new LiDAR technologies for inference about a number of important forests structural features including vertical biomass distribution, tree allometry and light environments. 3D Forest is a timely application designed for this growing field of research. Detailed description of used methods and the complete TLS processing pipeline can be found in PAPER II and on web pages www.3dforest.eu.

4. CONCLUSIONS

In this Ph.D. thesis the potential of terrestrial laser scanning in forestry and forest ecology research was investigated. The three presented studies (PAPERS I-III) guide readers thought the processing of TLS data and can help with effective data acquisition, tree segmentation and reconstruction.

By using conventional field measurement techniques such as Field-Map (Černý *et al.*, 2006), the stem-position map is ready to use almost instantly after the fieldwork. In contrast, massive data processing must be performed after TLS measurements. The point clouds, on the other hand, include much more information than necessary for simple stem-position mapping, especially for the canopy layer.

The 3D Forest application presented in the theses contributes to better exploitation this great information potential focusing on forest stand description by means of individual trees and their mutual spatial arrangement in real 3D space. It allows users to take the advantage of TLS data for detailed spatially-oriented forestry and forest ecology studies in a user friendly environment. Currently it can provide standard census data such as tree positions, DBHs and heights; it also provides more complex tree parameters such as stem curve, convex/concave planar projection, crown dimensions, crown volume, surface, center of mass, crown to crown intersections and others. In the comparison with other applications the 3D Forest appeared as comparable with the best tools world-wide.

The advantages of TLS technology revealed also in its unconventional use for reconstruction and quantification of the ancient coppice stool root system. TLS allowed quantification of the root system biomass, while preserving and documenting its in situ spatial architecture resulting from its long-time development. Combining TLS results with other data brings new insight into the complex forest ecosystem and can help in understanding of the complex natural processes taking place there.

5. SOUHRN

V této disertační práci jsou zkoumány možnosti využití pozemního laserového skenování v lesnictví a ekologii lesa. Tři přiložené studie (PAPER I-III) jsou průvodcem po jednotlivých problémových oblastech, které brzdí širší využití pozemního skenování v lesnictví. Tyto problémové oblasti jsou jak v počátečním sběru dat, tak i v jejich zpracování.

Použití běžných metod sběru dat jako je průměrka, výškoměr nebo technologie Field-Map (Černý *et al.,* 2006) nám poskytnou potřebné údaje téměř okamžitě nebo jen s malým mezistupněm zpracování dat. Naproti tomu pozemní laserové skenování potřebuje velké množství dalšího zpracování dat, aby bylo možno dosáhnout podobných výsledků. Výsledkem ale není jen několik základních stromový parametrů. Z pozemního laserového skenování je možné získat velmi detailní model stromu i jeho okolí, a spolu se základními parametry i další informace, které jsou běžnými způsoby velmi nákladně zjistitelné.

Aby bylo možno získat detailní informace o jednotlivém stromu nebo jeho části, je potřeba si správně zvolit postup sběru dat v terénu. V současné době se nejčastěji používají dva základní přístupy – jeden sken na ploše a více skenovacích pozic. Výhodou jednoho skenu z plochy je rychlost nastavení a sběru dat. Tento přístup má velké negativum v množství zastíněných míst, a tím i nezachycení jednotlivých detailů nebo celých stromů. Použitím více skenů na jedné ploše se množství zastíněných míst snižuje, ale vzrůstá náročnost na nastavení skeneru a možnost změny povětrnostních podmínek, které výsledek znehodnotí. Z prezentované studie (PAPER I) je patrné, že pokud jsou cílem stromy s výčetní tloušťkou nad 10 cm, je možné počítat s úspěšným zachycením 85% stromů, pokud budou jednotlivé pozice od sebe vzdáleny 40 m.

Po pořízení dat je potřeba jednotlivé skeny spojit, registrovat do souřadnicového systému, vybrat zájmové území a výsledné mračno bodů zpracovat na jednotlivé stromy. Část z těchto kroků je běžně řešena v aplikacích výrobců dodávaných ke skeneru. Pro samotné zpracování jednotlivých stromů je již potřeba speciální aplikace a právě pro tento účel je vytvořena a v PAPER II prezentována aplikace 3D Forest. Tato aplikace je kolekcí algoritmů, které se osvědčily při zpracování dat z TLS. Implementované algoritmy umožňují získat automaticky body představující terén, jednotlivé stromy a tyto stromy i dále popsat pomocí jednotlivých parametrů jako jsou: pozice stromu, výčetní tloušťka, výška a délka stromu, profil kmene, planární projekce

a další korunové parametry. Přesnost výpočtu základních parametrů (výčetní tloušťka, výška) je srovnána s měřením běžnými prostředky jako je průměrka nebo výškoměr. Dále je studována i přesnost automatické segmentace jednotlivých stromů, kde dosahuje 90% správně přiřazených bodů jednotlivým stromům.

Výsledkem pozemního laserového skenování v lesním prostředí jsou, jak už bylo nastíněno, požadované parametry jednotlivých stromů, a také detailní mračno bodů reprezentující daného jedince. Toto mračno bodů je možno dále zpracovat a vytvořit tak jasně definovaný objekt, pro který je snadné již určit např. objem nebo plochu. Jedním z takových výsledků je i detailní model kořenového systému (PAPER III), který odhalil, jak jsou jednotlivé stromy propojeny pod zemí a kolik biomasy je tam uloženo nebo jaká byla jeho historie. Díky pozemnímu laserovému skenování lze odvodit poměr nadzemní a podzemní biomasy, který tvoří u studovaného polykormonu dubu 2:1 ve prospěch nadzemní části. Takový poměr je celkem zásadním zjištěním, jelikož běžně se používá poměr 5:1 (Barbaroux *et al.*, 2003). Toto zjištění může pomoci například pro zjištění množství zadržených látek jako je dusík, uhlík, vodík nebo kyslík v lesním prostředí.

Výsledky z jednotlivých studií mohou přispět k lepšímu získání podrobných dat o lesním ekosystému, pomocí aplikace k detailnímu popisu jedinců i celých lesních porostů. Ze zjištěných informací můžeme lépe porozumět komplexní struktuře a fungování lesního ekosystému a zpřesnit dopady lidské činnosti na přírodu a také lépe zajistit udržitelnost hospodaření člověka s přírodními zdroji.

6. REFERENCES

Aschoff, T., Spiecker, H., 2004. Algorithms for the automatic detection of trees in laser scanner data. International Archives.of Photogrammetry, Remote Sensing and Spatial.Information Sciences 36(Part 8) W2.

Barbaroux, C., Bréda, N., Dufrêne, E., 2003. Distribution of above-ground and below-ground carbohydrate reserves in adult trees of two contrasting broad-leaved species (Quercus petraea and Fagus sylvatica). New Phytologist 157(3) 605-615.

Bayer, D., Seifert, S., Pretzsch, H., 2013. Structural crown properties of Norway spruce (Picea abies [L.] Karst.) and European beech (Fagus sylvatica [L.]) in mixed versus pure stands revealed by terrestrial laser scanning. Trees. 1-13.

Bienert, A., Scheller, S., Keane, E., Mullooly, G., Mohan, F., 2006. Application of terrestrial laser scanners for the determination of forest inventory parameters. International Archives.of Photogrammetry, Remote Sensing and Spatial.Information Sciences 36(5).

Bremer, M., Rutzinger, M., Wichmann, V., 2013. Derivation of tree skeletons and error assessment using LiDAR point cloud data of varying quality. ISPRS Journal of Photogrammetry and Remote Sensing 80(0) 39-50.

Brolly, G., Kiraly, G., 2009. Algorithms for stem mapping by means of terrestrial laser scanning. Acta.Silva.Lign.Hung. 5 119-130.

Calders, K., Newnham, G., Burt, A., Murphy, S., Raumonen, P., Herold, M., Culvenor, D., Avitabile, V., Disney, M., Armston, J., Kaasalainen, M., McMahon, S., 2015. Nondestructive estimates of above-ground biomass using terrestrial laser scanning. Methods in Ecology and Evolution 6(2) 198-208.

Côté, J.F., Fournier, R.A., Egli, R., 2011. An architectural model of trees to estimate forest structural attributes using terrestrial LiDAR. Environmental Modelling & Software.

Côté, J.F., Widlowski, J.L., Fournier, R.A., Verstraete, M.M., 2009. The structural and radiative consistency of three-dimensional tree reconstructions from terrestrial lidar. Remote Sensing of Environment 113(5) 1067-1081.

Crowther, T.W., Glick, H.B., Covey, K.R., Bettigole, C., Maynard, D.S., Thomas, S.M., Smith, J.R., Hintler, G., Duguid, M.C., Amatulli, G., Tuanmu, M.N., Jetz, W., Salas, C., Stam, C., Piotto, D., Tavani, R., Green, S., Bruce, G., Williams, S.J., Wiser, S.K., Huber, M.O., Hengeveld, G.M., Nabuurs, G.J., Tikhonova, E., Borchardt, P., Li, C.F., Powrie, L.W., Fischer, M., Hemp, A., Homeier, J., Cho, P., Vibrans, A.C., Umunay, P.M., Piao, S.L., Rowe, C.W., Ashton, M.S., Crane, P.R., Bradford, M.A., 2015. Mapping tree density at a global scale. Nature 525(7568) 201-205.

Černý, M., Buksha, I., Pasternak, V., 2006. Usage of field technology Field-Map in forest management and nature protection. Geoinformatics, Kiev, Ukraine.

Danson, F.M., Hetherington, D., Morsdorf, F., Koetz, B., Allgower, B., 2007. Forest canopy gap fraction from terrestrial laser scanning. Geoscience and Remote Sensing Letters, IEEE 4(1) 157-160.

Ducey, M.J., Astrup, R., 2013. Adjusting for nondetection in forest inventories derived from terrestrial laser scanning. Canadian Journal of Remote Sensing 39(05) 410-425.

Duffy, J.E., 2009. Why biodiversity is important to the functioning of real-world ecosystems. Front. Ecol. Environ 7 437-444.

Forests of Europe, 2011. UNECE and FAO (2011) State of Europe's Forests 2011. Status and Trends in Sustainable Forest Management in Europe, Ministerial conference on the protection of forests in Europe, Oslo, p. 337.

Fernández-Sarría, A., Martínez, L., Velázquez-Martí, B., Sajdak, M., Estornell, J., Recio, J.A., 2013. Different methodologies for calculating crown volumes of Platanus hispanica trees using terrestrial laser scanner and a comparison with classical dendrometric measurements. Computers and Electronics in Agriculture 90(0) 176-185.

Hackenberg, J., Morhart, C., Sheppard, J., Spiecker, H., Disney, M., 2014. Highly Accurate Tree Models Derived from Terrestrial Laser Scan Data: A Method Description. Forests 5(5) 1069-1105.

Hackenberg, J., Spiecker, H., Calders, K., Disney, M., Raumonen, P., 2015. SimpleTree — An Efficient Open Source Tool to Build Tree Models from TLS Clouds. Forests 6(11) 4245-4294.

Hauglin, M., Astrup, R., Gobakken, T., Naesset, E., 2013. Estimating single-tree branch biomass of Norway spruce with terrestrial laser scanning using voxel-based and crown dimension features. Scandinavian Journal of Forest Research(ahead-of-print) 1-14.

Hector, A., Bagchi, R., 2007. Biodiversity and ecosystem multifunctionality. Nature 448 188-190.

Hopkinson, C., Chasmer, L., Young-Pow, C., Treitz, P., 2004. Assessing forest metrics with a ground-based scanning lidar. Canadian Journal of Forest Research 34(3) 573-583.

Hosoi, F., Nakai, Y., Omasa, K., 2013. 3-D voxel-based solid modeling of a broad-leaved tree for accurate volume estimation using portable scanning lidar. ISPRS Journal of Photogrammetry and Remote Sensing 82(0) 41-48.

Keenan, R.J., Reams, G.A., Achard, F., de Freitas, J.V., Grainger, A., Lindquist, E., 2015. Dynamics of global forest area: Results from the FAO Global Forest Resources Assessment 2015. Forest Ecology and Management 352 9-20.

Liang, X., Hyyppä, J., 2013. Automatic stem mapping by merging several terrestrial laser scans at the feature and decision levels. Sensors 13(2) 1614-1634.

Liang, X., Kankare, V., Hyyppä, J., Wang, Y., Kukko, A., Haggrén, H., Yu, X., Kaartinen, H., Jaakkola, A., Guan, F., 2016. Terrestrial laser scanning in forest inventories. ISPRS Journal of Photogrammetry and Remote Sensing 115 63-77.

Liang, X., Litkey, P., Hyyppä, J., Kaartinen, H., Kukko, A., Holopainen, M., 2011. Automatic plot-wise tree location mapping using single-scan terrestrial laser scanning. Photogrammetric.Journal of Finland. 22(2).

Livny, Y., Yan, F., Olson, M., Chen, B., Zhang, H., El-Sana, J., 2010. Automatic reconstruction of tree skeletal structures from point clouds. ACM Transactions on Graphics (TOG) 29(6) 151.

López-Mondéjar, R., Voříšková, J., Větrovský, T., Baldrian, P., 2015. The bacterial community inhabiting temperate deciduous forests is vertically stratified and undergoes seasonal dynamics. Soil Biology and Biochemistry 87 43-50.

Maas, H.G., Bienert, A., Scheller, S., Keane, E., 2008. Automatic forest inventory parameter determination from terrestrial laser scanner data. International Journal of Remote Sensing 29(5) 1579-1593.

Ministerstvo Zemědělství, 2015. Zpráva o stavu lesa a lesního hospodářství České republiky v roce 2014, In: Krejzar Tomáš, I., Ph.D. (Ed.), Ministerstvo Zemědělství, Praha: Praha.

Naeem, S., Bunker, D.E., Hector, A., Loreau, M., Perrings, C., 2009. Biodiversity, Ecosystem Functioning, and Human Wellbeing: An Ecological and Economic Perspective.

Naesset, E., 1997. Determination of mean tree height of forest stands using airborne laser scanner data. ISPRS Journal of Photogrammetry and Remote Sensing 52(2) 49-56.

Olofsson, K., Holmgren, J., Olsson, H., 2014. Tree stem and height measurements using terrestrial laser scanning and the ransac algorithm. Remote Sensing 6(5) 4323-4344.

Pfeifer, N., Gorte, B., Winterhalder, D., 2004. Automatic reconstruction of single trees from terrestrial laser scanner data, pp. 114-119.

Piboule, A., Krebs, M., Esclatine, L., Hervé, J., 2015. Computree: a collaborative platform for use of terrestrial LiDAR in dendrometry.

Puttonen, E., Lehtomäki, M., Kaartinen, H., Zhu, L., Kukko, A., Jaakkola, A., 2013. Improved Sampling for Terrestrial and Mobile Laser Scanner Point Cloud Data. Remote Sensing 5(4) 1754-1773.

Raumonen, P., Kaasalainen, M., Åkerblom, M., Kaasalainen, S., Kaartinen, H., Vastaranta, M., Holopainen, M., Disney, M., Lewis, P., 2013. Fast automatic precision tree models from terrestrial laser scanner data. Remote Sensing 5(2) 491-520.

Rusu, R.B., Cousins, S., 2011. 3d is here: Point cloud library (pcl). IEEE, pp. 1-4.

Rutzinger, M., Pratihast, A.K., Oude Elberink, S., Vosselman, G., 2010. Detection and modelling of 3D trees from mobile laser scanning data. International Archives.of Photogrammetry, Remote Sensing and Spatial.Information Sciences 38(5) 520-525.

Seidel, D., Hoffmann, N., Ehbrecht, M., Juchheim, J., Ammer, C., 2015. How neighborhood affects tree diameter increment – New insights from terrestrial laser scanning and some methodical considerations. Forest Ecology and Management 336(0) 119-128.

Seidel, D., Leuschner, C., Müller, A., Krause, B., 2011. Crown plasticity in mixed forests - Quantifying asymmetry as a measure of competition using terrestrial laser scanning. Forest Ecology and Management 261(11) 2123-2132.

Srinivasan, S., Popescu, S.C., Eriksson, M., Sheridan, R.D., Ku, N.-W., 2014. Multi-temporal terrestrial laser scanning for modeling tree biomass change. Forest Ecology and Management 318(0) 304-317.

Tao, S., Wu, F., Guo, Q., Wang, Y., Li, W., Xue, B., Hu, X., Li, P., Tian, D., Li, C., 2015. Segmenting tree crowns from terrestrial and mobile LiDAR data by exploring ecological theories. ISPRS Journal of Photogrammetry and Remote Sensing 110 66-76.

TreeMetrics, 2015. AutoStem Forest: http://www.treemetrics.com/.

Trochta J., Král K., Janík D., Adam D., 2013. Arrangement of terrestrial laser scanner positions for area-wide stem mapping of natural forests. Canadian Journal of Forest Research 43: 355-363.

Trochta, J., Krůček, M., Vrška, T., Král, K., 2016. 3D Forest: an application for descriptions of three-dimensional forest structures using terrestrial LiDAR. Manuscript submitted for publication (copy on file with author).

True Reality Geospatial Solutions, L., 2015. LiForest -LiDAR software for forestry applications, 2 ed: http://www.liforest.com/.

Van der Zande, D., Stuckens, J., Verstraeten, W.W., Mereu, S., Muys, B., Coppin, P., 2011. 3D modeling of light interception in heterogeneous forest canopies using ground-based LiDAR data. International Journal of Applied Earth Observation.and Geoinformation. 13(5) 792-800.

Vrška T., Janík D., Pálková M., Adam D., Trochta J., 2016. Below and above-ground structure and patterns in ancient lowland coppices. iForest - Biogeosciences and Forestry (Manuscript Accepted).

Widlowski, J.L., Côté, J.F., Béland, M., 2014. Abstract tree crowns in 3D radiative transfer models: Impact on simulated open-canopy reflectances. Remote Sensing of Environment 142(0) 155-175.

Zheng, G., Moskal, L.M., 2012. Spatial variability of terrestrial laser scanning based leaf area index. International Journal of Applied Earth Observation and Geoinformation 19(0) 226-237.

List of papers

I: Trochta J., Král K., Janík D., Adam D., 2013. Arrangement of terrestrial laser scanner positions for area-wide stem mapping of natural forests. Canadian Journal of Forest Research 43: 355-363.

II: Trochta, J., Krůček, M., Vrška, T., Král, K., 2016. 3D Forest: an application for descriptions of three-dimensional forest structures using terrestrial LiDAR. Manuscript submitted for publication in Journal Plos One.

III: Vrška T., Janík D., Pálková M., Adam D., Trochta J., 2016. Below and above-ground structure and patterns in ancient lowland coppices. iForest - Biogeosciences and Forestry (Manuscript Accepted).

PAPER I

Arrangement of terrestrial laser scanner positions for area-wide stem mapping of natural forests.

Jan Trochta[1,2], Kamil Král [1], David Janík [1], Dušan Adam [1]

1. *The Silva Tarouca Research Institute for Landscape and Ornamental Gardening,*

Department of Forest Ecology, Lidická 25/27, Brno 602 00, Czech Republic

2. *Mendel University in Brno, Faculty of Forestry and Wood Technology, Department of Geoinformation Technologies, Zemědělská 3, Brno 613 00 , Czech Republic*

Abstract:

With the development of terrestrial laser scanning and applications in forestry, the question arises as to how the scanners should be ideally placed for the best possible data acquisition. We searched for an optimal scanning distance for recognition of stems in natural beech-dominated forests, focusing particularly on the shading effect of tree stems and terrain. Recognised tree stems in TLS point clouds were compared with reference stem maps. A GIS based visibility simulation was carried out to enhance the quantitative assessment and generalizability of results. The analyses also include the additive effect of multiple scanning positions. Single scans only have a tree recognition rate above 80% up to a distance of 15 m from the scanner; using at least three scanning positions a comparable recognition rate was attained up to 20–25 m. A simulated coverage of a beech-dominated natural forest by laser beams using a 40 m square grid of scanning positions captured at least half of the stem perimeter for more than 90% of trees with a DBH ≥10 cm. In sites with rough terrain, the relief configuration has a more significant effect of occlusion than present tree stems.

1. INTRODUCTION

Forest inventories are one of the main tools for decision making for forest managers, policy makers, conservation planners and forest scientists. Traditional approaches such as area-wide stem-position mapping or statistical inventory methods can provide much of the desirable information. Research on forest ecology and dynamics (e.g., Janik *et al.* 2011; Král *et al.* 2010a; Šebková *et al.* 2011) are examples of the recent extensive use of such spatially oriented data. However, further insight into many questions of forest ecology and management still require more detailed studies with a greater use of spatial information. An increase in the speed and objectivity of data collection and extraction is thus highly desirable.

LiDAR (Light Detection And Ranging) technology provides the capacity for detailed mapping of 3D structures of forests with millimetre accuracy (van Leeuwen & Nieuwenhuis 2010). It has great promise for collecting spatial information in forests because of its excellent measurement precision, short acquisition time and level of detail. Due to these various advantages, LiDAR has been used widely to replace conventional methods of spatially oriented measurement of trees and forest structures since 2001 (Dassot *et al.* 2011). Both platforms of LiDAR data acquisition, Airborne Laser Scanning (ALS) and Terrestrial Laser Scanning (TLS), have been utilized for this purpose.

ALS is generally used for plot level investigations. The basic characteristics of a forest such as: canopy height (Naesset 1997; Parker & Russ 2004), determination of relief under the tree canopy (Kraus & Pfeifer 1998), the detection of individual trees (Chen *et al.* 2006; Heurich 2008), and biomass (Popescu 2007) have been successfully derived from ALS data.

TLS is used to describe forest vegetation at the tree level and is capable of acquiring levels of detail far beyond that of which ALS is capable. Basic parameters of individual trees, such as the diameter at breast height (DBH) (Bienert *et al.* 2006; Maas *et al.* 2008), or tree height (Bienert *et al.* 2007; Király & Brolly 2007) can be derived via this automated method. Other variables of tree structure (e.g., crown, stem or whole tree dimensions) can be observed and measured in the point cloud by time-consuming manual interpretation (Côté *et al.* 2009; Fleck *et al.* 2007; Hopkinson *et al.* 2004), although (semi)-automatic algorithms have recently been developed with various degrees of success (Bienert *et al.* 2007; Côté *et al.* 2011; Lefsky & McHale 2008). Data

describing specific characteristics of individual trees can also be summarized to describe characteristics at the plot level, e.g. stem density (Hopkinson *et al.* 2004), overall volume of biomass (Lefsky & McHale 2008; Huang *et al.* 2008), or the fuel capacity in a forest (García *et al.* 2011). The early applications of TLS in area-wide stem mapping have been also presented (Brolly & Kiraly 2009; Hopkinson *et al.* 2004). More details on the use of terrestrial LiDAR in developing a forest inventory can be found in several books, e.g. Vosselman & Maas (2010), or in recent reviews by van Leeuwen & Nieuwenhuis (2010) and van Leeuwen *et al.* (2011).

Various field conditions can greatly affect the quality and character of data acquired by TLS. Weather conditions (e.g., fog, drizzle, rain or even wet surfaces after rain) can cause a significant reduction in the resulting point cloud density and measurement range due to the absorption of the laser pulse energy by water. Wind that moves leaves, branches and even tree trunks is a limiting factor for precise measurements. Leaves are also a physical obstacle for laser beams penetrating the forest stand and decrease the attainable range for measurement. On the other hand, the presence of leaves is beneficial when the actual shape of individual tree crowns is investigated (e.g. Rutzinger *et al.* 2010). Thus, studies that combine the measurement of leaf-off and leaf-on states are common (e.g., Clawges *et al.* 2007; Hill & Broughton 2009; Kim *et al.* 2009). For area-wide forest measurements (e.g., complete census-stem position mapping) that are preferably carried out when leaves have dropped, the shading of stems and branches is another key limiting factor. The presence of rough terrain appears to be another pronounced occlusive effect in TLS, which can significantly reduce the visibility of tree individuals in the surrounding area. Although numerous forestry applications have employed TLS, these limiting conditions have not yet been adequately studied. To some extent, the increase of scanning positions can overcome the effect of occlusion, although at increased cost both in terms of labour as well as financially (van Leeuwen & Nieuwenhuis 2010). As general rules of the configuration of optimal scanners have not yet been established (Hopkinson *et al.* 2004), the positioning of TLS stations is usually selected subjectively, depending on local site conditions and plot visibility. This may lead to sub-optimal coverage of a target area that is detected only in post-processing, i.e., too late to effectively correct the problem. Moreover, subjective scan-head locations might lead to biased sampling.

In this study we focus on the optimal spatial arrangement of scanning positions, taking into account the shading effect of tree stems and relief. For natural forests that have often been

preserved on sites with rugged terrain and that are characterised by a rich stand structure, these two limiting factors are of high importance. We addressed the following fundamental questions: What is an effective acquisition range for recognition of stems from a single TLS position? What is the 'synergic effect' of multiple scans and what distance between scanning positions is best for capturing stems? How should the TLS ideally be spaced in the forest for the best possible data acquisition? What is the shading effect of trees and relief? Can TLS be used for a complete census (stem mapping) if placed in a regular grid? To answer these questions we compared TLS data to reference stem maps and supported and extended the findings through visibility modelling.

2. MATERIAL AND METHODS

2.1. Study sites and data acquisition

Our research took place in beech-dominated natural forests the Žofínský prales and Boubínský prales National Nature Reserves, Czech Republic (hereafter referred to as the Žofín and Boubín forests, respectively).

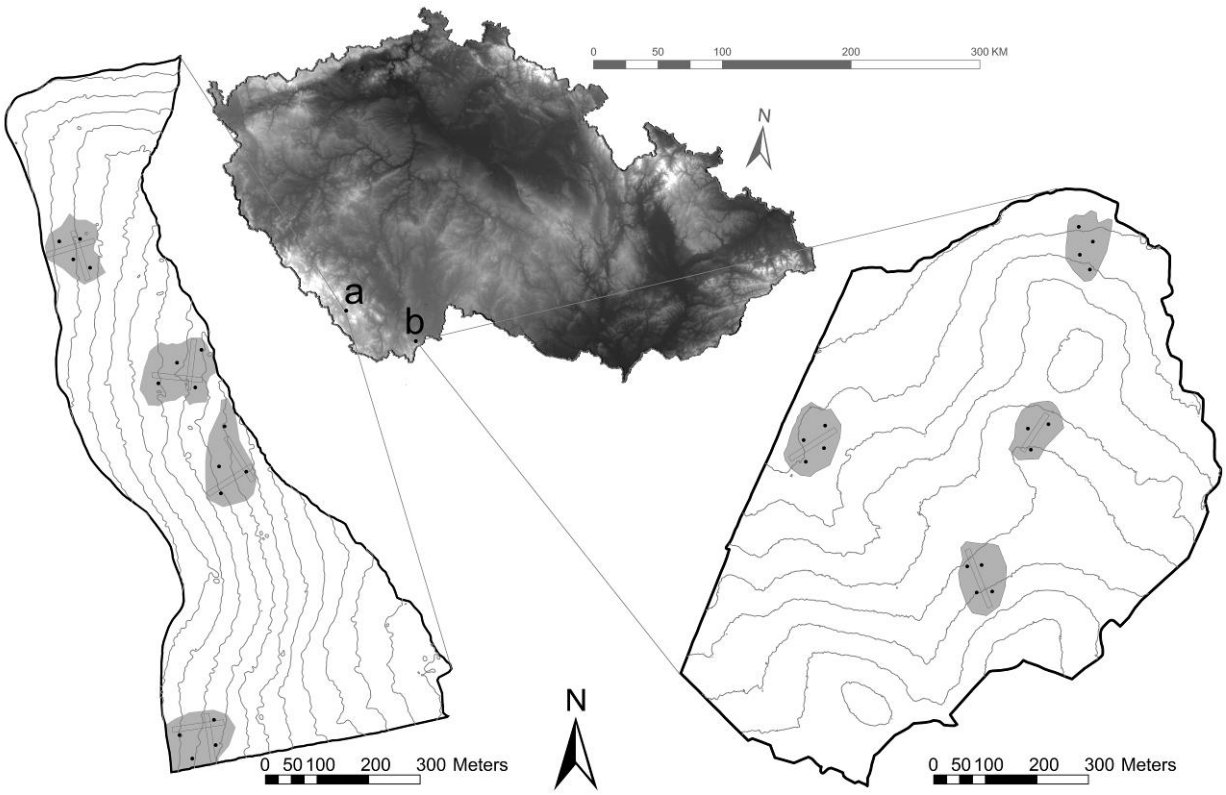

Figure 1: Study sites – a) Boubín forest and b) Žofín forest with 10 m contours and location in the Czech Republic . Each site with four study plots measured by TLS (grey areas) and marked positions of LiDAR scanner (black dots).

The core area of the Žofín forest (74,5 ha) has been under strict protection since 1838. The altitude ranges from 735 to 825 m. The mean slope of the study site is about 8.8 °, and the mean local altitudinal differences within a 10 m radius are about 3 m (see description of relief filters below). Mean annual precipitation varies between 800 and 950 mm and the mean annual temperature is 4.3 °C (Průša 1985). According to the last census carried out in 2008, the mean density of living trees with DBH ≥ 10 cm is about 226 per hectare, mean basal area 36.05 m^2/ha, and with mean volume 584.62 m^3/ha. The study site is composed mainly of European beech (*Fagus sylvatica L;* 65%.), Norway spruce (*Picea abies (L.) Karsten;* 33%) and an admixture of silver fir (*Abies alba Mill*.; less than 2%).

The Boubín forest (45.1 ha) has also been under strict protection since 1858. The altitude of the Boubín forest ranges from 930 to 1110 m, the mean slope is 15.5 ° and local altitudinal differences within 10 m radius are on average 5.5 m. The mean annual temperature is 4.0 °C. (Vrška *et al.* 2001). According to last census carried out in 2010, the mean stand density is about

204 living trees per hectare, mean basal area 41.39 m^2/ha, with mean volume 659.40 m^3/ha. Similarly as in the Žofín forest, the Boubín forest is composed mainly of European beech (54%.), Norway spruce (44%) and an admixture of silver fir (2%; as calculated according to tree counts).

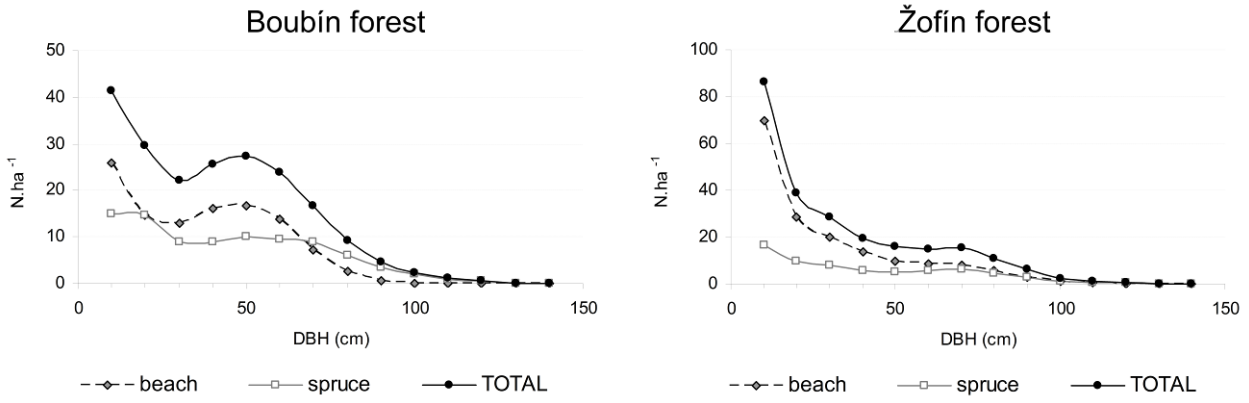

Figure 2: DBH distribution of living trees for the Boubín and Žofín study sites.

The DBH distributions of the study sites (Fig. 2) have reverse J-shaped (Žofín) or rotation sigmoid (Boubín) curves typical for European natural beech forests (Westphal *et al.* 2006). However, the stand structure of both sites is locally highly variable (Král *et al.* 2010a), formed by a fine-scale mosaic of patches in different phases of forest development, which implies that local DBH distributions can be right skewed, bell-shaped or bi-modal (Král *et al.* 2010b). Also, the understory varies locally with significant patches of natural regeneration occurring mostly in canopy gaps, while the presence of shrubs and tall herbs is quite scarce.

All standing and downed trees of a DBH ≥ 10 cm within the core areas of both study sites have previously been mapped by conventional field measurements using Field-Map technology (computer aided field data collection equipment composed of software, field computer, laser rangefinder, inclinometer and electronic compass and angle encoder – for details see www.fieldmap.cz, Pecheur *el al.* 2010). The resulting stem-position maps with linked databases were used as reference data for the LiDAR data assessment (the conventional stem mapping and TLS positionally aligned in decimetres, which was sufficient for comparing the presence/absence of individual trees in both datasets).

Within both study sites, four permanent plots were established in the 1970s as transects for detailed studies of temporal changes in vertical stand structure (Fig. 1). These plots were re-

measured in 2010 by TLS using the Optech ILRIS-3_6D laser scanner with an automated pan/tilt base mounted on a tripod. The scanner has a dynamic scanning range of 3–1,500 m for an 80% reflectivity target, 3–800 m for a 20% reflectivity target and 3–350 m for a 4% reflectivity target, with a positional accuracy of 8 mm at a distance of 100 m. Thanks to the automated pan/tilt base, the scanner can acquire data from -20 ° through 90 ° (zenith) x 360 ° with no loss of accuracy or functionality (Optech, 2009). The scans were acquired in early spring when the deciduous trees had no leaves and when the snow had already melted off. These conditions ensured the best possible visibility of stems. In the Žofín forest, one plot was scanned from 3 scanning positions and three plots were scanned using 4 scanning positions. In the Boubín forest, all four plots were scanned using 4 scanning positions (Fig. 1). The distance among scanning positions within plots varied from 20 to 110 m for scanning pairs, with the mean distance among four scans ranging from 40 to 85 m. The area fully scanned at one plot was on average about 1.2 ha. The scanning resolution (density) was set to 2 cm spacing for a 20 m distance from the scanner. Data acquired at each plot were consequently fitted together using artificial targets on a geodetically-measured grid (44 m per side) and cloud-to-cloud fitting using ICP algorithm, then registered in the S-JTSK Czech national coordinate system with a mean positional error varying between 6.5–9.8 cm for the Žofín plots and from 3.1–6.9 cm for the Boubín plots. For each scan a horizontal layer (slice) of points 120–140 cm explicitly above the derived terrain was created for recognition of the trees and their DBH.

In order to examine the effects of terrain on stem recognition explicitly, the roughness and morphology of the relief of both study sites was quantified by two focal filters at several spatial scales. The range filter calculates the difference between the largest and smallest value of DEM in a given neighbourhood. When normalized by filter diameter, the resulting values represent the average slope percentage at the scale of the filter extent. The slope shape filter (Kimball & Weihrauch 2000) estimates the convexity/concavity of terrain morphology from DEM. It is calculated by applying a pixel kernel that has -1 as the coefficient at the N,S,E and W borders of the kernel, 4 in the middle (the target pixel) and 0 everywhere else. The result is a raster layer in which negative values represent concave landforms (pits) and positive values represent convex landforms (mounds). If normalized by the number of directions used and the filter radius, the absolute values represent the average of the slope percentage from the target pixel in all examined directions at the distance of the filter radius employed (Kimball & Weihrauch 2000). In

other words, it also denotes the 'acuteness' of the given morphological relief form (Samonil *et al.* 2008). For both filters the 10 m radius seemed to be the most indicative of the relief roughness, and thus was used in subsequent statistical evaluations.

2.2. Stem identification and validation

Firstly, we observed what proportion of standing trees could be recognised from each of the scanning positions and how that recognition is affected by the distance from the scanner. Eight concentric circles were made at 5 m radius steps around each scanning position as follows: r_1 = 5 m, r_2 = 10 m, …., r_8 = 40 m. The circles formed seven 5 m lags (i.e., 5–10 m, … 35–40 m; see Table 1). The "zero" lag, 0–5 m is not included in the analyses because the ILRIS-3D registers the closest point at a distance of 3 m from the scanner. In these lags the trees recognised by visual interpretation from LiDAR data were counted and compared with the number of existing trees in the reference data (stem-position map measured by Field-Map). The stem interpretation was carried out on the top plan view with a sliced point cloud at a height of 120-140 cm above terrain. The tree stems thus appeared as full or partial rings. The presence of at least an approximate semicircle was set as the criteria for recognizing the presence of a tree stem. The ratio of recognised trees from the LiDAR data (N_L) to present trees in the reference data (N_R) for each lag was used as a measure of successful tree recognition (R) by LiDAR, i.e., $R_{\text{lag X}} = N_{L\,\text{lag X}} / N_{R\,\text{lag X}}$ (%); where *X* is the number of the lag. The 90% nonparametric bias-corrected and accelerated (Bca) confidence intervals based on 1000 bootstrap replications (Efron & Tibshirani, 1993) were constructed for mean values of LiDAR tree recognition for each lag and number of scanning positions.

For each of the seven study plots (grey areas in Fig. 1) scanned from 4 scanning positions, there are six unique scanning position pairs, four scanning position triplets and one tetrad of scanning positions. In the one study plot scanned from 3 scanning positions there are three scanning position pairs and one scanning position triplet. Therefore, the number of real observations *m* (the count of single scanning positions and all unique combinations of multiple scanning positions) varies according to the number of combined scanning positions within the study plots (Table 1).

Table 1: Number of real observations *m* (count of single scanning positions and unique combinations of multiple scanning positions) and appropriate sums of observed trees in the reference data for a given lag.

Lag	1 scan [m=31]	2 scans [m=45]	3 scans [m=29]	4 scans [m=7]
5-10	142	401	414	136
10-15	255	693	735	240
15-20	322	899	930	304
20-25	425	1152	1221	398
25-30	480	1316	1382	451
30-35	620	1670	1758	569
35-40	655	1785	1871	608

The increased recognition of trees using data from additional scanning positions depends on the distance between scanning positions. Scans which are too close together have similar viewing angles of the same trees, and scans too far apart sight at different trees. Therefore, to evaluate the effect of mutual scanning position spacing, we assessed the dependency of increased recognition on the distance between scanning positions whereby the mean distance of three or more scans was used). The increase of tree recognition (%) was determined by comparing the sum of the trees recognised separately from individual scans, to the number of trees recognised from merged scans.

2.3. Modelling tree stem visibility

The results of the two previous analyses were tested and extended by GIS modelling at the Boubín study site, selected because it has higher variability in terrain conditions. We simulated the visibility of tree stems from TLS positions with an estimated optimal distance and lay out. Based on the results of previous analysis (percentage of tree detection in point clouds depending on the distance and number of scans), a regular (squared) 40 m grid of scanning positions was

designed. If there was a spatial coincidence with a standing tree, the scanning position was shifted slightly (as would be the case in real field measurements). The Viewshed tool in the Spatial Analyst for ArcGIS 10 was used to determine the raster surface locations visible to a particular set of observer features. To determine the visibility of a target cell, each cell between the viewpoint cell and target cell was examined for line of sight. When there were cells of higher value between the viewpoint and the target cells, this meant that the line of sight was blocked, in which case the target cell was determined not to be part of the viewshed. If line of sight was not blocked then this cell was included in the viewshed (Kim *et al.*, 2004).

For the modelling, the stem-position map (trees of DBH ≥10 cm) from conventional field measurements and a digital elevation model were used, and is thus based on an existing actual dataset. The 296 simulated scanning positions and more than 11,000 standing trees in the reference data were entered into the analysis. The height of the observation towers (representing TLS sensors) was set at 1.8 m and the maximal visible range from one scanning position set at 100 m. For the purpose of visibility modelling, the stems were represented by cylinders of width equal to the DBH. For the final tree visibility assessment, the perimeter of each stem was divided in ArcGis by default into 37 points. Values of the visibility raster resulting from the viewshed analysis were extracted into these points and thus the ratio of the visible and non-visible parts of the perimeter of each tree was calculated. In order to augment the portability of the results to other sites, quantitative measures of the stand structure and local relief conditions were compared to corresponding visibility rates. All visibility models were created with a 5 cm spatial resolution.

Initially, the effect of relief was neglected (a plane was used) so that the results only represented the net shading of stems with a DBH ≥ 10 cm. The influence of the stand variables local number of trees, number of mature trees, volume of biomass and basal area (BA) of standing trees was tested on a 40 m grid defined by the scanner positions located at the corners of the grid. The mean visibility of stems within a grid cell was correlated with the local hectare-based variables for that cell. The Pearson's correlation coefficient and coefficient of determination were calculated. This comparison was repeated on an 80 m grid (cells of the 40 m grid were grouped by 4) in order to test the effect on a coarser scale.

A subsequent analysis took into account the pure shading effect of the terrain only. The detailed digital elevation model (DEM) of the Boubín forest used was interpolated from the *Z* values of

tree coordinates of the stem map that provides a dense point set of known coordinates (average nearest neighbour distance is about 3.3 m). The rasters resulting from the normalized terrain morphology filters applied to the DEM were divided into 5 relative intervals from lowest to highest according to the distributions of their values. The values of the range filter were split into the following categories: very low (values less than 20), low (20-25), medium (25-31), high (31-40) and very high (above 40), representing the relative classes of increasing local terrain differences. The values of the shape filter were split into their relative classes representing the local relief shapes as follows: deep pits (values less than -4), moderate pits (from -4 to -1), planes (from -1 to 1), moderate mounds (from 1 to 4) and high mounds (above 4). The modelled visibility of the ground was sampled in a 5 m point grid and separated into each of the defined relief morphology classes. The differences in visibility were tested by one-factorial ANOVA and Tukey's Honestly Significant Differences Test for significant differences in all pair-wise comparisons. Finally, the composed (real) shading effect of relief and stems for the whole study site was quantified.

3. RESULTS

3.1. Distance from the scanner

Figure 3 shows the percentage of successfully recognised trees in a given distance interval (lag) from the scanner, using mean values and a BCa 90% confidence interval. Single scans only have a recognition rate above 80% for up to 15 m from the scanner. At further distances from the scanner (35-40 m away), recognition rapidly and almost linearly decreases to 40–50%. It is apparent that multiple scanning positions significantly improve the percentage of recognised trees, especially at greater distances from the scanner. By employing at least two scanning positions, 80% of trees are still recognised at 15–20 m. By using at least three scans, there is a comparable recognition rate of approximately 80% at 20–25 m and greater. Similarly, with the use of at least three scans, 65% of trees are recognised at 35–40 m.

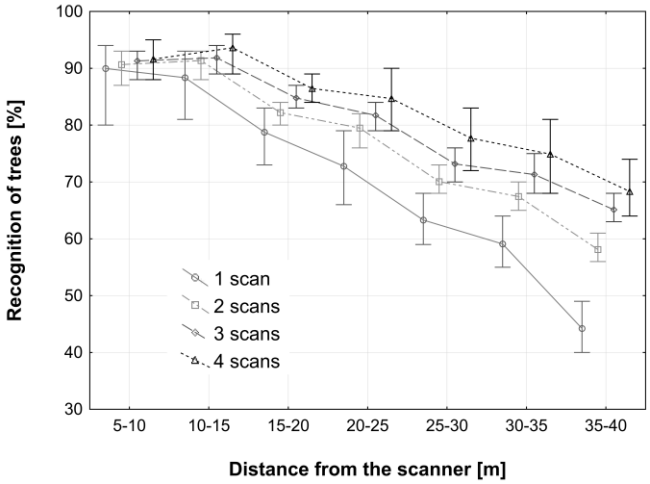

Figure 3: Successfully recognized trees according to the number of scans divided into lags (distance from the scanner). Points – bootstrap mean values; whiskers – bootstrap 90% confidence interval.

3.2. Distances among scanners

Not only does the number of scanning positions significantly affect successful tree recognition, but the distance between them also has great importance. Figure 4 shows the relative impact of an additional scan at a given distance on tree recognition. The increase in tree recognition (which we also call a 'synergic effect') was defined as the percentage increase of the number of recognised trees in merged multiple scans, compared with the number of recognised trees in separated scans. A statistically significant relationship was found for scanning pairs only; the synergic effect markedly decreased with increasing distance ($p < 0.001$). The highest increase in tree recognition (about 20%) was detected for inter-scanner distances of about 40 m, while the lowest (insignificant) increase was at distances above 110 m. The triplets and tetrads of scanning positions exhibit no significant relationship between the synergic effect and inter-scanner distance.

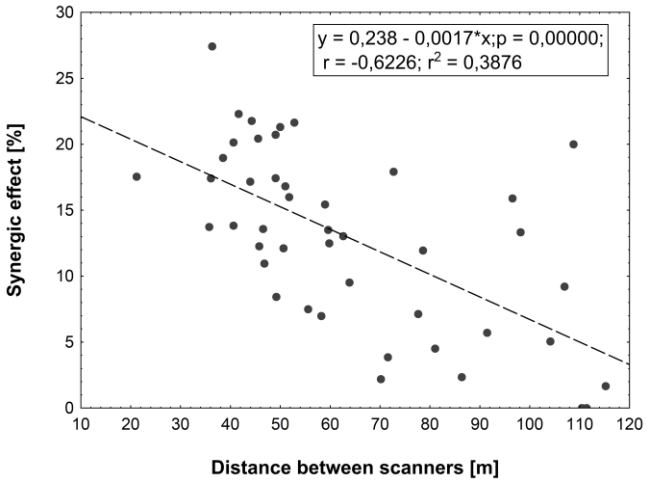

Figure 4: The increase of tree recognition (%) merging two scans in relation to the inter-scanner distance.

3.3. Visibility modeling

GIS modelling of tree visibility for the whole Boubín forest (45.1 ha) was carried out using a 40 m regular grid of scanning positions. Such spacing should, according to the previous analysis, ensure at least 80% success in tree recognition (i.e. trees were well visible).

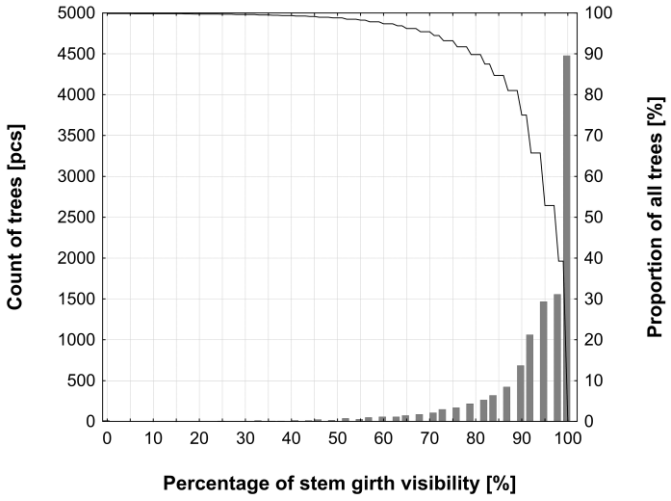

Figure 5: Modelled visibility of standing trees (DBH ≥ 10 cm) in Boubín from 296 regularly spaced scanning positions arranged in a 40 m square grid; the shading effect of relief was neglected. Grey bars – the tree counts (left axis); black line – the cumulative cumulative (from right to left) percentage of all standing trees (right axis).

When the shading effect of relief was not taken into account (i.e. a plane was used), 98.8% of all trees were demonstrated as having at least 50% of the stem perimeter visible (Fig. 5). Almost 4500 trees (i.e., 40%) were completely visible, and out of the 132 potentially unrecognisable trees (those exhibiting less than 50% of the stem perimeter) only 16 trees were completely undetected.

No significant effect of all tested stand variables on the local visibility of trees was detected in the 40 m or the 80 m grids. The local tree density, basal area, volume and density of mature trees were not correlated with the proportion of well-visible trees, which in all grid cells always exceeded 98% detection.

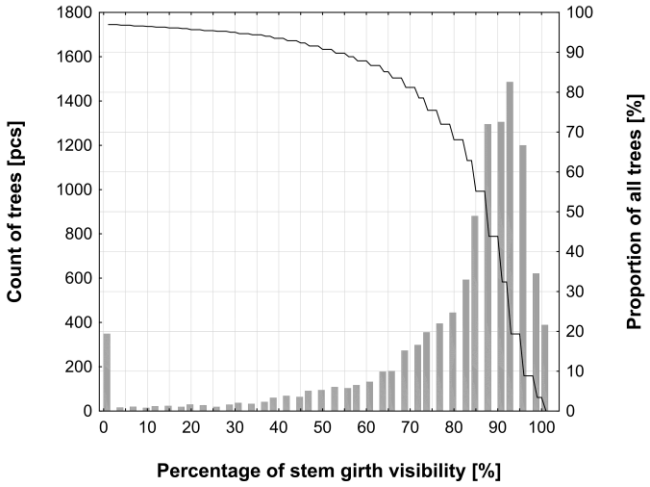

Figure 6: Modelled visibility of all trees in Boubín from 296 regularly spaced scanning positions arranged in a 40 m square grid; combined shading effect of stems and relief (real conditions). Grey bars – the tree counts (left axis); black line – the cumulative

When the shading effects of stems and terrain were combined, a total of 90.7% of standing trees were shown to have at least 50% of the stem perimeter visible (Fig.6). Only 3.4% of stems were completely visible and of the 1048 potentially unrecognised trees, only the 3% were completely undetected. The frequency of undetected trees seems generally to decrease slightly with increasing DBH class, mainly due to the proportion of completely missed trees (Fig. 7).

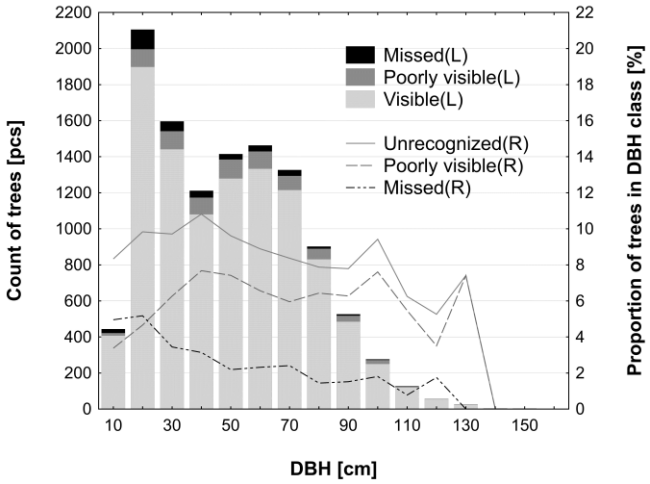

Figure 7: Proportion of potentially unrecognized trees in visibility modelling across 10 cm DBH classes; combined shading effect of stems and relief. Unrecognised trees are divided into missing (all of the stem perimeter is in shadow) and poorly visible (less than 50% of the stem perimeter is visible). Bars refer to the number of trees in a given DBH class (left axis); the lines refer to the percentage of poorly visible and missing trees (right axis).

We also compared the pure shading effect of stems, terrain and their combination by comparing the number of scanners targeting the forest ground (see Fig. 8). In the Boubín forest the stems have a smaller shading effect in comparison with bare terrain. Although some parts of the site were targeted maximally by 'only' 14 scanners, there was only 0.01 ha of pure shadow (i.e. places not covered by any scanner) and all points within the site were on average detected by 6.1 scanners. The shading effect of terrain is more variable, although the mean scanner coverage is comparable (i.e. average point detection by 5.9 scanners). The coverage ranges from 0 (on 0.84 ha) up to 19 scanners. Thus, the pure shadow is much higher even though the maximum scanner coverage is also higher. The combined shadow of stems and terrain cover ca. 2.3 ha, which is about 5% of the study site. On average, the entire site in this case, is covered by 3.2 scanners.

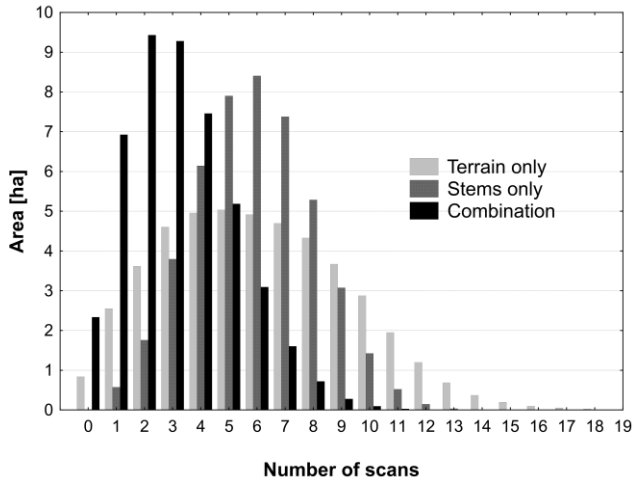

Figure 8: Number of scanners targeting forest ground in the visibility model when the effect of occlusion of terrain, stems and their combination is applied.

The pure shading effect of terrain was further analysed using the quantitative measures of local relief conditions. Following significant ANOVA results, post-hoc Tukey tests revealed significant differences between the mean values of visibility among most classes of local terrain differences and all local relief shapes. As expected, increasing local terrain differences gradually decrease the mean number of scanners targeting the forest ground from about 7.5 scanners to less than 5 scanners (Fig. 9a). They also increase the proportion of pure shadow from 0.4% to 5% (Table 2). The effect of local relief shape is a bit different (Fig. 9b). In particular, the presence of pits especially points to a decrease in the mean visibility of the ground from about 7 scanners on planes and mounds to less than 2.5 in deep pits. Also, the proportion of pure shadow in deep pits was markedly higher (12.2%) in comparison to all other relief shapes (less than 1% of pure shadow).

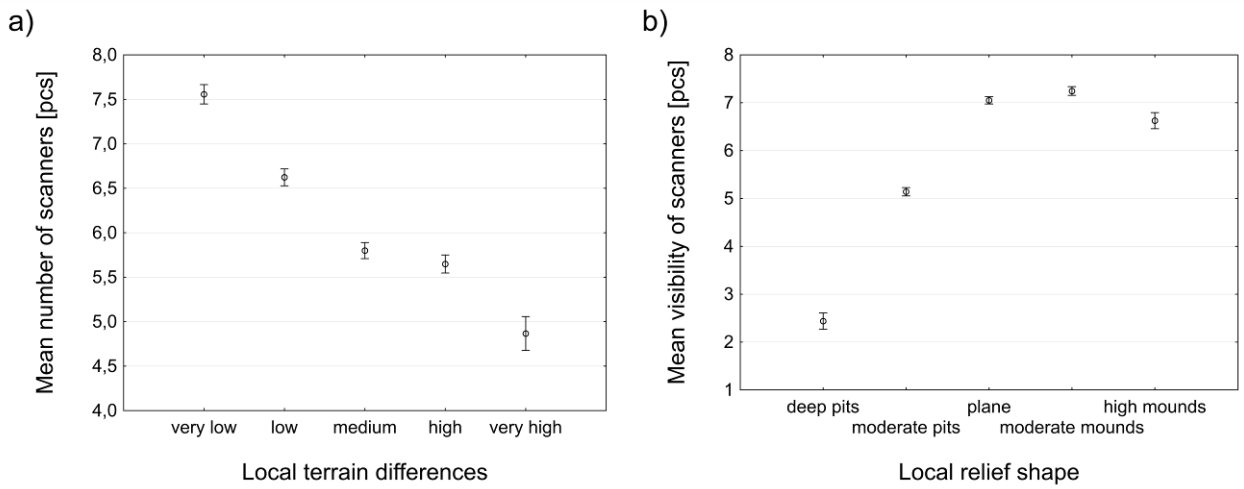

Figure 9: The mean number of scanners targeting forest ground depending on a) local terrain differences and b) the local relief shapes.

Table 2: Proportion of pure shadow (i.e. no scanner is targeting the ground) depending on local terrain differences and relief shapes.

Local terrain differences				
very low	low	medium;	high	very high
0,4%	0,8%	1,3%	1,6%	5,0%
Local relief shapes				
deep pits	moderate pits	plane	moderate mounds	high mounds
12,2%	1,0%	0,4%	0,2%	0,3%

4. DISCUSSION

Using TLS in natural forests poses various complications due to complex stand structures such as shadows behind trees, heterogeneous tree density and the distribution of stems and branches in space, as well as due to relief morphology. All of these aspects affect the successful recognition of trees.

4.1. Distance from the scanner

The main relationship observed is simple and unsurprising; the closer a tree is to the scanner, the better its recognition (see Fig. 3). This better recognition at close ranges is most likely due to less shadowing. The scanning resolution at these distances is still sufficient and therefore not as critical. The only exception is the ‘zero lag’ (0–5 m), where the tree capture is reduced because of the 3 m minimum scanning range of the ILRIS 3D scanner. Therefore, this lag was not included in the analysis. This effect can be eliminated using alternative scanning devices with a lower minimum range (e.g. a ScanStation C10 with a minimum range of 0.1 m).

The second relationship observed was also predictable; the more scanners that target an area the better the rate of tree recognition in the area. As in the first case, the benefit of this analysis is the explicit quantification of the expected relationship of the number as well as the distance of the scanners to the rate of recognition. The acceptable resolution rate (above 80%) employing four scanning positions is achieved at distances shorter than 25 m. These results were taken into consideration in designing the visibility analysis.

The higher observed variance (and wider confidence interval) for one scanning position can be explained by the specific spatial arrangement of trees and their shadows around a single scanner. The use of additional scanning positions reduced the effect of the unique spatial arrangement of trees, thereby resulting in a narrower confidence interval. The wider confidence interval of a tree recognition rate for cases when four scanning positions are combined is the result of the low number of real observations (only 7 tetrads of scans entered the bootstrap – see Table 1).

The question still remains as to the additive effect of further and more distant scanning positions. By using the proposed 40 m grid of scanning positions and realistic effective range of 100 m, one place, in theory, can be targeted by up to 21 scans. Under real conditions some places were visible by 11 scanners (see Fig. 8). Supposing that all the partial point clouds are aligned properly, then further improvement in tree recognition is anticipated, as supported by the results of visibility modelling (see below).

4.2. Distance between scanners

The mutual spatial arrangement and spacing of scanning positions is another important aspect of effective wide-scale TLS of stand structure. Adjacent scanning positions mutually complement each other and therefore only partially captured trees in individual scans can be recognised when individual point clouds are merged. Consequently, the number of recognised trees in merged multiple scans is higher when compared with the number of successfully recognised trees in identical scans that are analysed separately, creating a kind of 'synergic effect' (see Fig. 4).

However, scanning positions that are too close together have similar viewing angles of the same trees and therefore do not complement each other in the detection of the cylindrical shape of a stem that is necessary for successful recognition. Scanning positions that are too far apart detect different trees rather than cross-recognising common trees from different viewing angles. The synergic effect of multiple scanning positions is in both cases low, although for different reasons. Naturally, there is some optimal range of scanner spacing where adjacent scans effectively mutually complement each other. Theoretically, for the full range of possible inter-scanner distances, the synergic effect should exhibit a 'bell-shaped' curve. Instead however, in Fig. 4, a linear decreasing trend is observed for scan pairs. One can conclude that the tested inter-scanner distances are behind the peak of the theoretically expected bell-shaped curve. In other words, the spacing of the scanners (21–115 m) was probably always within a reasonable range, and unreasonably close scanning positions were not used during the field measurements and therefore are missing from the chart. It would appear that the inter-scanner spacing of about 40 m shows evidence of the highest synergic effect.

In the case of 3 and 4 scans, no significant relationship was observed between their spacing (distance) and the synergic effect. This may be attributable to the fact that the mean distance among multiple scanners was used, which most likely weakened any observable dependence.

4.3. Visibility simulation

The spacing of scanning positions for the visibility analysis was designed to match the results of the preceding analyses. Thus, a 40 m square grid of scanning positions was tested, ensuring that

each part of the grid can theoretically be targeted from the 4 closest scanning positions with a maximum nearest distance of 28.3 m as well as by up to 17 additional surrounding positions within the 100 m visible range. Moreover, the regular distribution of scanning positions to some extent reduces the variability of point cloud density caused by the variable distance of scanned objects from the scanner. Considering the angular nature of laser scanner resolution and the actual scanning resolution used in the field (0.01 rad), the reasonable scanning range was probably less than that which was actually used (i.e., 10 cm point density at 100 m). In contrast, the physical range of the scanner was actually much higher (in our case ca. 800 m for a 20% reflectivity target). As the reasonable (effective) scanning range can be adjusted to some extent by adjusting the scanning resolution, the 100 m distance was ultimately setup as the maximal visible range for the viewshed analysis, which is also in accordance with the assumed acquisition range of TLS in a forest environment (Hopkinson *et al.* 2004; Jupp *et al.* 2009; van Leeuwen *et al.* 2011).

The visibility modelling assessed the real viewing conditions and real shading effect of standing stems and terrain of the Boubín study site (45 ha). The interpretation of the analysis, however, should be cautious. The visibility of particular objects is essential but not a sufficient condition of valid object detection. Strictly speaking, the fact that a tree is visible from a scanning position does not necessarily mean that it will be correctly recognised in the point cloud, which may potentially be attributable to insufficient point density or to the detection of only a small part of the stem perimeter. Therefore, only trees with at least half the stem perimeter visible were likely to be recognised. In these cases, the DBH can be measured directly, although it could also be determined by fitting a circle to a smaller part of the stem perimeter (e.g. Aschoff, 2004).

When the net shading effect of tree stems was assessed by approximating the terrain as a plane, nearly 99% of all trees were likely to be recognised (Fig. 5). Only 132 of the stems were missed throughout the whole study site. The percentage of directly visible trees was not dependant on the local stand variables tested (tree density, BA and volume). The arrangement of scanners in a 40 m grid on a planar surface is probably dense enough to eliminate most of the tree shadows if a visibility range of 100 m is applied (i.e. if a shorter scanning range had been simulated this relation would more likely have been detected). In the case of the real composed shading effect of relief and stems, about 90% of trees were still likely to be recognised (Fig.6). Comparing the area

of pure shadow, the effect of occlusion for relief was 50 times higher than the effect of occlusion for stems (Fig. 8). The variation in relief thus proved to be a very important aspect of visibility. Although this aspect is unique for each study site, such results indicate that TLS spacing could be sparser in flat forests (depending on the presence and density of the understory). Interestingly, the total effect of occlusion was more than 3 times higher than the sum of the separate shadows of stems and terrain. While the shading effect of stems is more uniform throughout the study area, the relief exhibits places of both poor visibility (particularly with the occurrence of pits) and excellent visibility, though occasionally high levels of visibility may be obscured by stems when both effects are combined. The overall estimated recognition rate resulting from the visibility analysis is about 10% higher compared with the results of point cloud interpretation (Fig. 3). This can be attributed to the additive effect of further scanning positions (up to 17 additional surrounding scanning positions within the 100 m range used), and to the fact that visibility modelling only takes into account the shading effect of terrain and tree stems above 10 cm DBH, while in real conditions there are other objects that might also reduce visibility.

In terms of applicability, we should therefore bear in mind that other shading effects (e.g. the presence of lying deadwood), as well as that of areas of dense natural regeneration of trees under the 10 cm DBH threshold are not included in the analysis. In any case, visibility modelling appears to be a useful tool for planning extensive TLS measurements in forest ecosystems. If existing data of the study site is available, such as a DEM and/or an old stem-position map, one could predict the minimal spacing of scanner positions to cover a particular study site (e.g., Figs. 6 and 7). This could be accomplished in a relatively short period of time (it took us 25 hours for a visibility analysis of 45 ha). Performing an iterative visibility analysis in terms of changing scanner spacing, the optimal spatial arrangement of scanning positions for a particular site can be estimated prior to commencing field work. Moreover, the effects of terrain occlusion and tree stems can be isolated and quantified depending on the local terrain and forest stand conditions. Keeping the prescribed 40 m scanner spacing and 100 m visibility range, site visibility might be quickly and easily approximated from ancillary data using above described relations (Fig. 9, Table 2). As the local stand variables do not significantly change the proportion of well-visible trees in the model, a quick approximation can be performed with only the site's DEM.

5. CONCLUSIONS

Due to the peculiarities of both field measurement approaches, TLS methodology and conventional (Field-Map, Peucheur *et al.* 2010) stem mapping are not directly comparable. In the case of traditional stem mapping, much of the interpretation work is carried out in the field, whereas TLS field measurements only produce huge amounts of raw data. Keeping these differences in mind, it is not surprising that the TLS field work in itself is far less labour-intensive and faster than conventional stem mapping. For example, the Boubín study site was measured in 155 field days by a group of 3 people using Field-Map devices (www.fieldmap.cz). The TLS measurement could be done in 888 hours (111 days with 8 hour shifts) using the ILRIS 3_6D and 296 scanning positions. These estimates assume that the net scanning time of one hemisphere can be calculated in about 2 hours plus about 1 additional hour necessary to transfer among scanning positions, and for the adjustment of scanners and the supporting tripod, etc.). Similarly, this could be performed in 43 days by a device with a higher scanning frequency (e.g., the ScanStation C10 with which the net scanning time of one hemisphere can be performed in ca. 10 minutes using the same scanning resolution).

In the case of using conventional field measurement techniques, the stem map is ready to use almost instantly after the fieldwork. In contrast, massive data processing must be performed after TLS measurements. This includes the fitting and merging or aligning of individual point clouds, registering in the particular coordinate system, and particularly point cloud segmentation with backward field verification. The point clouds, on the other hand, include much more information than necessary for simple stem-position mapping, especially for the canopy layer. The data can be used for precise DEM and DSM (digital surface model) or DCM (digital canopy model) extraction, gap fraction estimates of the whole study site, detailed descriptions and quantification of stand structure including suppressed trees and sub-canopy regeneration, measurement of the majority of individual tree heights, etc. (see van Leeuwen & Nieuwenhuis 2010). As forest dynamics should be regarded as a three-dimensional process (Falkowski *et al.* 2009), the above analyses could significantly improve our understanding of the underlying developmental and analytical processes.

It is unlikely that potential of TLS data would be fully exploited on extensive areas by manual interpretation, as it would be too labour-intensive and too costly to carry out. The LiDAR point cloud data do offer the potential for automated tree identification and counting and location estimation (van Leeuwen *et al.* 2011) but in forest areas other than uniform single-tier plantations this process would require some kind of sophisticated feature recognition and extraction process (Hopkinson *et al.* 2004). This being the case, there is a need for researchers to develop point cloud processing algorithms for automatic object recognition, classification and measurements. The successful incorporation of these algorithms in a processing chain could significantly enhance the speed and efficiency of point cloud 'data mining'. However, a thorough labour-consumption analysis of the complete processing chain of the stem mapping has yet to be undertaken. It would seem that the greatest advantage of TLS will be in the multiple utilisations of point clouds for a range of analyses, rather than in expediting the implementation of fast and easy stem mapping alone.

6. ACKNOWLEDGEMENTS

Thanks to GeoVAP Ltd. for LiDAR data acquisition and preprocessing. The research was supported by the Czech Science Foundation, project No.P504/10/2018 and, by IGA foundation of Mendel University in Brno, project No. 5/2011.

7. REFERENCES

Aschoff,T., Spiecker,H., 2004. Algorithms for the automatic detection of trees in laser scanner data. International Archives of Photogrammetry, Remote Sensing and Spatial Information Sciences 36, W2.

Bienert,A., Scheller,S., Keane,E., Mohan,F., Nugent,C., 2007. Tree detection and diameter estimations by analysis of forest terrestrial laserscanner point clouds. ISPRS Workshop on Laser Scanning 2007, 50-55. 2007.
Ref Type: Conference Proceeding

Bienert,A., Scheller,S., Keane,E., Mullooly,G., Mohan,F., 2006. Application of terrestrial laser scanners for the determination of forest inventory parameters. International Archives of Photogrammetry, Remote Sensing and Spatial Information Sciences 36.

Brolly,G., Kiraly,G., 2009. Algorithms for stem mapping by means of terrestrial laser scanning. Acta. Silva. Lign. Hung. 5, 119-130.

Chen,Q., Baldocchi,D., Gong,P., Kelly,M., 2006. Isolating individual trees in a savanna woodland using small footprint lidar data. Photogrammetric Engineering and Remote Sensing 72, 923-932.

Clawges,R., Vierling,L., Calhoon,M., Toomey,M., 2007. Use of a ground-based scanning lidar for estimation of biophysical properties of western larch (Larix occidentalis). International Journal of Remote Sensing 28, 4331-4344.

Côté,J.F., Fournier,R.A., Egli,R., 2011. An architectural model of trees to estimate forest structural attributes using terrestrial LiDAR. Environmental Modelling & Software 26, 761-777.

Côté,J.F., Widlowski,J.L., Fournier,R.A., Verstraete,M.M., 2009. The structural and radiative consistency of three-dimensional tree reconstructions from terrestrial lidar. Remote Sensing of Environment 113, 1067-1081.

Dassot,M., Constant,T., Fournier,M., 2011. The use of terrestrial LiDAR technology in forest science: application fields, benefits and challenges. Annals of Forest Science 68 (5), 959-974.

Efron, B. and Tibshirani, R.1993. An introduction to the bootstrap. Chapman & Hall.

Falkowski,M.J., Evans,J.S., Martinuzzi,S., Gessler,P.E., Hudak,A.T., 2009. Characterizing forest succession with lidar data: An evaluation for the Inland Northwest, USA. Remote Sensing of Environment 113, 946-956.

Fleck,S., Obertreiber,N., Schmidt,I., Brauns,M., Jungkunst,H.F., Leuschner,C., 2007. Terrestrial LiDAR measurements for analysing canopy structure in an old-growth forest. International Archives of the Photogrammetry, Remote Sensing and Spatial Information Sciences.XXXVI. , Part 3, W52.

García,M., Danson,F.M., Riaño,D., Chuvieco,E., Ramirez,F.A., Bandugula,V., 2011. Terrestrial laser scanning to estimate plot-level forest canopy fuel properties. International Journal of Applied Earth Observation and Geoinformation. 13, 636-645.

Heurich,M., 2008. Automatic recognition and measurement of single trees based on data from airborne laser scanning over the richly structured natural forests of the Bavarian Forest National Park. Forest Ecology and Management 255, 2416-2433.

Hill,R.A., Broughton,R.K., 2009. Mapping the understorey of deciduous woodland from leaf-on and leaf-off airborne LiDAR data: A case study in lowland Britain. ISPRS Journal of Photogrammetry and Remote Sensing 64, 223-233.

Hopkinson,C., Chasmer,L., Young-Pow,C., Treitz,P., 2004. Assessing forest metrics with a ground-based scanning lidar. Canadian Journal of Forest Research 34, 573-583.

Huang,H., Gong,P., Cheng,X., Clinton,N., Cao,C., Ni,W., Li,Z., Wang,L., 2008. Forest structural parameter extraction using terrestrial LiDAR. AGU.Fall.Meeting.Abstracts 1, 0726. 2008.
Ref Type: Conference Proceeding

Janik,D., Adam,D., Vrška,T., Hort,L., Unar,P., Král,K., Šamonil,P., Horal,D., 2011. Field maple and hornbeam populations along a 4-m elevation gradient in an alluvial forest. European Journal of Forest Research 130, 197-208.

Jupp,D.L.B., Culvenor,D.S., Lovell,J.L., Newnham,G.J., Strahler,A.H., Woodcock,C.E., 2009. Estimating forest LAI profiles and structural parameters using a ground-based laser called Echidna. Tree physiology 29, 171-181.

Kim,Y., Rana,S., Wise,S., 2004. Exploring Multiple Viewshed Analysis Using Terrain Features and Optimisation Techniques. Computers and Geosciences, 30(9), 1019.

Kim,S., McGaughey,R.J., Andersen,H.E., Schreuder,G., 2009. Tree species differentiation using intensity data derived from leaf-on and leaf-off airborne laser scanner data. Remote Sensing of Environment 113, 1575-1586.

Kimball,K.D., Weihrauch.D., 2000. Alpine vegetation communities and the alpine treeline ecotone boundary in New England as biomonitors for climate change. USDA Forest Service Proceedings 3, 93–101.

Király,G., Brolly,G., 2007. Tree height estimation methods for terrestrial laser scanning in a forest reserve. Proceedings of the ISPRS Workshop Laser.Scanning, 12-14. 2007.
Ref Type: Conference Proceeding

Král,K., Janík,D., Vrška,T., Adam,D., Hort,L., Unar,P., Šamonil,P., 2010a. Local variability of stand structural features in beech dominated natural forests of Central Europe: Implications for sampling. Forest Ecology and Management 260, 2196-2203.

Král,K., Vrška,T., Hort,L., Adam,D., Šamonil,P., 2010b. Developmental phases in a temperate natural spruce-fir-beech forest: determination by a supervised classification method. European Journal of Forest Research 129, 339-351.

Kraus,K., Pfeifer,N., 1998. Determination of terrain models in wooded areas with airborne laser scanner data. ISPRS Journal of Photogrammetry and Remote Sensing 53, 193-203.

Lefsky,M., McHale,M.R., 2008. Volume estimates of trees with complex architecture from terrestrial laser scanning. Journal of Applied Remote Sensing 2, 023521.

Maas,H.G., Bienert,A., Scheller,S., Keane,E., 2008. Automatic forest inventory parameter determination from terrestrial laser scanner data. International Journal of Remote Sensing 29, 1579-1593.

Naesset,E., 1997. Determination of mean tree height of forest stands using airborne laser scanner data. ISPRS Journal of Photogrammetry and Remote Sensing 52, 49-56.

Optech, 2009. ILRIS summary specification sheet [online]. Available from http://optech.ca/pdf/ILRIS_SpecSheet_110309_Web.pdf [accessed 30 October 2012].

Parker,G.G., Russ,M.E., 2004. The canopy surface and stand development: assessing forest canopy structure and complexity with near-surface altimetry. Forest Ecology and Management 189, 307-315.

Pecheur, A.L., Bartoli, M., Müller, P., 2010. Field-Map, un outil de terrain pour estimer les peuplements forestiers. La foret privée n°315:42-46.

Popescu,S.C., 2007. Estimating biomass of individual pine trees using airborne lidar. Biomass and Bioenergy 31, 646-655.

Průša, E.1985. Die bohmischen und mährischen Urwälder-ihrer Struktur und Őkologie. Academia.

Rutzinger,M., Pratihast,A.K., Oude Elberink,S., Vosselman,G., 2010. Detection and modelling of 3D trees from mobile laser scanning data. International Archives of Photogrammetry, Remote Sensing and Spatial information Sciences 38, 520-525.

Šamonil,P., Král,K., Douda,J., Šebková,B., 2008. Variability in forest floor at different spatial scales in a natural forest in the Carpathians: effect of windthrows and mesorelief. Canadian Journal of forest research 38, 2596–2606.

Šebková,B., Šamonil,P., Janík,D., Adam,D., Král,K., Vrška,T., Hort,L., Unar,P., 2011. Spatial and volume patterns of an unmanaged submontane mixed forest in Central Europe: 160 years of spontaneous dynamics. Forest Ecology and Management 262, 873-885.

van Leeuwen,M., Hilker,T., Coops,N.C., Frazer,G., Wulder,M.A., Newnham,G.J., Culvenor,D.S., 2011. Assessment of standing wood and fiber quality using ground and airborne laser scanning: A review. Forest Ecology and Management 261, 1467-1478.

van Leeuwen,M., Nieuwenhuis,M., 2010. Retrieval of forest structural parameters using LiDAR remote sensing. European Journal of Forest Research 129, 749-770.

Vosselman, G. and Maas, H. G.2010. Airborne and Terrestrial Laser Scanning. Taylor & Francis.

Vrška,T., Hort,L., Odehnalova,P., Horal,D., Adam,D., 2001. The Boubin virgin forest after 24 years (1972-1996)development of tree layer. Journal of Forest Science 47, 439-460.

Westphal,Ch., Tremer,N., von Oheimb,G., Hansen,J., von Gadow,K., Härdtle,W., 2006. Is the reverse J-shaped diameter distribution universally applicable in European virgin beech forests?. Forest Ecology and Management 223, 75-83.

PAPER II

3D Forest: an application for descriptions of three-dimensional forest structures using terrestrial LiDAR

Jan Trochta[a] *, Martin Krůček[a,b], Tomáš Vrška[a], Kamil Král[a]

[a] *The Silva Tarouca Research Institute, Department of Forest Ecology, Lidicka, Brno Czech Republic;*

[b] *Mendel University in Brno, Faculty of Forestry and Wood Technology, Department of Geoinformation Technologies, Zemedelska , Brno Czech Republic*

Abstract

Terrestrial laser scanning (TLS) is a powerful technology for capturing the three-dimensional structure of forests with a high level of detail and accuracy. Over the last decade many algorithms have been developed to extract various tree parameters from TLS data.

Here we present 3D Forest, an open-source non platform specific software application with an easy-to-use GUI with compilation of algorithms focused on forest environment and tree parameters extraction. The current version (0.4) extracts important parameters of forest structure from TLS data, such as stem positions (*X*, *Y*, *Z*), tree heights, diameters at breast height (DBH), as well as more advanced parameters such as tree planar projections, stem profiles or detailed crown parameters including convex and concave crown surface and volume. Moreover, 3D Forest provides quantitative measures of between-crown interactions and their real arrangement in 3D space. We present new method of automatic tree segmentation algorithm and crown segmentation. Comparison with field data measurement show no significant difference in measuring DBH or tree height using 3D forest.

1. INTRODUCTION

Big part of forest ecosystem research is based on spatially oriented data. Research on forest dynamics commonly makes use of large census plots, where the position and size of every tree individual is measured and recorded (Anderson-Teixeira *et al.*, 2014). These observations are fundamentally two-dimensional, trees being represented as points with X, Y coordinates of the tree base and other parameters (e.g. species, DBH, height) only recorded in a database. However, forests are intrinsically three-dimensional systems. Canopy disturbances, tree regeneration, tree growth and competition (especially aboveground competition for light) all take place in real space and time. These processes cannot be explicitly represented in two-dimensional forest plots.

The technology of terrestrial laser scanning (TLS) undoubtedly has the potential to change this state of affairs and bring real 3D insights to research in forest ecology and dynamics. It has great promise for collecting spatial information in forests because of its excellent measurement precision, short acquisition time, and level of detail (van Leeuwen and Nieuwenhuis, 2010). TLS is capable of acquiring levels of detail far beyond the capabilities of airborne laser scanning (Côté *et al.*, 2012; Hackenberg *et al.*, 2014), and thus may be used to describe forest stand vegetation at the level of individual trees including juvenile sub-canopy trees (Seidel *et al.*, 2011a).

The output of TLS data preprocessing are registered and aligned point clouds with millions of points oriented in 3D space with millimeter accuracy. This specific data format requires specific methods of processing. Due to the extensive amounts of data and their high information potential, the automated processing of TLS point clouds is of crucial importance. Numerous algorithms have been introduced during past decade(s), with early studies focusing on basic tree parameters such as tree height, DBH and position (Maas *et al.*, 2008) and recent works dealing with more advanced issues such as crown shape and dimensions (Metz *et al.*, 2013), light propagation in forest gaps (Seidel *et al.*, 2015) and individual-specific estimates of woody biomass (Calders *et al.*, 2015). The recent development of several applications for extraction of various tree parameters from TLS point clouds (e.g. SimpleTree (Hackenberg *et al.*, 2015), CompuTree (Piboule *et al.*, 2015), Liforest (True Reality Geospatial Solutions, 2015) or AutoStem (TreeMetrics, 2015)) prove that using TLS has great potential to help foresters and forest researcher in detailed tree parametrization.

Therefore, we introduce 3D Forest, a software application for describing forest 3D structure based on tree parameters. The application is not platform-specific, and has an easy-to-use graphical interface also suitable for non-experts in TLS data processing. It provides a free, open-source solution for computing the following tree parameters: tree base position, DBH, tree height, stem curve, tree planar projection and crown parameters like: crown centroid, crown base, height, crown volume and surface using convex hull or concave hull or volume of crown intersection. It also produces a detailed DTM of the study plot.

In the following sections, we introduce the algorithms employed for extraction of terrain and individual tree parameters, briefly describe the workflow in 3D Forest and present a comparison of two principal TLS derived tree parameters with conventional field measurements. We conclude by describing current and future developments to be incorporated in future versions of 3D Forest with relation to the forest dynamics.

2. 3D FOREST WORKFLOW

To better demonstrate the workflow of 3D Forest and its outputs, we present an example of TLS data processing using a subplot (2.4 ha) of a larger study site known as the Velká Pleš Forest Dynamics Plot (VPFDP) (Fig. 1).

Prior to importing to 3D Forest, the data scanned from multiple scanner positions are fitted and registered in the proprietary software usually provided with the ground-based laser scanner. 3D Forest can import data in the following formats: txt, xyz, pcd, pts, ptx and las. For version 0.4 only data with X, Y, Z and Intensity fields can be imported. In the 3D Forest workflow, the imported point cloud prior to any segmentation is called the Base cloud (Fig. 1a).

The Base cloud is then separated into two parts: i) the points representing the terrain surface, i.e. the Terrain cloud; and ii) all other points, which in forests usually represent vegetation and therefore called the Vegetation cloud (Fig. 1b).

The next step is segmentation of the Vegetation cloud into individual trees – i.e. Tree clouds (Fig. 1c). This is done automatically by the above described algorithm (section 2.2.) with possible manual adjustment.

Individual Tree clouds are the subject of further automatic processing. Tree and crown parameters can be extracted, e.g. tree base position with DBH and tree height (Fig 1d) and/or crown surface, volume and other crown parameters can be estimated (Fig. 1e). Between-crown interactions can be quantified by crown concave hull intersections (Fig. 1f) and its parameters. All extracted tree parameters are simultaneously visualized in the 3D Forest viewer, which allows a direct visual check of their fit with appropriate tree clouds. Results can be exported as a table of extracted tree parameters, images of viewer or segmented point clouds (e.g. terrain cloud or tree clouds) for further analyses in other software. The geometry of tree planar projections can be exported in a .txt file of polygon vertices coordinates and imported as a polygon vector layer into common GIS software.

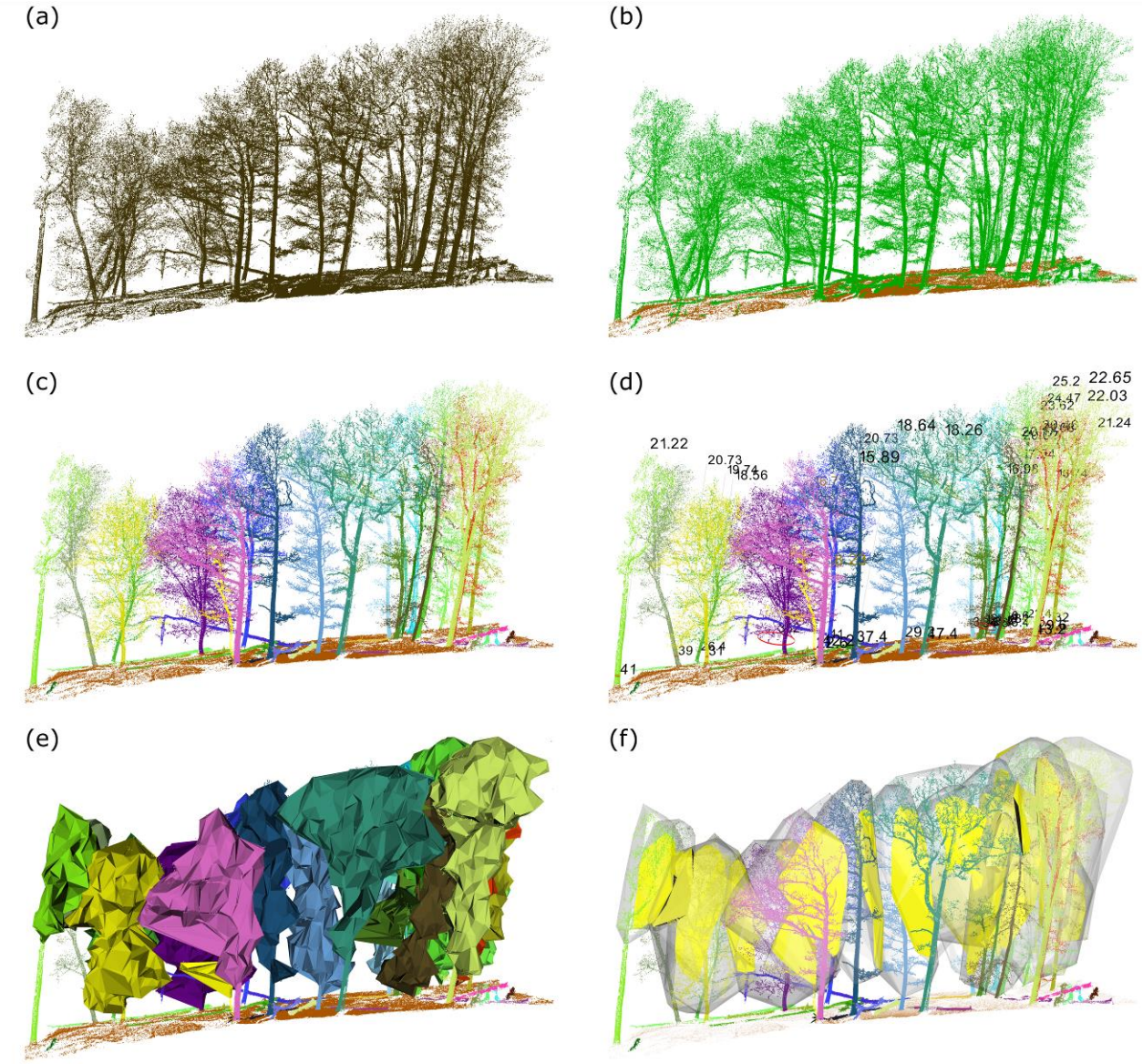

Fig. 1 Demonstration of the 3D Forest workflow on a small sub-sample of the VPFDP: (a) TLS data imported into 3D Forest (i.e. the Base cloud) prior to any segmentation; (b) automatically segmented Terrain cloud (brown) and Vegetation cloud (green) using the octree search method, refined by manual adjustment; (c) individual trees segmented into Tree clouds displayed in random colors; (d) DBH and tree height displayed for each tree; (e) concave hulls of tree crowns; (f) crowns represented by 3D convex hulls and their intersections (in yellow).

3. ALGORITHMS USED IN 3D FOREST

The application 3D Forest 0.4 released in year 2016 is licensed under the terms of GNU GPL v3 and is not platform specific written in programming language C++. Source code, compiled version, user manual and subsample of testing data are available at web page www.3dforest.eu. Compiled version is prepared for Windows 64 bit operating system only. Hardware requirements are 64 bit processor with at least 4 GB RAM memory.

Application has benefit of using free libraries like: PCL (Rusu and Cousins, 2011), VTK (Hanwell *et al.*, 2015), Boost (Boost, 2015), LibLAS (Isenburg, 2014) or Qt (Qt, 2015). Only brief decription of the software algorithms follows, more details are available in the User Guide and source code at web site.

3.1. Terrain extraction

The first presented algorithm is used for terrain extraction since almost all forest and tree parameters are connected with a distance from the ground (DBH, tree height, etc.). |TLS data provide not only detailed view into forest, but also cover terrain and other reflective elements of the environment. Automated terrain extraction methods have been widely developed in airborne laser scanning (ALS); in TLS processing, however, only a few studies have dealt with DTM extraction in forests in more detail (Bienert *et al.*, 2006; Brolly and Kiraly, 2009). In 3D Forest we implement two methods: i) Segmentation of the lowest points on Z axis based on search in octree with given resolution; and ii) Voxelization of the input could and selecting of the lowest voxels on Z axis as a terrain.

The first method using an octree search recursively subdividing the 3D space of the point cloud into eight cubes (all axis are divided in half) until arriving at the specified resolution R (R = length of the cube edge). Using a too-coarse resolution leads to missing spots in the terrain, while too-fine resolution leads to a very noisy terrain cloud. Two pass algorithm is incorporated: In the first pass a temporary sub-cloud containing all points of the lowest cubes of the tenfold resolution (10R) is created. Then, a new octree search of resolution R is carried out within this temporary

sub-cloud and saved into a new terrain point cloud, the rest is saved as a vegetation point cloud. The octree search provides more detailed results, but with more noise included.

The second method calculates centroid for points within every voxel of given input size (defined by the user) and creates new point cloud of voxels centroids. The centroids of the lowest voxels on Z axis are selected and saved as a terrain point cloud; the rest is classified as a vegetation point cloud.

The noise points in output can be removed using filters or adjusted manually. Missing points in the terrain point cloud (e.g. in stem shadows) can be filled in by inverse distance weighted interpolation incorporated into application.

3.2. Segmentation of trees

After terrain extraction a rest of vegetation needs to be segmented into single trees for computing its parameters. For segmentation of forest vegetation into individual trees (Fig. 1c), autors are aware only of two automated methods. Raumonen *et al.* (2015) use two main principles - tree topology and cover-sets – to segment vegetation into trees. The segmentation of the point cloud into stems and branches is based on using large surface patches of a fixed size. The stem bases and approximate stems are located heuristically, based on the assumption that stems are vertical. Tao *et al.* (2015) use strategy for individual tree segmentation consisted of three major parts: point cloud normalization, trunk detection and DBH estimation, and finally crown segmentation. Trunks are detected using density-based spatial clustering and while all trunks are segmented, for each trunk DBH and mean horizontal distance to its center is measured. Crown points are segmented based on weighted distance to the tree base and tree DBH.

In 3D Forest we present automatic approach based on distance between points and minimal number of points forming clusters and an angle between centroids of the clusters. In the first step of segmentation, the whole vegetation is divided into horizontal slices with user-defined input size [cm] S (S is a fundamental parameter of the segmentation used also in subsequent steps). Within these slices the clusters with user defined minimal number of points N and maximal distance S between two nearest points are constructed. Next step is to reconstruct bases of the trees. For each cluster with centroid height lower than 1.3 m above terrain the 10

neighboring (nearest) clusters up to distance 2S are found. We suppose those clusters come from the same tree base. All such clusters are merged into segments and tested if they are formed by at least 5 clusters and if the maximal dimension of segment is at least 1 m to be identified as the tree. When all segments are tested and evaluated, we use different approach to add more clusters to the tree. A cluster is added to the tree if its centroid lies within the distance 4S to the nearest centroid of the tree and the angle between the vector of these two centroids and the Eigen vector of the 5 closest centroids of the stem is less than 10 degrees. For non-selected clusters we test distance betweeen cluster points and tree points and if the clusters fit condition of S they are joined to the tree. At the final step all non- selected points are tested if they can be joined to any tree according to rising distance (maximaly to 3S). Automatically segmented trees can be visually checked and in case of need adjusted by manual segmentation. Resulting individual tree clouds are used for estimation of tree parameters.

3.3. Tree parameters

Trees segmented are ready for computing tree parameters. 3D Forest 0.4 can compute following parameters: tree position, tree DBH, tree height, stem curve and tree planar projection.

Tree position in censuses is usually understood as the position of the center of the tree base (Condit, 1998), and this convention was also adopted in 3D Forest (green sphere in Fig. 1b). Two methods for extracting the tree position are implemented. The first method uses all points up to a user specified height (default is 60 cm) above the lowest point of the tree and computes median coordinates of X and Y. The Z coordinate is defined as the median Z value of the n (default value is 5) closest points of terrain to that X, Y position. The second method use approach of Bienert *et al.* (2006), who applied a Randomized Hough Transform (RHT) for circle detection (Xu and Oja, 1993) on tree points at 1.3 m and 0.65 m above the lowest point of the tree cloud. The tree position is defined as the intersection of vector formed by centers of the two estimated circles with the DTM surface.

The two available methods for the computation of Tree DBH (red cylinder with size in cm in Fig. 1b) are: i) Randomized Hough Transform for circle detection (RHT) with adjustable number of iterations (default is 200) of circle estimation (Xu and Oja, 1993); and ii) Least Square

Regression (LSR) with an algebraic estimation of the circle and geometric reduction of squared distances to the computed circle (Chernov and Lesort, 2003). Both methods use a sub-set of the tree point cloud – a horizontal slice from 1.25 to 1.35 cm above the calculated tree position - called the DBH cloud in the 3D Forest environment. For successful circle fitting at least 4 points in this slice are needed. Both methods were tested for sensitivity of input data and computational time in a manner to find the best use and setup for each method in manner to get precise and reliable results in appropriate time. Manual editing (i.e. elimination of all points not representing the DBH) is available at this stage of the 3D Forest workflow.

The Tree Height (TH) / Length is defined as the difference in Z coordinates between the highest point of the tree point cloud and the tree base position (vertical line and number above the tree in Fig. 2b). The second method (tree length) computes the largest Euclidean distance between any two points of the tree point cloud. This method is thus suitable for calculation of the total length of leaning trees or even the length of lying deadwood.

For analysis of the Stem curve and its shape we use a similar approach as in Maas *et al.* (2008). The position of stem centers and stem diameters are calculated at different heights above the tree base position, starting at 0.65m followed by 1.3m, 2m and then every next meter above terrain (yellow cylinders in Fig. 2b). The circles (defining the local stem center and diameter) are fitted by the RHT algorithm to horizontal 7cm slices of the tree point cloud defined at appropriate heights. The algorithm stops when the estimated diameter is two times greater than in both of the two previous circles, which indicates expansion of the tree cloud into the crown.

3D Forest can compute and visualize an area of Tree planar projection using a 2D convex/concave hull of the tree point cloud orthogonally projected on the horizontal plane at the height of the tree base position. The convex hull (Fig. 2e) is calculated using the Gift wrapping algorithm (Preparata and Hong, 1977), then the area of the resulting polygon is calculated. Since convex shapes do not fit well the actual shape of many irregular trees, we also implemented a concave planar projection (Fig. 2d). The concave projection extends the convex hull algorithm using the Divide and conquer algorithm to split the sides of the polygon according to the given maximal polygon side length. The level of detail/generality as well as the area of the concave polygon can vary according to the maximal side length value defined by the user.

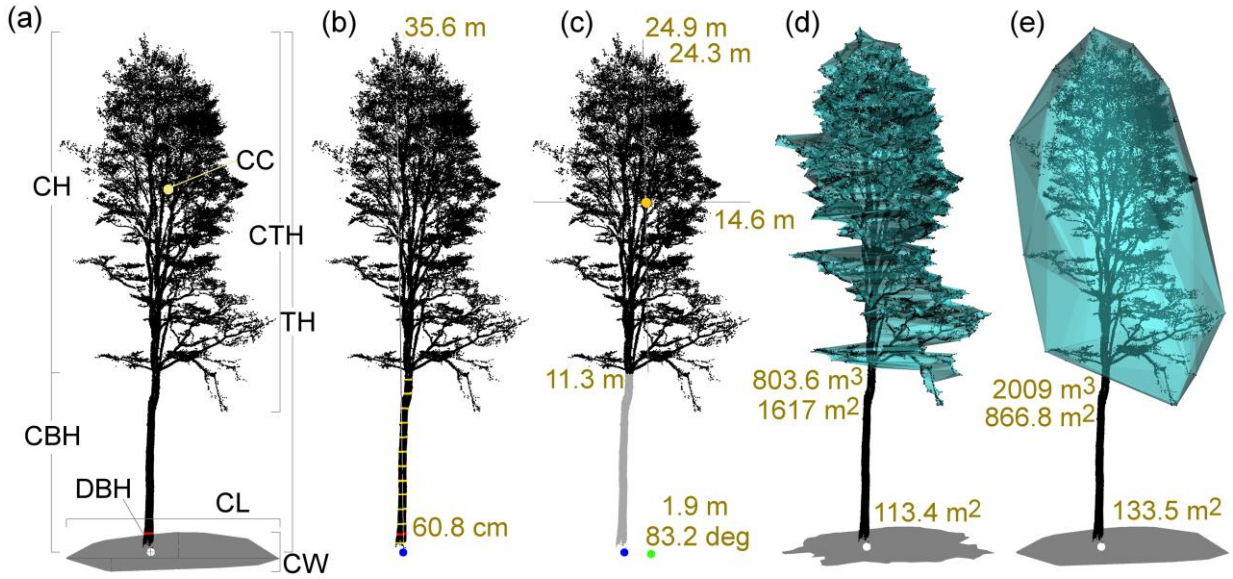

Fig. 2 Extraction and visualization of tree parameters from a single tree cloud: (a) visualization of tree parameters: CBH – crown base height, CH – crown height, CTH – crown total height, CL – Crown length, CW – crown width, CC –crown centroid, DBH – diameter at breast height, TH – tree height, white sphere – tree position; (b) tree with computed basic parameters –position (blue sphere), DBH (60.8 cm), TH (35.6 m) and stem profile (yellow cylinders); (c) tree crown (black cloud) represented by CTH (24.3 m), CH (24.1 m), CL(14.6 m), CBH (11.3 m), crown centroid (orange sphere) and its planar projection (green sphere) with distance and azimuth from the tree position; (d) concave hull of the crown with volume (803.6 m3) and surface(1617 m2) and orthogonal projection into plane with its surface area (113.4 m2); (e) 3D convex hull of the crown with volume (2009 m3) and surface (866.8 m2) and orthogonal projection into plane with appropriate surface area (133.5 m2).

3.4. Crown Segmentation

In our application, trees are divided into stem and crown of the tree. Separation of the crown cloud from the single tree cloud is possible manually or using automatic extraction.

In the first step of the automatic extraction algorithm the tree cloud is divided into 0.5 m high horizontal sections and its widths (average x and y axis extension) are compared one by one from the lowest section. If three (or more) consecutive sections are wider than the previous one, the last thin section is used as a starting position for detailed search. As the first step of the detailed search, the circles are fitted by LSR to the two 10 cm high horizontal sections. From centers of those circles the position of the fitted circle center of the next 10 cm high horizontal section is approximated. The subset of points for consecutive circle fitting is limited to the points

within a radius two times greater than the last fitted circle. This should avoid using points representing overhanging branches for diameter computation. If the new (uppermost) section diameter is not 25 % wider than the previous one, algorithms continues by predicting next stem center from the last two fitted circles and computing the next section diameter. Height of the last section diameter complying the examined limit is considered as the crown base. All points of the tree cloud above this position are considered as the tree crown together with points which were excluded from fitting circles in detailed search.

When crown manual separation is used, all stem points below the crown are manually removed from the tree cloud. Z coordinate of the highest point from the removed points is taken as the crown base height.

3.5. Crown parameters

As for the whole tree also for tree crown can be computed parameters. All available parameters are listed below with brief description.

The Crown Base Height (CBH) is in relation to the tree position and might be defined as the height where the lowest branch is connected to the stem. It is computed like the difference between tree base position Z coordinate and the Z coordinate of the crown base resulting from the crown extraction (Fig. 2a, c).

Crown Height (CH) is the difference between the Z coordinate of the crown base and the Z coordinate of the highest point of the crown (Fig. 2a, c).

Crown Total Height (CTH) represents the difference between Z coordinates of crowns highest and lowest points (Fig. 2a, c).

Crown Length (CL) is the longest distance between the two vertices of convex hull of the crown planar projection (Fig. 2a, c).

Crown Width (CW) is the sum of the two longest perpendicular distances from the crown length line to a convex hull vertex (Fig. 2a).

Crown centroid (CC) is computed from border points, which are defined by 2D concave hulls of crown horizontal sections (orange point in Fig. 2a, c). Height of the horizontal sections and the maximal length of concave hull edge are adjustable by the user. Position of the crown centroid is then computed as average coordinates from border points; this avoids displacement of the crown centroid caused by different cloud density when all crown points are used. The second option is the calculation of centroid of the 3D convex hull.

Crown position deviation (CPD) is defined by distance, direction (azimuth angle) and inclination. The distance and direction are measured between the tree base position and orthogonal projection of the crown center position (green sphere in Fig. 2c). Crown inclination is the inclination of the line connecting the tree base position and the position of the crown center from the vertical.

Crown volume and surface area may be estimated by its concave and/or convex 3D representation. Concave representation (Fig. 2d) is based on horizontal sections (slices) of user defined height and its concave hulls. Crown volume is then a sum of volumes of all horizontal sections (which are calculated as section 2D concave hull area multiplied by section height). Surface area is computed by specific triangulation algorithm. For triangulation, polygons created by concave hull of each section are used (border points). Top and bottom of the crown is triangulated by creating triangles between highest/lowest point of the crown and highest/lowest polygon edges respectively. The rest is triangulated by strip triangulation of two consecutive polygons.

3D convex hull created by 3D Voronoi triangulation (Fig. 2e) is another option for obtaining crown volume and surface area. For the reduction of calculation time only boarder points and all points from two uppermost and lowermost horizontal sections are used implicitly. If needed, computation using all crown points is also available.

Volume of crown by voxels of user specified size is also available; crown volume is then the sum of voxels volumes. All voxels that contain at least one point are counted.

Last but not least, 3D Forest allows user to compute Intersecting mass of two neighboring crowns (Fig. 1f). Intersection is computed as Boolean AND in 3D space using objects created by 3D convex hull (only). The intersection parameters like volume and center of mass are computed. To provide additional information about the competition pressure in canopies, direction from crown

center to intersection center of mass is expressed by horizontal azimuth and vertical angle, the distance in 3D space of these two points is also computed.

4. COMPARISON WITH CONVENTIONAL MEASUREMENTS

To demonstrate the actual applicability of 3D Forest in real conditions, we compared outputs from 3D Forest with results from a standard census of the VPFDP. The VPFDP (10.3 ha) is a xerophilous open forest on steep slopes and rocky outcrops. The stand is dominated by sessile oak (Quercus petraea Matt.), with admixtures of European ash (Fraxinus excelsior L.), European hornbeam (Carpinus betulus L.), small-leaved lime (Tilia cordata Mill.), and 14 other tree species. The position and DBH of all trees with DBH ≥10 cm were recorded in a census from year 2013. Tree positions were measured by a Field-Map device (www.fieldmap.cz) using a regular grid (44x44m) of reference points positioned by total station; DBHs were measured by a standard Haglöf caliper (recorded precision of 1 cm). Tree heights were measured for 181 trees using a TruPulse laser rangefinder / digital inclinometer (recorded precision of 10 cm based on).

At the same time, the whole plot was scanned in the leaf-off state using a Leica ScanStation C10 terrestrial laser scanner at a resolution of 2 mm in 10 m and using the regular multiple scanning position setup (44x44m) as proposed by Trochta *et al.* (2013). Scanned data were aligned, co-registered and exported into txt file in the Cyclone Register software provided with the scanner. After importing of files and automated terrain/vegetation segmentation, 824 individual trees of DBH ≥ 10cm on the 2.4 ha sub-plot were segmented both manually and automatically from the vegetation point cloud.

4.1. Automated segmentation

The first task was to evaluate the automatic tree segmentation algorithm depending on algorithm input parameters (Input cluster size, point cluster density). The outputs were compared in

confusion matrix to the manual tree segmentation used as a reference. Overall accuracy of the segmentation, mapping accuracy and omission and commission errors for each tree were calculated on the bases of individual points of particular tree clouds. The latter three indicators were tested by Kruskal-Wallis nonparametric ANOVA test (statistical significance level $\alpha = 0.05$) for identifying the best combination of input parameters.

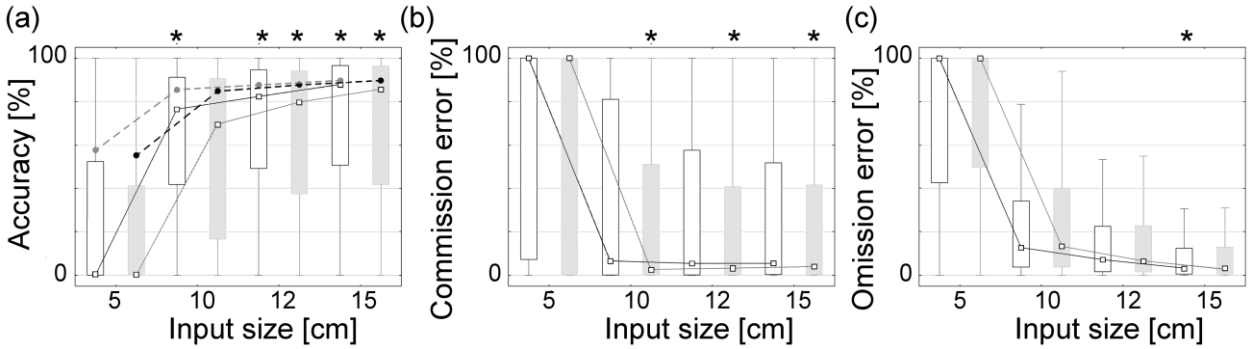

Fig. 3 Accuracy of automated segmentation as compared to manually segmented trees used as a reference. Four basic input cluster size (input size) and two point cluster density were tested: (a) overall segmentation accuracy (points connected by dashed line) and mapping accuracies of individual trees; (b) commission errors and(c) omission errors. In all charts rectangles connected by solid line represent medians, box upper and lower quartiles and whiskers represents upper and lower extremes; white box represents minimal cluster size of 10 points in a cluster and grey box minimum of 5 points in a cluster. Asterisk above boxplot represent the statistically significant group with the best values from all segmentation.

The analysis showed that overall and mapping accuracy rise with greater input size (Fig. 3a). Overall accuracy gained 89.9 % in combination of 15cm input size (S) and 5 number of points (N); still all setups with input size greater than 5 cm achieved more than 85 % overall accuracy. Since the overall accuracy gives us only general information about the whole segmentation, we used also mapping accuracy of each tree as a more detailed descriptor. The best mapping accuracy (median value 87.8 % was achieved with S of 15 cm and N of 5 points. Still, Kruskal-Wallis test found no significant differences in mapping accuracy using S of 10, 12 and 15 cm and N of 10 points and using S of 15 and 12 cm and N of 5 points per cluster (group of marked in Fig. 3a). Median commission error decreased to the minimal value of 2% at input size of 10, 12 and 15 cm and N of 5 points (Fig. 3b). Omission error (Fig. 3c) had a similar trend as the commission error but smallest value (3%) was reached with S of 15 cm and N of 10 points.

Opposed to commission error, differences in omission error were statistically significant for each input size and number of points in a cluster.

Results are quite comparable with similar study (Tao *et al.*, 2015) even when scanning setup and study area are different. Overall accuracy is comparable (89% vs 93%). The omission error (recall) and Commission error (precision) has also similar results and 3D forest has slightly better result (3%) than comparing study (5%).

The optimal values of S and N can vary with overall density of the TLS point cloud used - with more dense clouds the optimal segmentation distance can be smaller than 10 cm or clusters of more points might be preferable. Anyway, we demonstrated that with appropriate settings the automatic segmentation algorithm may provide fairly acceptable results. Still, in closed canopy forests with abundant understory and numerous stem and branch junctions of neighboring trees the visual check and manual adjustment will be needed.

4.2. Tree DBH and height

Since 3D Forest provides two methods of DBH estimation we compared both methods with field measurements by paired t-tests; the pairs were arranged by joining the spatially nearest tree positions in both datasets. The tree height measurement was compared in the same way. The LSR method provided slightly higher values than conventional caliper measurements (mean difference 1.17 cm). The RHT method provided results quite comparable to the conventional field census (mean difference 0.3 cm; see Table 1). The tree heights derived by 3D Forest were comparable to conventional TruPulse field measurements, with a mean difference of 12 cm (Table 1).

Result of DBH estimation can be compared with other study (Maas *et al.*, 2008), where DBH was evaluated. Maas *et al.* (2008) achieve slight overestimation in DBH using TLS (about 1 cm) which almost the same result as using LSR method in 3D Forest. RHT method underestimate results (0.3 cm) but still has smaller difference in results than Maas *et al.* (2008).

Table 1 Results of paired t-tests comparing automated methods of estimating DBH (Least Square Regression and Randomized Hough Transform) and tree height with conventional measurements using calipers and a digital inclinometer; computed for the significance level α = 0.05.

	Mean	Sdt. Dv.	N	Diff	Std. Dv. Diff	t	df	p	Confidence interval -95%	Confidence interval +95%
Caliper DBH	32,30	9,06								
LSR DBH	33,47	10,48	824	-1,17	5,338	-6,32	823	**4,4E-10**	-1,540	-0,809
Caliper DBH	32,30	9,06								
RHT DBH	31,96	10,04	824	0,332	5,113	1,864	823	0,062633504	-0,018	0,682
TruePulse height	15,25	5,01								
3D Forest height	15,38	4,96	181	-0,12	1,620	-1,03	180	0,304122889	-0,362	0,114

5. ANALYSIS OF SENSITIVITY FOR DBH COMPUTATION

With the analysis of sensitivity we tried to find optimal setup and limits of the two implemented methods of DBH computation. Five factors likely affecting the result were selected for testing: stem DBH, missing part of stem perimeter, proportion of noise points and number of points creating the DBH ring. For the RHT computation also the number of iterations was tested and for both methods time complexity of computation evaluated. The time complexity of RHT computation is O(n * i3) and LSR is O(n); where n is number of trees and i is the number of iterations. The testing was performed on artificial dataset designed as a pooled sample of simulated DBH clouds with points representing mixture of different levels of all tested factors. Full factorial design was used to simulate in total 48 300 trees; DBH for each artificial tree was estimated by both methods implemented in 3D Forest. The correct DBH estimation was rigorously defined as ± 1 mm difference from the expected DBH value. Results were analyzed by ANOVA for multiple factors at a statistical significance level α = 0.05 and post-hoc Tukey test to find differences among factors levels.

Table 2 Result of two-way ANOVA analysis for each factor of DBH computation by both methods. Significant tests are signed by "<" in the "Pr(>F)" column of the table.

		Df	Sum Sq	Mean Sq	F value	Pr(>F)	p
LSR	**DBH [mm]**	22	5,63	0,2557	60,842	<	2,00E-16
	Number of points	20	0,02	0,0008	0,192		0,998
	Noise [%]	3	8,4	0,9337	222,156	<	2,00E-16
	Missing part [%]	9	1,22	0,1359	32,343	<	2,00E-16
	Residuals	48239	202,74	0,0042			
RHT	**DBH [mm]**	22	1158	53	570,3	<	2,00E-16
	Number of points	20	5274	264	2857,5	<	2,00E-16
	Noise [%]	9	46331	5148	55780,9	<	2,00E-16
	Missing part [%]	9	223	25	268,8	<	4,38E-16
	Iterations	7	6609	944	10229,8	<	2,00E-16
	Residuals	386332	35654	0			

According to ANOVA (Table 2) it is evident that each factor except number of point at LRS is statistically significant; how each factor affects correct DBH estimation is depicted in Fig. 4. From the Tukey test we can conclude that LSR method is suitable for trees with DBH in the range of 10 – 50 cm (Fig. 4a). DBH clouds have to be composed of at least 3 points (Fig. 4b) representing at least 60% of the stem perimeter (Fig. 4e). The most importantly, the method is extremely sensitive to the presence of noise points - already 10 % of noise causes a total failure of the correct DBH estimation (Fig. 4d).

The RHT method proved to be more robust, showing significantly lower sensitivity to noise (Fig. 4d), DBH size (Fig.4a) and the missing part of the stem perimeter (Fig.4e). Using the RHT the tree DBH can be estimated since 1 cm; the DBH cloud should have at least 4 points to provide at least 50% rate of successful DBH recognition (Fig. 4b) with the best fit around 20-40 (100) points. The correct DBH estimation declines slowly with noise increasing to 50% and then rapidly drops to 0 (Fig. 4d). The RHT is on the other side more time consuming depending on the number of iterations (Fig. 4f). Tukey test showed that from 500 iterations successful recognition rate is not further increasing with the increasing number of iterations and additional iterations are thus only time consuming (Fig. 4c, Fig. 4f).

Due to the overall slight overestimation of the LSR method (Table 1) and the rigorous difference from the expected DBH value (± 1 mm) used in the definition of the correct DBH estimate for the

sensitivity analysis, the LSR provided generally significantly lower rates of successful DBH recognition there.

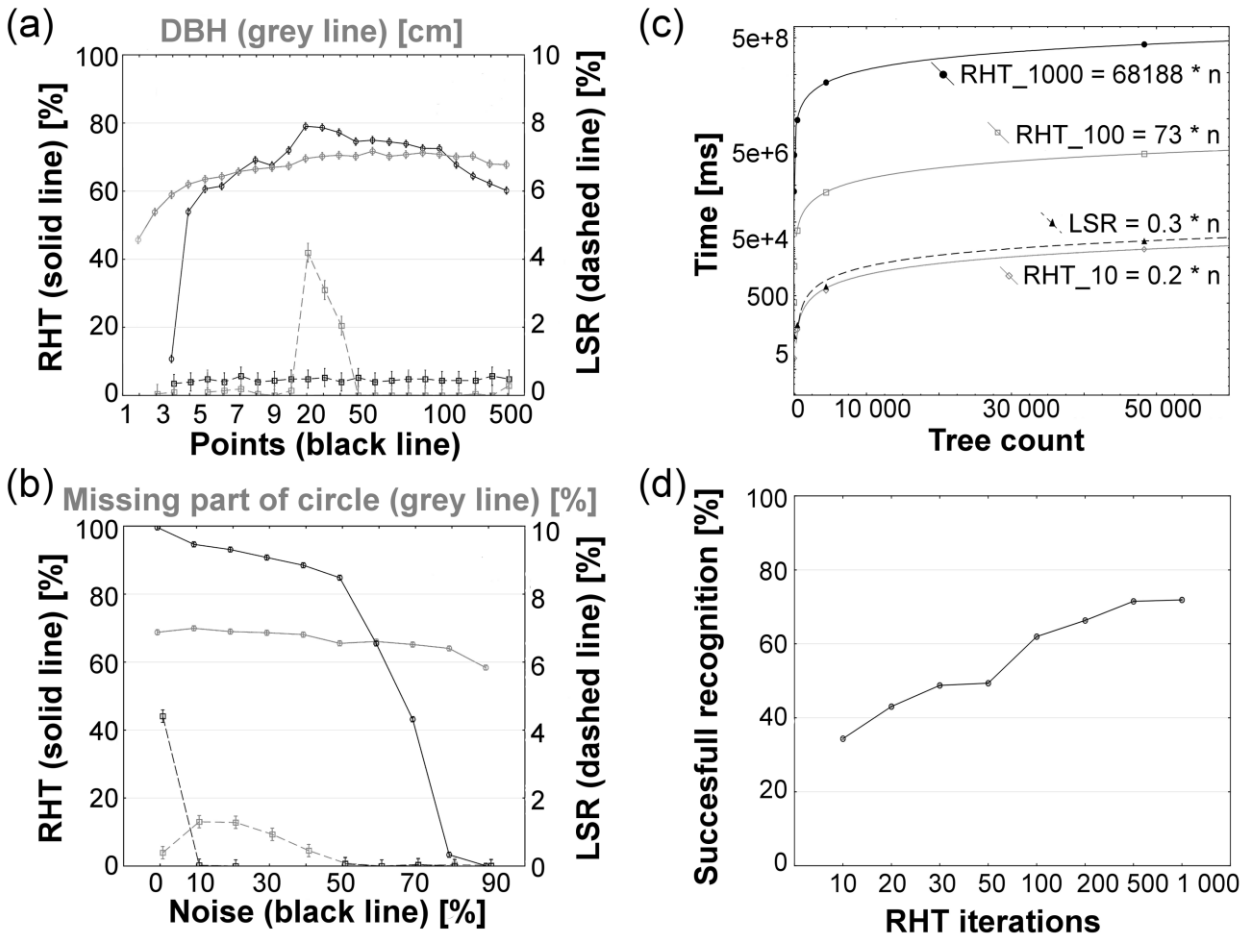

Fig. 4 Analysis of sensitivity of RHT and LSR estimation of DBH to selected factors expressed by successful DBH recognition rate (%); the tested factors were as follow: (a) DBH; (b) Number of points in DBH cloud perimeter; (c) Number of iterations (RHT only); (d) Portion of noise ; (e) Missing part of stem perimeter and (f) Computational time where Y axis have logarithmic scale. All values are displayed as means with 95% confidence intervals. The black marks and solid line represent RHT method - left Y axis is used; grey marks and dotted line represent LSR method with range of values on right Y axis of graphs.

6. CONCLUSIONS

The use of LiDAR technology undoubtedly has great potential in forest ecosystem research. While for processing ALS data several software packages may be used (e.g. FUSION, TerraScan, LiForest), only few free software specialized for tree description is available for TLS data so far. The 3D Forest contributes to filling this gap focusing on forest stand description by means of individual trees and their mutual spatial arrangement in a 3D space. It allows users to take the advantage of TLS data for detailed spatially-oriented forestry and forest ecology studies in a user friendly environment. Currently it can provide standard census data such as tree positions, DBHs and heights; it also provides more complex tree parameters such as stem curve, convex/concave planar projection, crown dimensions, crown volume, surface, center of mass and others. Implemented methods are comparable with other literature findings on automatic segmentation of trees (Tao *et al.*, 2015), tree parameters (Maas *et al.*, 2008) or crown parameters (Seidel *et al.*, 2011b).

In addition, the 3D Forest allows to compute intersecting mass of two neighboring crowns, which affords superior identification and quantification of aboveground competition of trees e.g. (Metz *et al.*, 2013; Seidel *et al.*, 2015) or testing the canopy related predictions of metabolic scaling theory of forests (Coomes *et al.*, 2012; Pretzsch and Dieler, 2012) with authentic data on tree crowns. On the other hand, 3D forest is still rather limited in pinpoint biomass estimates and detailed modeling of a single tree as provided e.g. by SimpleTree (Hackenberg *et al.*, 2015), on branch and leaves level (Côté *et al.*, 2012; Raumonen *et al.*, 2013).

The future development of 3D forest is aimed at the realistic modeling of the potential direct solar irradiance of individual tree crowns based on real tree shapes, positions and sun-path at the respective latitude, year season and daytime. This will enable studies of the competition for light in a new individualistic manner (e.g. which tree crown overshadows which, when and how much).

The 3D Forest software including the source code is freely available at www.3dforest.eu. Researchers and developers are openly invited to join our effort in further development of the software. The 3D Forest users can also leave comments and suggestions at forum or via ticket system on the web page.

7. ACKNOWLEDGEMENT

This research was supported by the Czech Science Foundation (GAČR), project No. P504/15-23242S and by institutional support (VUKOZ-IP-00027073). We would like to thank Sean M. McMahon for his useful comments and suggestions.

8. AUTHORS CONTRIBUTIONS

The contribution of the authors to this work: Jan Trochta developed and implemented the foundations of the 3D Forest application and functionality and is the main author of this manuscript. Martin Krůček developed and described planar projections functions and methods for estimation of crown parameters and provided useful feedback and suggestions in other parts. Tomáš Vrška contributed on manuscript writing and suggested several improvements of the manuscript. Kamil Král contributed on manuscript writing and supervised the development of the 3D Forest application.

9. CONFLICTS OF INTEREST

The authors declare no conflict of interest.

10. REFERENCES

Anderson-Teixeira, K.J., Davies, S.J., Bennett, A.C., Gonzalez-Akre, E.B., Muller-Landau, H.C., Joseph Wright, S., Abu Salim, K., Almeyda Zambrano, A.M., Alonso, A., Baltzer, J.L., 2014. CTFS-ForestGEO: a worldwide network monitoring forests in an era of global change. Global change biology.

Bienert, A., Scheller, S., Keane, E., Mullooly, G., Mohan, F., 2006. Application of terrestrial laser scanners for the determination of forest inventory parameters. International Archives.of Photogrammetry, Remote Sensing and Spatial.Information Sciences 36(5).

Boost, 2015. Boost C++ Libraries.

Brolly, G., Kiraly, G., 2009. Algorithms for stem mapping by means of terrestrial laser scanning. Acta.Silva.Lign.Hung. 5 119-130.

Calders, K., Newnham, G., Burt, A., Murphy, S., Raumonen, P., Herold, M., Culvenor, D., Avitabile, V., Disney, M., Armston, J., Kaasalainen, M., McMahon, S., 2015. Nondestructive estimates of above-ground biomass using terrestrial laser scanning. Methods in Ecology and Evolution 6(2) 198-208.

Condit, R., 1998. Tropical forest census plots: methods and results from Barro Colorado Island, Panama and a comparison with other plots. Springer Science & Business Media.

Coomes, D.A., Holdaway, R.J., Kobe, R.K., Lines, E.R., Allen, R.B., 2012. A general integrative framework for modelling woody biomass production and carbon sequestration rates in forests. Journal of Ecology 100(1) 42-64.

Côté, J.F., Fournier, R.A., Frazer, G.W., Olaf Niemann, K., 2012. A fine-scale architectural model of trees to enhance LiDAR-derived measurements of forest canopy structure. Agricultural and Forest Meteorology 166GÇô167(0) 72-85.

Hackenberg, J., Morhart, C., Sheppard, J., Spiecker, H., Disney, M., 2014. Highly Accurate Tree Models Derived from Terrestrial Laser Scan Data: A Method Description. Forests 5(5) 1069-1105.

Hackenberg, J., Spiecker, H., Calders, K., Disney, M., Raumonen, P., 2015. SimpleTree—An Efficient Open Source Tool to Build Tree Models from TLS Clouds. Forests 6(11) 4245-4294.

Hanwell, M.D., Martin, K.M., Chaudhary, A., Avila, L.S., 2015. The Visualization Toolkit (VTK): Rewriting the rendering code for modern graphics cards. SoftwareX 1–2 9-12.

Chernov, N., Lesort, C., 2003. Least squares fitting of circles and lines. arXiv preprint cs/0301001.

Isenburg, M., 2014. LAStools: software for rapid LiDAR processing. URL: http://www. liblas. org/. Plaça Ferrater Mora 1 17071.

Maas, H.G., Bienert, A., Scheller, S., Keane, E., 2008. Automatic forest inventory parameter determination from terrestrial laser scanner data. International Journal of Remote Sensing 29(5) 1579-1593.

Metz, J., Seidel, D., Schall, P., Scheffer, D., Schulze, E.D., Ammer, C., 2013. Crown modeling by terrestrial laser scanning as an approach to assess the effect of aboveground intra- and interspecific competition on tree growth. Forest Ecology and Management 310(0) 275-288.

Piboule, A., Krebs, M., Esclatine, L., Hervé, J., 2015. Computree: a collaborative platform for use of terrestrial LiDAR in dendrometry.

Preparata, F.P., Hong, S.J., 1977. Convex hulls of finite sets of points in two and three dimensions. Communications of the ACM 20(2) 87-93.

Pretzsch, H., Dieler, J., 2012. Evidence of variant intra-and interspecific scaling of tree crown structure and relevance for allometric theory. Oecologia 169(3) 637-649.

Qt, 2015. Qt Development team.

Raumonen, P., Casella, E., Calders, K., Murphy, S., Åkerblom, M., Kaasalainen, M., 2015. Massive-scale tree modelling from TLS data. ISPRS Ann. Photogramm. Remote Sens. Spat. Inf. Sci 189-196.

Raumonen, P., Kaasalainen, M., Åkerblom, M., Kaasalainen, S., Kaartinen, H., Vastaranta, M., Holopainen, M., Disney, M., Lewis, P., 2013. Fast automatic precision tree models from terrestrial laser scanner data. Remote Sensing 5(2) 491-520.

Rusu, R.B., Cousins, S., 2011. 3d is here: Point cloud library (pcl). IEEE, pp. 1-4.

Seidel, D., Beyer, F., Hertel, D., Fleck, S., Leuschner, C., 2011a. 3D-laser scanning: A non-destructive method for studying above- ground biomass and growth of juvenile trees. Agricultural and Forest Meteorology 151(10) 1305-1311.

Seidel, D., Hoffmann, N., Ehbrecht, M., Juchheim, J., Ammer, C., 2015. How neighborhood affects tree diameter increment – New insights from terrestrial laser scanning and some methodical considerations. Forest Ecology and Management 336(0) 119-128.

Seidel, D., Leuschner, C., Müller, A., Krause, B., 2011b. Crown plasticity in mixed forests - Quantifying asymmetry as a measure of competition using terrestrial laser scanning. Forest Ecology and Management 261(11) 2123-2132.

Tao, S., Wu, F., Guo, Q., Wang, Y., Li, W., Xue, B., Hu, X., Li, P., Tian, D., Li, C., 2015. Segmenting tree crowns from terrestrial and mobile LiDAR data by exploring ecological theories. ISPRS Journal of Photogrammetry and Remote Sensing 110 66-76.

TreeMetrics, 2015. AutoStem Forest: http://www.treemetrics.com/.

Trochta, J., Král, K., Janík, D., Adam, D., 2013. Arrangement of terrestrial laser scanner positions for area-wide stem mapping of natural forests. Canadian Journal of Forest Research 43(4) 355-363.

True Reality Geospatial Solutions, L., 2015. LiForest -LiDAR software for forestry applications, 2 ed: http://www.liforest.com/.

van Leeuwen, M., Nieuwenhuis, M., 2010. Retrieval of forest structural parameters using LiDAR remote sensing. European Journal of Forest Research 129(4) 749-770.

Xu, L., Oja, E., 1993. Randomized Hough transform (RHT): basic mechanisms, algorithms, and computational complexities. CVGIP: Image understanding 57(2) 131-154.

PAPER III

Below- and above-ground biomass, structure and patterns in ancient lowland coppices

Tomáš Vrška[a,b]*, David Janík[a], Marcela Pálková[a,b], Dušan Adam[a], Jan Trochta[a]

[a] *Silva Tarouca Research Institute, Department of Forest Ecology, Lidická 25/27, 602 00 Brno, Czech Republic*

[b] *Faculty of Forestry and Wood Technology, Mendel University in Brno, Department of Silviculture, Zemědělská 3, 613 00 Brno, Czech Republic*

Abstract

Ancient coppice woods are areas that reflect long-term human influence and contain high species biodiversity. In this type of forest we aimed: i) to analyse the below- and above ground biomass of stools and to estimate the age of largest stool; ii) to define a "zone of interference" for coppices; iii) to describe and classify variability in the shape and size of coppice stools; iv) to define the specific characteristics of the spatial distribution of stems and stools;

The study was conducted in the Podyjí National Park, Czech Republic, where two old oak coppice stands were fully stem mapped: Lipina (3.90 ha) and Šobes (2.37 ha). Cores were processed using TimeTable and PAST4. Below- and above-ground biomass of largest stool was computed using the data from terrestrial laser scanner. Tree zones of influence were analysed with V-Late landscape analysis tools using Shape Index. The pair correlation function and L function were used to describe the spatial patterns of trees with DBH $\geq$ 7 cm, and the null model of Complete Spatial Randomness and Matérn cluster process were tested. For the modelled old stool we estimated a ratio of 2:1 for above/below ground volume with no reduction of below ground biomass regarding the hollow roots. The age of the largest stool was estimated 825 years (SE ± 145 years). An "Inner Zone of Influence" was defined, with a total area covering 323 m^2/ha. The median area of this zone in both plots was 0.40 m^2 for all trees, 0.23 m^2 for singles and 0.87 m^2 for stools. The Matérn cluster process was successfully fitted to our empirical data. In this model the mean cluster radius ranged between 1.9 to 2.1 m and mean number of points per cluster was 1.7 and 1.9. The most prevalent characteristics of these ancient oak coppices were their compact shape and clustered spatial distribution up to 10 m.

1. INTRODUCTION

Ancient coppice woods are a specific type of habitat, reflecting long-term human influence and containing high species biodiversity. They conserve local tree ecotypes, and at some sites are the only remnants of original woods with natural species composition, even if the structure of the stands has been modified (Bechmann 1990, Fuller & Warren 1993, Rackham 2006). Coppices demonstrate vast variability and adaptability in the tree and herb layers and in their processes as a whole (Peterken 1996, Verheyen et al. 1999, Rackham 2006, Schweingruber 2007). Coppicing is considered to be one of the most important ways to manage temperate lowland (oak-dominated) or highland (beech-dominated) woodlands of West and Central Europe, Eastern Asia and North-East America in reserves or urban areas where this kind of management was historically used (Evans & Barkham 1992, Iida & Nakashizuka 1995, Joys et al. 2004, Rackham 2006, Nielsen & Møller 2008, Itô et al. 2012).

For coppice or coppice with standards systems, the most common tree species have traditionally been oaks (Quercus sp.), chestnut (*Castanea sativa*), lindens (*Tilia* sp.), hornbeam (*Carpinus betulus*), and beech (*Fagus sylvatica*), though others have been used as well (Rackham 2006). The main tree species in lowlands is sessile oak *Quercus petraea* (Matt.) Liebl - a slower-growing but long-lived deciduous tree species whose wood, bark, acorns and litter have versatile uses. Sessile oak can tolerate a considerable lack of moisture and rocky substrates. Late to leaf, this species is associated with spring geophytes, and natural oak or oak-hornbeam woods are generally considered to host light-demanding species of flora and fauna (Dey 2002, Ducousso & Bordacs 2003, Linford 2007).

For the purposes of this paper, one or more stems of the same origin creating a single interconnected system were considered as one ‘tree’. Individual stems were designated as ‘singles’, while multi-stemmed trees as ‘stools’. Stools are formed by clonal stems forming interconnected groups or clusters of individuals that originated through vegetative propagation, such as layering, root suckers, stolons or stump shoots, from the same parent plant (Falinska 1985, Oldeman 1990, Kull 1995, Jeník & Soukupová 1999).

What distinguishes coppiced trees from trees of seed origin is the root and stool system, which can be very old, crooked and extremely large (Peterken 1996, Bauhus 2009). A single coppice

stool can have stems several meters away from each other, which nevertheless can be visually identified in the field by experienced observers due to curvatures at the stem bases (Coles 1978) or the typical concentric or linear formations of stems. The age of a stool may be estimated from its diameter; the largest stools are thought to have been continuously coppiced for centuries (Rackham 1980, Pigott 1989, Bouwer 2008).

Since the mid 19th century, continuous coppicing and the ageing of coppice stools have been blamed for lower stand productivity and quality throughout Europe, and especially for the worsening of soil conditions (Vyskot 1961). However, recent scientific research has not confirmed previous assumptions and has even concluded that in coppice systems, in comparison with high forests, the decomposition rate and transport of nutrients is faster and soil chemical conditions more favourable, argued to be the consequence of higher light and heat consumption (Hölscher et al. 2001, Bruckman et al. 2011).

In 1985 Wu et al. introduced the term 'ecological field theory' based on interactions and interferences among plants. Graded circular zones surrounding individual plants ('influence domain' (Walker et al. 1989) or 'zone of influence' (Weber & Bardgett 2011) were defined. For herbaceous plants, even a Generalized Linear Model concerning the belowground zone of influence has been drawn. This showed that belowground zones of influence are not of fixed circular shapes (Casper et al. 2003). The aim of this paper is to describe and define zones of interference for new seedling recruitment in the case of coppiced trees. Such zones are undoubtedly different from those around trees of seed origin, and for coppiced trees the belowground part is of outstanding importance. We hypothesized that large coppice stools influence the interference potential to a high degree, which a newly germinated seedling would have to overcome to establish itself and successfully grow at a site within the area of a stool.

To describe spatial patterns of stools we used the method of spatial point process analysis, in which the "points" are tree locations and the "marks" tree characteristics such as species, diameter, height, social status etc. (Stoyan & Penttinen 2000). Due to vegetative reproduction, coppice stands tend to be characterized by high clumping intensities at small spatial scales, i.e. clustered formations. The size and shape of the stool cluster could therefore also be characteristic for different tree species or ecotope conditions, such as terrain exposition, and they play a significant role in determining the age of the stool, in other words the length of continuous human

activity - coppicing. Therefore, we also attempted to better define the specific characteristics of the stems and stools in ancient coppices.

To foster a better understanding of the structure and patterns in ancient coppices both below and above ground, we asked the following questions:

- What is the ratio of below- and above-ground structure and biomass of ancient Central European coppices and how old are the largest stools?
- What is size of "zone of interference" for coppices – the area around every tree (stool) that is practically inaccessible for natural seed regeneration?
- What is the variability in the shape and size of coppice stools?
- What the specific characteristics of the spatial distribution of stems and stools in ancient coppices are?

2. MATERIAL AND METHODS

2.1. Study site

We studied long abandoned sessile oak (Quercus petraea) dominated ancient coppices in the Podyjí National Park (hereafter PNP), Czech Republic. Average yearly temperature in the PNP is between 8°C and 9°C, average precipitation is 550–600 mm (Tolasz et al. 2007). In a biogeographical sense, the PNP lies in the transition zone between the Hercynian and Pannonian provinces (the mesophytic and the thermophytic) that, together with the varied morphology of the river valley and the plateaux, creates high species diversity (Chytrý & Vicherek 1995). The PNP is among the longest settled areas in Central Europe, and has been continuously inhabited since 5-6,000 BC (Čižmář 2002, Neruda 2007). The forest history in the PNP has been described by Škorpík (1993), Vrška (1998), and Reiterová & Škorpík (2012). Woodlands in the PNP were intensively influenced by deforestation, pasture, burning, litter raking, cultivation terraces and coppicing.

Two research plots, Lipina - 3.90 ha (48°49'19"N, 15°57'47"E) and Šobes - 2.37 ha (48°49'32"N, 15°58'21"E) (Fig. 1.), are located in the core (non-intervention) zone of the PNP. Lipina lies on the eastern side of the National Park with an average inclination of 20˚ and elevation ranging between 300-365 m a.s.l. Šobes lies on the transition ridge between the valley and the plateaux, and has more moderate slopes at elevations between 382-395 m a.s.l. The geological bedrock at both sites consists of granites and similar rocks of Proteozoic to Paleozoic age (Škorpík 1993). The vegetation and soil conditions at Lipina were described in Janík et al. (2007). The ancient coppices at Lipina, Šobes and other stands in the PNP were left unmanaged after active coppicing started to be abandoned at the end of 19th century and definitively ceased in the 1950s.

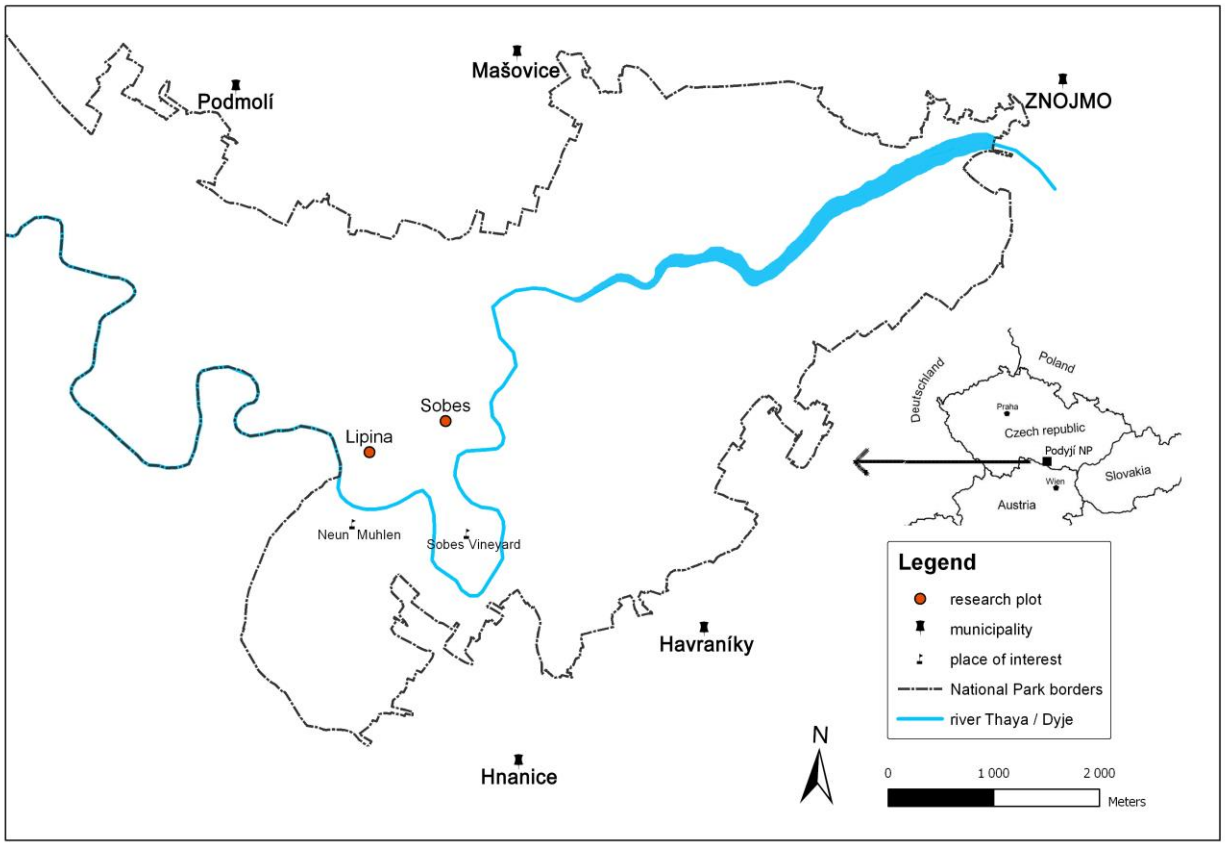

Figure 1 The location of the research plots within the Podyjí National Park (Czech Republic).

2.2. Stool mapping and biomass computation

Tree and stand data were acquired using Field-Map technology, with a MapStar compass module, laser rangefinder, Impulse altimeter (Laser Technology) and Hammerhead field computer (WalkAbout Computers) (www.fieldmap.cz). All standing and lying trees with diameter at breast height (DBH) ≥ 7 cm and stumps with diameter at the base ≥ 7 cm were measured and stem position maps were constructed, for Lipina in 2006 (Janík et al. 2007) and for Šobes in 2010. For standing stems the following categories were distinguished: live normal, live breakage - snap, full dead stem and snag. Lying deadwood was measured and classified into three stages of decay: hard, touchwood and disintegrated (Král et al. 2014). For growing shape construction the heights were measured for 10% of standing stems. Height curves were constructed with Naeslund's function. During fieldwork in 2010, every standing stem and stump was classified as a single or part of a stool, and the affiliation of stems to stools was recorded in the database using unique IDs for each stool.

In 2010, we exposed the root systems of three old stools of different sizes and shapes (Fig. 2). Unearthing was performed manually using hand tools, pneumatic drills and an air-spade supersonic nozzle (Nadezhdina & Cermak 2003). We removed the earth to the underlying bedrock at a maximum depth of 65 cm. Exposing the root and stool systems served as a basis for the assessment and mapping of these stools by terrestrial laser scanning. Each uncovered stool was scanned from 9 different positions to record all shapes. After merging all scans into a single one, the resulting point cloud was used to create a model of a stool and its stems (Fig 2a) for estimating biomass and stem positions. For scanning, a Leica ScanStation C10 was used together with Cyclone software for merging single scans and exported to ASCII file. From the ASCII data, the model of stems, branches and roots was created using Geomagic Studio 2014 software. A closed manifold surface of all stems and roots that were recognized in stools was generated, and the volume of each part was estimated and a planar projection of each tree and the whole stool was created.

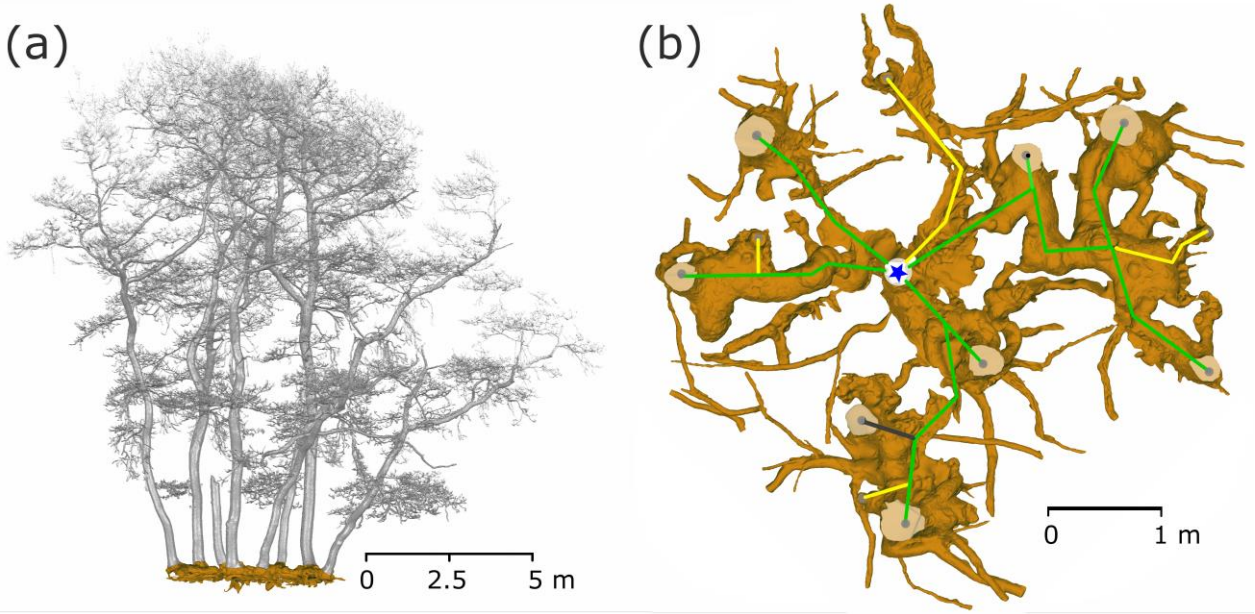

Figure 2 Exposed coppice stool root system (Lipina research plot). The current state was captured by a terrestrial laser scanner and saved as a mesh for further analysis. In part (a) the stems are visualized as a side view of the single stool with the whole root system (brown) as a realistic model. A detailed root system model (b) shows all coarse roots, positions of the living stems (grey dots on stem profiles) and their connections (green – living trees; yellow – historical stumps; grey – standing snags) to the origin (blue star) of the stool.

2.3. Stand age analysis and stool age estimation

To survey the age structure of living stems, we sampled the research plots for dendrochronological analysis with an increment borer in 2010. On the basis of stem position maps, we created a regular square network of 44.25 m. At each network point the 2-3 closest live stems were cored. We collected 115 increment cores of individual stems (Lipina 72, Šobes 43). The cores were processed using TimeTable and PAST4 with an accuracy of 0.01 mm. To extrapolate the age of cores bored off-pith, missing tree rings were calculated from the measured distance to the estimated pith with a compass and the average width of the first five measured tree rings. Only cores with a maximum of 6 extrapolated tree rings were included into the age analyses (Lipina 38; Šobes 26).

For stool age (SA) estimation we used the following formula, in which:

AGR is the average growth rate based on annual radial increment;

DSR is the average distance of current stems from the parent central root (Fig. 2b);

AAS is the average age of current stems minus 20 as the age used for the AGR;

$$SA = AGR * DSR + (AAS - 20)$$

AGR is based on the radial growth of individual stems (shoots), which is simultaneous with the growth of the stool radius; therefore the growth rate of the entire stool should be twice the radial increment measured on shoots. In practice, the real rate of radius growth of the stool cluster is not twice the mean annual radial growth but is rather somewhat smaller. The reason behind this is that the ground plan projection of the stem circumference is an „inclined plane". New coppice shoots always spread outwards from the original stump, but because of space restrictions by the original stump, they bend as they grow larger, creating stem curvature at the base and oblique growth. Based on Pigott (1989), we used a coefficient rate of 1.8 of the mean width increment.

Based on forest management plans from the beginning of the 20th century (Vrška 1998) we established that the rotation period at our research plots was intended to be 40 years. Older written material was not so detailed, but previous research has demonstrated that the further one goes back in time, the shorter the coppice cycle tended to be. For instance, in the Middle Ages coppicing was done every seven to ten years (Evans & Barkham 1992, Rackham 2006). A twenty-year period was chosen as a long-term average rotation period. According to the historical surveys the AGR was calculated as the average radial increment of the first 20 tree rings from the dendrochronological analysis of the entire research plot.

DSR was calculated using the 3D model of the stool root and standard image analysis.

2.4. Tree inner zone of influence

In order to determine the tree interference zone – the area practically inaccessible for the successful establishment and growth of tree seedlings – we defined the Tree Inner Zone of Influence ($Tree_{IZI}$). $Tree_{IZI}$ is a closed polygonal area which constituted a projection of i) the basal area(s) of standing stem(s) or stump(s), ii) a buffer(s) around the basal area(s), and in the case of stools: iii) the stool polygon and iv) a buffer around the polygon (Fig. 3). The circumference of the stool polygon was created as a link among standing stems or stumps through a procedure of searching nearest neighbours in the stool such that i) all stems or stumps should lie inside the polygon, and ii) the circumference line should go directly through each stem or stump position (i.e. a convex hull of stems positions). The buffer size (BS) around each stem or stump was determined by linear scaling according to the diameter (DBH). For smaller trees the buffer radius is a little larger than DBH, while larger trees have a buffer radius almost equal to the DBH value.

$$\mathbf{BS = 0.85 * DBH + 7.386.}$$

For the circumference, the line of stool buffers with r = the mean diameter of stool was used. Variability analysis and categorization of $Tree_{IZI}$ shapes were carried out with landscape analysis tools V-Late (Lang & Tiede 2003) using the Shape Index, where:

P_{ij} = the perimeter of patch ij in terms of the number of cell surfaces.

$\min P_{ij}$ = the minimum perimeter of patch ij in terms of the number of cell surfaces

$$\mathbf{SHAPE = P_{ij} / \min P_{ij}}$$

The Shape Index (SI) is a dimensionless expression of compactness. Maximum compactness is represented by a circle; with increasing complexity, crookedness or jaggedness SI also increases. The range of SI is ≥ 1, and is without limit. The V-Late ArcGis extension is an implementation of procedures based on Fragstat (McGarigal & Marks 1995).

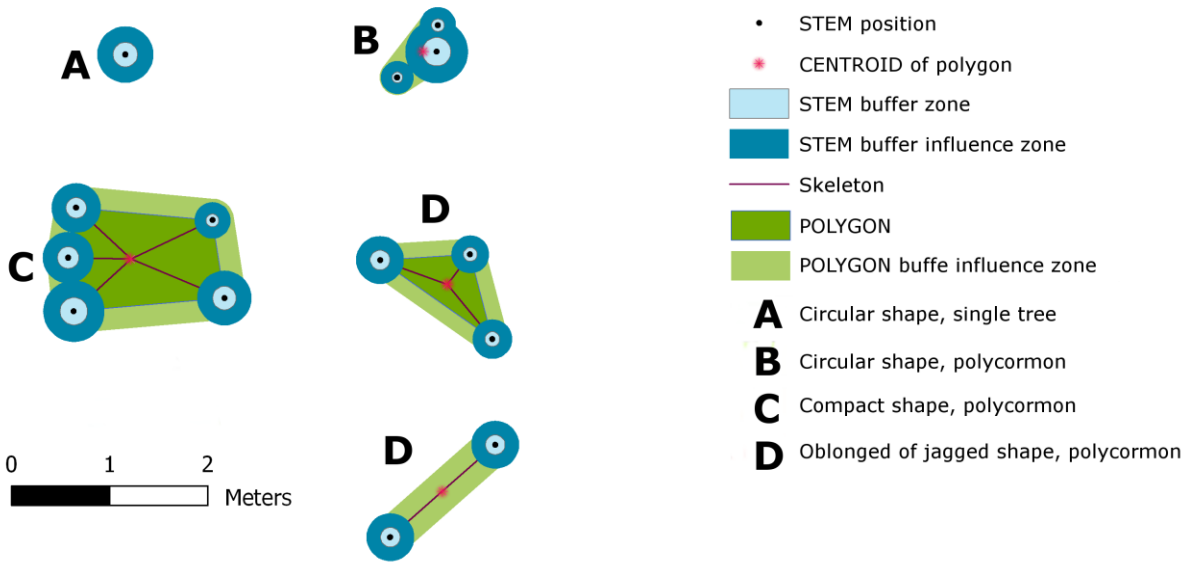

Figure 3 Construction of Tree Area (Tree Inner Zone of Influence) – projection of individual buffers around stool and and it shape class. Stools have benn classified by Shape Index into four classes: circular – single tree (A); circular polycormon (B); compact polygon(C) and oblonged (D).

2.5. Tree spatial patterns

To describe the density variability of both individual standing stems and stumps, we used the univariate pair correlation function. The pair correlation function is a second order characteristic, as are the frequently used K function (Ripley 1977) and L function (Besag 1977). Stoyan & Penttinen (2000) define the pair correlation function as follows: consider two infinitesimally small discs of areas dx and dy at distance r. Let p(r) denote the probability that each disc contains a point of the process. Then p(r) = λ2g(r)dx dy, where λ is density. Put in a different way, the pair correlation function g(r) is the probability of observing a pair of points separated by a distance r, divided by the corresponding probability for a Poisson process (Baddeley 2008). It is related to the K function by:

$$g(r) = d/dr * K(r)/(2 * \pi) \quad \text{for } r \geq 0$$

The essential difference between the K function and pair correlation function is the non-cumulative character of the latter. The pair correlation function uses annuli as distance classes,

not circles. Under the assumption of a homogenous Poisson process, g(r) = 1. Values of g(r) larger than one indicate clustering, while values smaller than one indicate regularity. The pair correlation function g(r) was estimated for each plot at steps of 1 m for r-values up to 20 m. A null model of complete spatial randomness (hereafter CSR) was used on the assumption that the first-order intensity λ is constant within plots. For the fixed value of r we used 199 Monte Carlo simulations of CSR to obtain pointwise critical envelopes for g(r). The significance level of tests was 0.01 (Besag & Diggle 1977). A fixed r had to be chosen prior to the simulation, since if all r values are considered simultaneously, the probability of rejecting H_0 increases and the true error probability is larger (Loosmore & Ford 2006, Illian et al. 2008). Therefore, if we had estimated continuous intervals of the distances over which an observed pattern deviates from the hypothesized model, the results could not have been considered significant with a significance level of 0.01.

A cluster process model was also fitted to the data as an alternative to the Poisson homogenous process. We used the Matérn cluster process, in which the parent points come from a homogeneous Poisson process with intensity κ, and each parent has a Poisson number (μ) of offsprings, independently and uniformly distributed in a disc of radius R centered on the parent (Baddeley 2008). We used the L function as summary statistics for fitting the model to the data (Ripley 1988). To determine the values of the parameters that achieve the best match between the fitted LΘ(r) and the empirical L-function of the data, we used the method of minimum contrast (Diggle 2003). Since maps of individual plant locations cannot be used to investigate processes occurring at scales that approach the accuracy of the measurements (Freeman & Ford 2002), and our spatial error was ±1.1 m, we focused primarily on large-scale processes, such as clustering. All spatial analyses were conducted using the package ‘‘spatstat’’ (Baddeley & Turner 2005) in the statistics software R (R Development Core Team 2006).

3. RESULTS

3.1. Below- and above-ground biomass and coppice stand structure

The basic characteristics of the tree layer at Lipina and Šobes are shown in Table 1. Approximately 640 live standing stems per hectare represented a timber stock of ± 260 m^3/ha and a basal area of ± 30m^2/ha. The number of stumps (mostly of artificial origin) was 41/ha at Lipina and 271/ha at Šobes. The median diameter of stems and stumps was 22 cm at both plots, but at Šobes there were more thick individuals (Fig. 4). Long-term coppicing significantly altered the forest structure and texture. The majority of stems and stumps were growing in stools; in total only ca. 25% were single-stemmed trees (Table 2). At Šobes there were proportionally more multi-stemmed trees (stools with 4 and more stems or stumps), but two- and three-stemmed stools still predominated (Fig. 5).

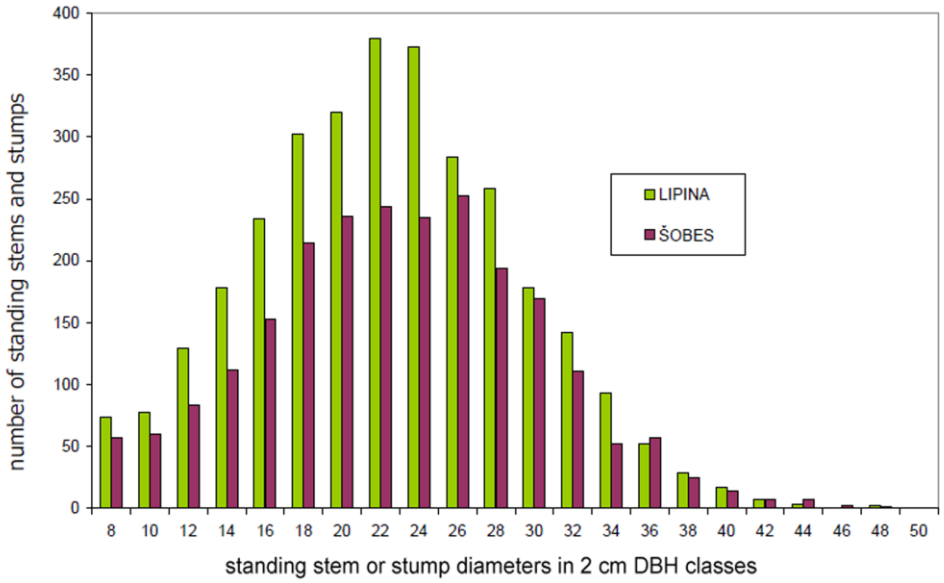

Figure 4 Histogram of the diameter distribution of standing stems and stumps at Lipina and Šobes.

Table 1 Main tree layer parameters at Lipina and Šobes

PLOT				ŠOBES		LIPINA	
				total	[*/ha]	total	[*/ha]
AREA			[ha]	2,37		3,90	
live standing trees		stem numbers	[N]	1503	634	2501	641
		basal area	[m^2]	75,8	32,0	642,0	164,6
		timber volume	[m^3]	621,0	262,0	115,4	29,6
dead standing trees		stem numbers	[N]	139	59	471	121
		basal area	[m^2]	3,0	1,3	9,9	2,5
		timber volume	[m^3]	18,0	7,6	65,0	16,7
stumps		stem numbers	[N]	643	271	160	41
		basal area	[m^2]	20,9	8,8	4,2	1,1
dead lying trees	stem numbers	decay stage	H	39		183	
			T	75		955	
			D	3		47	
		total	[N]	117	49	1185	304
	Timber volume	decay stage	H	6,0		48,0	
			T	11,0		166,0	
			D	0,0		4,0	
		total	[m^3]	17,0	7,2	218,0	55,9

The average upper height of the stand was ca. 18 metres at both plots. A distinctive difference between the plots was found for deadwood volume, which was more than 4 times higher at Lipina than at Šobes (73 m^3/ha and 15 m^3/ha, respectively). The dynamics of changes in the tree layer was more pronounced at Lipina, while at Šobes larger gaps in the crown canopy were missing because of the smaller number of fallen dead trees, which were also less disintegrated than at Lipina.

From the modelled stool, above and below ground biomass was calculated. The below ground biomass of the stool was estimated to be 1.02 m^3 of woody biomass connecting 7 living stems and one snag, and the sum of the above ground biomass was about 2.13 m^3. The stool had a planar projection area of 122.35 m^2 with an average stem planar projection area of 26.4 m^2. The uncovered area and the root system had an area of about 20 m^2.

Table 2 Representation of single and multi-stemmed trees (polycormons; stools) by numerical representation and Tree Inner Zone of influence coverage.

PLOT			ŠOBES		LIPINA		TOTAL	
			total	[*/ha]	total	[*/ha]	total	[*/ha]
AREA		[ha]	2,37		3,90		6,27	
standing stems and stumps	stools	[N]	1841	777	2298	589	4139	660
	singles	[N]	444	187	834	214	1278	204
	total	[N]	2285	964	3132	803	5417	864
tree zone of inner influence	stools	[N]	496	209	820	210	1316	210
		[m^2]	767,8	324,0	940,0	241,0	1707,8	272,4
	singles	[N]	444	187	834	214	1278	204
		[m^2]	116,0	48,9	198,8	51,0	314,8	50,2
	total	[N]	940	397	1654	424	2594	414
		[m^2]	883,8	372,9	1138,8	292,0	2022,6	322,6

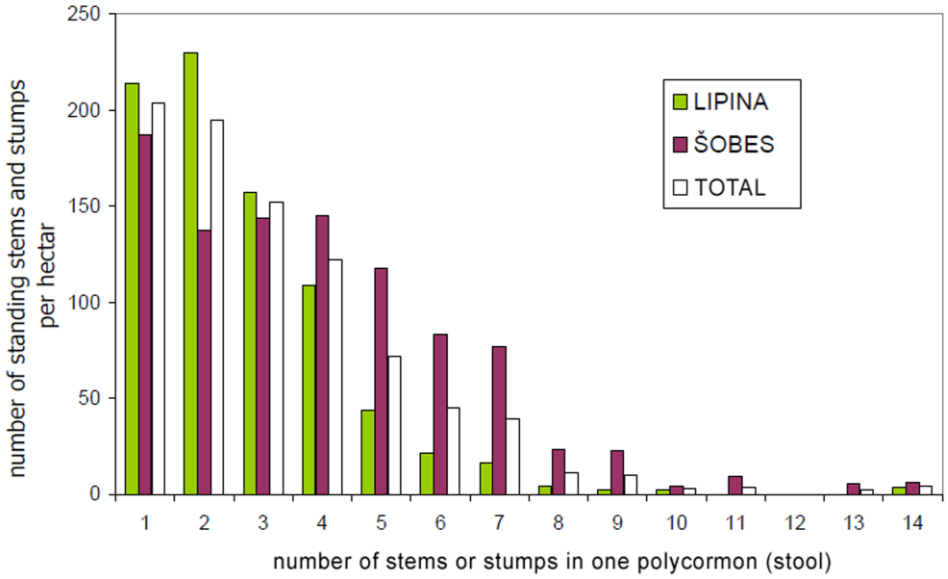

Figure 5 Histogram of the distribution according the number of stems or stumps in one stool

3.2. Stand age and stool age

According to the dendrochronological analyses, forest stands at the research plots were last coppiced in 1885 (Lipina) and 1890 (Šobes). The measured mean stem age was 124 years at Lipina (Q^{25-75}: 116-126 yrs) and 120 years at Šobes (Q^{25-75}: 109-122 yrs) (Fig. 6). Spot felling could be traced during the Great depression, World War II, and sporadically since the 1950s. During the 1980s/90s, Šobes was thinned as part of a planned transformation into high forest, and the number of stems in one stool was partially reduced. We also detected small-scale thinning at Lipina; stumps from these thinnings can still be easily recognized in the forest, and almost none has re-sprouted with new shoots.

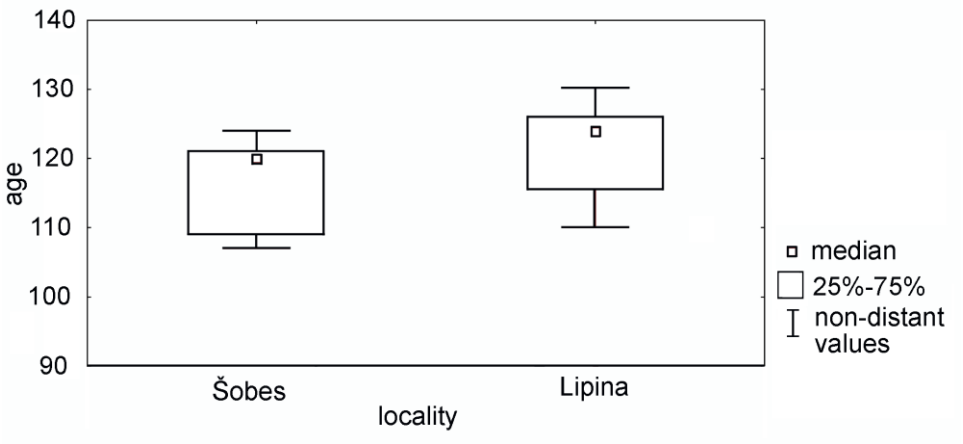

Figure 6 Box plot of age distribution at the Lipina and Šobes sites.

The largest stool (Fig. 2b) had an average distance of 2.13 m (SE ± 0.3 m) and an average annual radial increment of 1.46 mm (SE ± 0.06 mm). The age of this stool was 825 years (SE ± 145 years), which means that the stool originated in the 11^{th}–13^{th} centuries (High Middle Ages). Older roots were often hollow inside and we observed a secondary growth of cambium into this hollow space (Fig. 7). This obviously rules out any age analysis.

Figure 7 Stool root profile – internal cambium created in the root cavity

3.3. Tree inner zone of influence

Tree Inner Zone of Influence ($Tree_{IZI}$) area covered 292 m^2/ha at Lipina and 372 m^2/ha at Šobes (mean 323 m^2/ha). The median area of $Tree_{IZI}$ for a full set of both plots was 0.40 m^2 for all trees, 0.23 m^2 for singles and 0.87 m^2 for stools. At Šobes the Interquartile Range of $Tree_{IZI}$ values was wider compared with Lipina (Fig. 8), and the occurrence of larger stools ≈ larger $Tree_{IZI}$ was more frequent. While the distribution of stem and stump diameters tended to be normal or normal related, the distribution of $Tree_{IZI}$ area was strongly positively skewed and best fit with extreme values or lognormal distribution - even if very few large stools composed a relatively large total of the $Tree_{IZI}$ area.

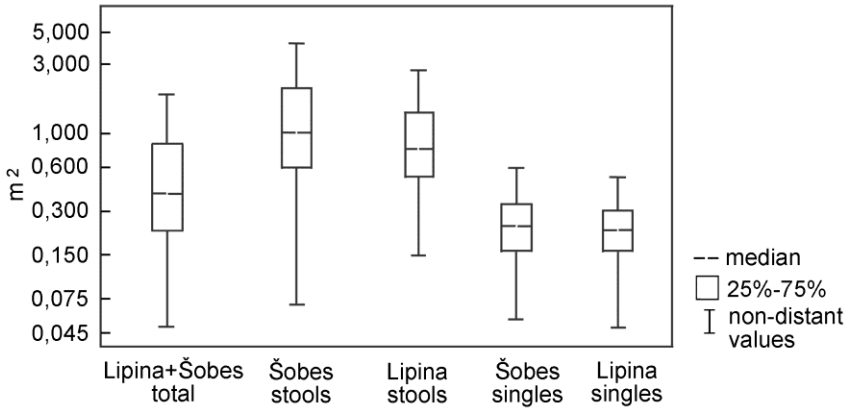

Figure 8 Total tree area (Tree Inner Zone of Influence) for single trees and trees in polycormons. The boxplots represent range of area for single trees and polycormons on study plot.

For a basic differentiation of the variety of $Tree_{IZI}$ areas, we used the Shape Index (SI). Based on the results, we defined three categories of $Tree_{IZI}$ shapes (I - rounded; II - compact; III – jagged, Table 3, Fig. 3), by comparing to the boundary values of SI for the basic, mathematically easily definable shapes of a pentagon (SI 1.075) and equilateral triangle (SI 1.285). Both in numbers and area, the most prevalent was category II (compact), (Table 3). Mean patch size at Lipina was smaller than at Šobes for all categories, most significantly in category III (jagged). In general, for our data raising SI raises the patch size of $Tree_{IZI}$ (Pearson's r 0.4856, significance of F for regression analysis: $p<0.0001$).

Table 3 Stool shapes and tree types according to assessed indexes. Representation of Tree Inner Zones of Influence categories and their basic characteristics

Class	Shape type	Tree type	Criterion	Number of Patches [N/ha]		Class Area [m2/ha]		Mean Patch Size (MPS) [m2]		PS Standard Deviation; (PSSD)		Mean Shape Index (MSI)	
				Šobes	Lipina	Šobes	Lipina	Šobes	Lipina	Šobes	Lipina	Šobes	Lipina
I	circular	single	SI ≤ 1,001	187	214	49	51	0,3	0,2	0,1	0,1	1,0	1,0
I			SI ≤ 1,075	13	10	10	5	0,8	0,5	1,0	0,2	1,1	1,0
II	compact	polycormon (stool)	1,075 < SI ≤ 1,285	167	149	251	174	1,5	1,2	1,2	1,0	1,2	1,2
III	elongated or jagged		SI > 1,285	29	52	62	62	2,1	1,2	2,2	1,3	1,4	1,4
Total				396	424	372	292	-	-	-	-	-	-

3.4. Tree spatial patterns

Our evaluation of the spatial distribution of all standing stems and stumps (both singles and stools) resulted in slight differences between the two plots (Fig. 9). While at Lipina stems and stumps were significantly clustered over all examined distances (Fig. 9 – a), at Šobes for the majority of distances complete spatial randomness (CSR) could not be rejected and a significantly clustered distribution was confirmed only for individual distances (1, 4, 5, 8, 16 and 19 m) (Fig. 9 – b). Since the CSR hypothesis was rejected for the distribution of trees at Lipina and partly at Šobes, the Matérn cluster process was fitted to our empirical data. The minimum contrast method based on the L function yielded the estimates R = 2.11 m (cluster radius), c=

1.85 (mean number of points per cluster) and intensity κ = 0.04 m-2 for Lipina stems and R= 1.22 m, c = 1.68 and κ = 0.05 m-2 for stems at Šobes. The empirical L function and envelopes from 199 simulations of the fitted model showed good agreement for Šobes trees in particular.

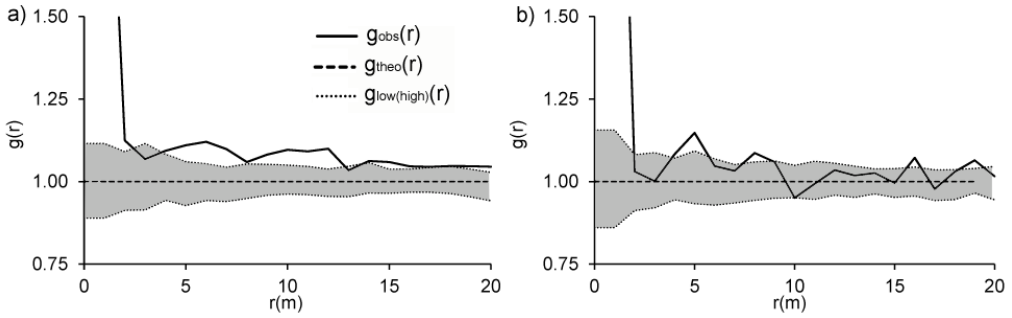

Figure 9 Pair correlation functions g(r) show spatial patterns of all stems at Lipina (a) and Šobes (b). gobs(r) – observed function, gtheo(r) – theoretical value of complete spatial randomness, glow(high)(r) – pointwise envelopes resulting from 199 Monte Carlo simulations of the null model of complete spatial randomness. If the value of gobs(r) is larger than the value of the ghigh(r) then the stems suggest positive association. If the value of gobs(r) is smaller than value of the glow(r) then the stems suggest negative association. In the grey zone, we cannot reject the null hypothesis of complete spatial randomness. The variable "r" refers to distance.

4. DISCUSSION

4.1. Ancient stool roots and age

Because roots are generally less accessible and more difficult to explore and measure, they are less well known than the aboveground parts of plants. A detailed morphological and anatomic analysis of root systems can potentially indicate relationships between roots, the outside environment and other organisms at a particular site. The analysis of root systems, especially in the case of older individuals, can be used to gain insights into the complex and long-term driving factors influencing individual stands. Analyses of roots of oak on skeletal soils have shown that in such conditions oak sometimes develops distorted plates or slats, which are pushed into the small spaces between rocks or fissures of the parent rock (Jeník 1957, Schweingruber 2007). Oak tree rings are visible only in root ends and adjacent areas of surface skeletal roots, which also show other signs of transitional anatomy between aboveground and underground organs (Jeník

1957, Bédéneau & Pagés 1984). As a result, dendrochronological cores of old roots cannot be used to determine the age of ancient coppice stools.

Structural differences in wood anatomy are more variable for broadleaf trees than for conifers (Gaertner 2001), making it much more difficult to detect changes in the wood in response to various events. Because the influences of climate, stand density, and social position of a tree causes large variability in ring width pattern, Copini et al. (2010) rejected using the pattern of wide rings around the pith, previously utilized by Haneca et al. (2005a, 2005b, 2009) as a fingerprint of coppice management. Our findings are in agreement with these views.

To examine the age of ancient stools and the processes that led to their current shape, one must go beneath the surface to uncover the root and stump system. We made a visual and acoustic evaluation (by tapping on roots) of the exposed underground of ancient stools and took cross sections of different roots. We concluded that the overwhelming majority of large roots were hollow because of heart rot or were preserved only as remnants of the original root in the form of slab roots. Because the oldest parts of the roots were decayed, the deadwood samples we were able to take could not serve as indicators of stool age. The approximated age of one of the largest oak stools at our research plots was 825 years (SE ± 145 years). Similar or even older coppice stools of oaks and lindens with respect to size and growth rate have been reported by Rackham (2006) and Pigott (1989).

For the modelled old stool we estimated a ratio of 2:1 for above/below ground volume with no reduction of below ground biomass regarding the hollow roots. This is in contrast to Barbaroux et al. (2003), who found a 5:1 biomass estimation ratio in a high forest. Stem bases were clustered only at 20 m^2 but the trees were spread into the neighbourhood and altogether covered a 5 times greater area than in high forest.

4.2. Tree inner zone of influence

In our study we simplified the shape of stool clusters into three categories (I - rounded; II - compact; III - jagged). However, the number of variants can be very high depending on tree species: coppicing ability and strength, mortality rate and its spatial distribution, length of rotation period, longevity and rate of growth.

The present form of ancient coppices was shaped by the mortality of new shoots due to mutual competition, the ageing and dying of old stools (Johnson 1977, Larsen & Johnson 1998, Rydberg 2000), as well as by natural habitat conditions and the length, intensity and frequency of human impact. The probability of sprouting steeply declines for stools with large DBH. If many sprouts persist on a single stump, they may develop a sweep in the lower part of the bole.

It appears that for most oak species the key factor limiting seedling recruitment is light availability, i.e. overstory crown closure. Seed regeneration is therefore far more likely in open sites away from the parent tree (Crow 1992, Dey 2002, Steele & Smallwood 2002). However, with the gradual decay and dying off of ancient oak stools, one can expect an increase in seedlings of tree species other than oak (lime, hornbeam, maple, pine) (Szymura et al. 2014).

4.3. Tree spatial patterns

In accordance with our assumptions, stems often showed a significantly clustered distribution. This reflects the vegetative origin of stems in stools. At Lipina, stems had clustering at all study intervals up to 20 m. A similar spatial distribution was observed in the Mondariz and Pantón coppice forests in Spain (Rozas et al. 2009). The maximum intensity of clumping in our study and in Mondariz and Pantón is almost identical, with ranges at ca. 1 m.

Interestingly, stool centroids also showed a clustered distribution at distances to 10m. This could be the effect of long-term human influence (short-rotation period). If the stems were cut at a young age (7-10, later 20 years), then the forest stand was essentially single-layered at all times. All stems needed a minimal crown area for survival, and less successful trees were gradually eliminated, so the forest stand tended towards a clustered spatial distribution.

5. CONCLUSIONS

For the modelled old stool we estimated a ratio of 2:1 for above/below ground volume with no reduction of below ground biomass regarding the hollow roots. The age of the largest stool was

estimated 825 years (SE ± 145 years). Total area of "Inner Zone of Influence" covers 323 m^2/ha. The median area of this zone in both plots was 0.40 m^2 for all trees, 0.23 m^2 for singles and 0.87 m^2 for stools. The Matérn cluster process was successfully fitted to our empirical data. In this model the mean cluster radius ranged between 1.9 to 2.1 m and mean number of points per cluster was 1.7 and 1.9. The most prevalent characteristics of these ancient oak coppices were their compact shape and clustered spatial distribution up to 10 m.

6. LIST OF ABBREVIATIONS

PNP - Podyjí National Park

CSR - Complete Spatial Randomness

7. ACKNOWLEDGEMENTS

We would like to thank the Podyjí National Park Administration for supporting our research. Ivana Plačková, Dagmar Koktová, Saly Šmíd and Fidel Švejda helped us to unearth the coppice stools. Thanks to Hanuš Vavrčík from the Faculty of Forestry and Wood Technology, Mendel University in Brno for consulting the dendroecology of roots. For comments on the manuscript, we thank to Martin Valtera. David Hardekopf carried out the proofreading. This paper was created with support of projects GA ČR P503-11-2301 and OPVK CZ.1.07/2.3.00/20.0267.

8. REFERENCES

Baddeley A (2008). Analysing spatial point patterns in R. CSIRO, Australia. 232 pp.

Baddeley A, Turner R (2005). Spatstat: an R package for analysing spatial point patterns. Journal of Statistic Software 12: 1-42.

Barbaroux C, Bréda N, Dufrêne E (2003). Distribution of above-ground and below-ground carbohydrate reserves in adult trees of two contrasting broad-leaved species (Quercus petraea and Fagus sylvatica). New Phytologist 157(3), 605-615.

Bauhus J (2009). Rooting patterns of Old-Growth Forest: is Aboveground Structural and Functional Diversity Mirrored Bellowgeound? In: "Old-Growth Forests: Function, Fate and Value" (Wirth C, Gleixner G, Heimann M, eds). Springer, Berlin, Germany. pp: 211-229.

Bechmann R. (1990). Trees and man: the forest in the middle ages. Paragon House, Saint Paul, MN, 326 pp.

Bédéneau M, Pagés L (1984). Etude des cernes d'accroissement ligneux du système racinaire d'arbres traités en taillis. [Studies about tree rings in coppice root system]. Annales des sciences forestières 41: 59-68.

Besag J (1977). Contribution to the discussion of Dr Ripley's paper. Journal of the Royal Statistical Society (Series B) 39: 193-195.

Besag J, Diggle PJ (1977) Simple Monte Carlo tests for spatial pattern. Applied Statistics 26: 327-333.

Bouwer K (2008). Voor profijt en genoegen; De geschiedenis van bos en landschap van de Zuidwest-Veluwe. [For profit and pleasure; The history of forest and landscape of the Southwest Veluwe] Uitgeverij Matrijs, Utrecht, The Netherlands. 432 pp.

Bruckman VJ, Yan S, Hochbichler E, Glatzel G (2011). Carbon pools and temporal dynamics along a rotation period in Quercus dominated high forest and coppice with standards stands. Forest Ecology and Management 262: 1853-1862.

Casper BB, Schenk HJ, Jackson RB (2003). Defining a plant's belowground zone of influence. Ecology 84: 2313-2321.

Chytrý M, Vicherek J (1995). Lesní vegetace NP Podyjí. [The Forest Vegetation in Podyjí National Park]. Academia, Praha, Czech Republic. 166 pp.

Čižmář Z (2002). Mašovice (okr. Znojmo). [Mašovice region]. In: PV 43 Brno. Archeologický ústav AV ČR Brno, Czech Republic. pp: 157-161.

Coles JM (1978). Man and landscape in the Somerset Levels. In: "The Effect of Man on the Landscape: the Lowland Zone" (Limbrey S, Evans JG, eds). C.B.A. Research Report No. 21. Council for British Archaeology, London, UK. pp: 86-89.

Copini P, Sass-Klaassen U, Den Ouden J (2010). Coppice fingerprints in growth patterns of pedunculate oak (*Quercus robur*). In: TRACE – Tree Rings in Archaeology, Climatology and Ecology (Levanic T, Gricar J, Hafner P, Krajnc R, Jagodic S, Gärtner H, Heinrich I, eds). Otočec, Slovenia. pp: 54-60.

Crow TR (1992). Population dynamics and growth patterns for a cohort of northern red oak (*Quercus rubra*) seedlings. Oecologia 91: 192-200.

Dey D (2002). The Ecological Basis for Oak Silviculture in Eastern North America. In: "Oak Forest Ecosystems: Ecology and Management for Wildlife" (McShea WJ, Healy WM, eds). The Johns Hopkins University Press, Baltimore, USA. pp: 60-79.

Diggle PJ (2003). Statistical Analysis of Spatial Point Patterns. Hodder Arnold, 2nd Edition, London. 159 pp.

Ducousso A, Bordacs S (2003). EUFORGEN Technical Guidelines for genetic conservation and use for pedunculate and sessile oaks (*Quercus robur*) and (*Quercus petraea*). International Plant Genetic Resources Institute, Rome, Italy. 6 pp.

Evans MN, Barkham JP (1992). Coppicing and natural disturbance in temperate woodlands - a review. In: "Ecology and Management of Coppice Woodlands" (Buckley GP ed.). Chapman and Hall, London, UK. pp: 79-98.

Falinska K (1985). The demography of coenopopulations of forest herbs. In: „The Population Structure of Vegetation" (Handbook of Vegetation Science 3) (White J, ed.). W. Junk, Dordrecht, The Netherlands. pp: 241-264.

Freeman EA, Ford ED (2002). Effects of data quality on analysis of ecological pattern using the K(d) statistical function. Ecology 83: 35-46.

Fuller RJ, Warren MS (1993). Coppice woodlands: their management for wildlife. Joint Nature Conservation Committee, Peterborough. 29 pp.

Gaertner H (2001). Holzanatomische Analyse diagnostischer Merkmale einer Freilegungsreaktion in Jahrringen von Koniferenwurzeln zur Rekonstruktion geomorphologischer Prozesse. [Wood-anatomical analysis of diagnostic characteristics of an exposure reaction in tree rings of coniferous roots to reconstruct geomorphological processes]. Rheinischen Friedrich-Wilhelms-Universität, Bonn, Germany. 118 pp.

Haneca K, Boeren I, Acker J, Beeckman H (2005a). Dendrochronology in suboptimal conditions: tree rings from medieval oak from Flanders (Belgium) as dating tools and archives of past forest management. Vegetation History and Archaeobotany 15: 137-144.

Haneca K, Čufar K, Beeckman H (2009). Oaks, tree-rings and wooden cultural heritage: a review of the main characteristics and applications of oak dendrochronology in Europe. Journal of Archaeological Science 36: 1-11.

Haneca K, Van Acker J, Beeckman H (2005b). Growth trends reveal the forest structure during Roman and Medieval times in Western Europe: a comparison between archaeological and actual oak ring series (*Quercus robur* and *Quercus petraea*). Annals of Forest Science 62: 797-805.

Heggenstaller DJ, Zenner EK, Brose PH, Peck JE (2012). How Much Older are Appalachian Oaks Below-Ground than Above-Ground? Northern Journal of Applied Forestry 29: 155-157.

Hölscher D, Schade E, Leuschner C (2001). Effects of coppicing in temperate deciduous forests on ecosystem nutrient pools and soil fertility. Basic and Applied Ecology 164: 155-164.

Iida S, Nakashizuka T (1995). Forest fragmentation and its effect on species diversity in sub-urban coppice forests in Japan. Forest Ecology and Management 73: 197–210.

Illian JB, Penttinen A, Stoyan H, Stoyan D (2008). Statistical Analysis and Modelling of Spatial Point Patterns. John Willey & Sons, Chichester, UK. 534 pp.

Itô H, Hino T, Sakuma D (2012). Species abundance in floor vegetation of managed coppice and abandoned forest. Forest Ecology and Management 269: 99-105.

Janík D, Vrška T, Šamonil P, Unar P, Adam D, Hort L, Král K (2007). Structure and Ecology of oak woods in the Podyjí National Park as exemplified by the Lipina locality. Thayensia 7: 175–206.

Jeník J (1957). Kořenový systém dubu letního a zimního: rhizologická studie. [Root system of oaks]. Nakladatelství ČSAV, Praha, Czech Republic. 85 pp.

Jeník J, Soukupová L (1999). On the growth form of bog pine, Pinus× pseudopumilio. Silva Gabreta 3: 25-32.

Johnson PS, 1977. Predicting oak stump sprouting and sprout development in the Missouri Ozarks. North Central Forest Experiment Station, Forest Service, US Department of Agriculture, USA. 43 pp.

Joys A, Fuller RJ, Dolman PM (2004). Influence of deer browsing, coppice history, and standard trees on the growth and development of vegetation structure in coppiced woods in lowland England. Forest Ecology and Management 202: 23–37.

Korpeľ Š (1991). Pestovanie lesa. [Silviculture]. Príroda, Bratislava, Slovak Republic. 465 pp.

Král K, Valtera M, Janík D, Šamonil P, Vrška T (2014). Spatial variability of general stand characteristics in central European beech-dominated natural stands – Effects of scale (suppl. mat.). Forest Ecology and Management 328: 353-364.

Kull K (1995). Growth form parameters of clonal herbs. Consortium Masingii: A Festschrift for Victor Masing, Tartu, Estonia. pp: 106-115.

Lang S, Tiede D (2003). vLATE Extension für ArcGIS - vektorbasiertes Tool zur quantitativen Landschaftsstrukturanalyse. In: „ESRI Anwenderkonferenz proceedings." Innsbruck, Austria. pp: 1-10.

Larsen DR, Johnson PS (1998). Linking the ecology of natural oak regeneration to silviculture. Forest Ecology and Management 106: 1-7.

Linford J (2007). A Concise Guide to Trees. Parragon Book Service Limited, UK. 256 pp.

Loosmore NB, Ford ED (2006). Statistical inference using the G or K point pattern spatial statistics. Ecology 87: 1925-1931.

McGarigal K, Marks BJ (1995). Fragstats spatial pattern analysis program for quantifying landscape structure, Version 2.0. Oregon State University, Corvallis, USA. 134 pp.

Nadezhdina N, Cermak J (2003). Instrumental methods for studies of structure and function of root systems of large trees. Journal of Experimental Botany 54: 1511-1521.

Neruda P (2007). Starší doba kamenná v Podyjí: Současný stav a perspektivy [Old stone age in the river Dyje region: An overview and perspectives]. Thayensia 7: 291–303.

Nielsen AB, Møller F (2008). Is coppice a potential for urban forestry? The social perspective. Urban Forestry and Urban Greening 7: 129-138.

Oldeman RA (1990). Forests: elements of silvology. Springer, Stuttgart. 624 pp.

Peterken GF (1996). Natural woodland: Ecology and conservation in northern temperate regions. Cambridge University Press, Cambridge, UK. 540 pp.

Pigott CD (1989). Factors controlling the distribution of *Tilia cordata* Mill. at the northern limits of its geographical range IV. Estimated ages of the trees. New Phytologist 112: 117-121.

R Development Core Team (2006). R: a language and environment for statistical computing.. URL: http://www.R-project.org. R Foundation for Statistical Computing, Vienna, Austria.

Rackham O (1980). The Medieval Landscape in Essex. In: "Archaeology in Essex to A.D. 1500" (Buckley DG, ed.). London, UK. pp: 103-107.

Rackham O (2006). Woodlands. Collins, London, UK. 608 pp.

Reiterová L, Škorpík M, eds (2012). Plán péče o Národní park Podyjí a jeho ochranné pásmo. [Management plan for Podyjí National Park and its protective zone]. Správa NP Podyjí, Znojmo, Czech Republic. 316 pp.

Ripley BD (1977). Modelling spatial patterns. Journal of the Royal Statistical Society (Series B) 39: 172-212.

Ripley BD (1988). Statistical inference for spatial processes. Cambridge University Press, Cambridge, UK. 148.

Rozas V, Zas R, Solla A (2009). Spatial structure of deciduous forest stands with contrasting human influence in northwest Spain. European Journal of Forest Research 128: 273-285.

Rydberg D (2000). Initial sprouting, growth and mortality of European aspen and birch after selective coppicing in central Sweden. Forest Ecology and Management 130: 27-35.

Schweingruber FH (2007). Wood structure and environment. Springer, Berlin - Heidelberg, Germany. 279 pp.

Škorpík M ed (1993). Plán péče o Národní park Podyjí a jeho ochranné pásmo. [Management plan for Podyjí National Park and its protective zone]. Správa NP Podyjí, Znojmo, Czech Republic. 173 pp.

Steele M, Smallwood PD (2002). Acorn Dispersal by Birds and Mammals. In: "Oak Forest Ecosystems: Ecology and Management for Wildlife" (McShea WJ, Healy WM, eds). The Johns Hopkins University Press, Baltimore, USA. pp: 182-195.

Stoyan D, Penttinen A (2000). Recent applications of point process methods in forestry statistics. Statistical Science 15: 61-78.

Szymura TH, Szymura M, Pietrzak M (2014). Influence of land relief and soil properties on stand structure of overgrown oak forests of coppice origin with *Sorbus torminalis*. Dendrobiology 71: 49-58.

Tolasz R, ed (2007). Atlas podnebí Česka. [Climate atlas of Czechia]. Czech Hydrometeorological Institute, Praha, Czech Republic. 255 pp.

Verheyen K, Bossuyt B, Hermy M, Tack G (1999). The land use history (1278–1990) of a mixed hardwood forest in western Belgium and its relationship with chemical soil characteristics. Journal of Biogeography 26: 1115-1128.

Vrška T (1998). Historický vývoj lesů na území NP Podyjí a v bližším okolí do roku 1948. [Historical development of forests in Podyjí National Park until 1948]. Thayensia 1: 101-124.

Vyskot M (1961). Výsledky nepřímých převodů pařezin přetvářením. [The results of coppice transformation management]. Lesnictví 12: 1061-1096.

Walker J, Sharpe PJ, Penridge LK, Wu HI (1989). Ecological Field Theory: the concept and field tests. Vegetatio 83: 81-95.

Weber P, Bardgett RD (2011). Influence of single trees on spatial and temporal patterns of belowground properties in native pine forest. Soil Biology and Biochemistry 43: 1372-1378.

Wu HI, Sharpe PJ, Walker J, Penridge LK (1985). Ecological field theory: a spatial analysis of resource interference among plants. Ecological Modelling 29: 215-243.